Ionospheric Research

NASA Grant No. Ns G 134-61

Scientific Report

on

"Density and Temperature Fluctuations in the
Daytime F Region of the Ionosphere"
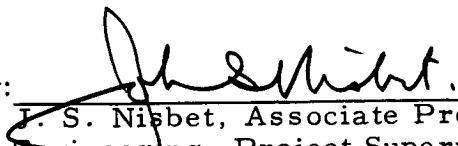
by

Joe R. Doupnik

August 10, 1967

Scientific Report No. 302

Ionosphere Research Laboratory

Submitted by: _____

J. S. Nisbet, Associate Professor of Electrical
Engineering, Project Supervisor

Approved by: _____

A. H. Waynick, Director, Ionosphere Research
Laboratory

The Pennsylvania State University
College of Engineering
Department of Electrical Engineering

TABLE OF CONTENTS

ABSTRACT

Large amplitude electron density and temperature fluctuations in the daytime F region were observed at Puerto Rico during incoherent backscatter experiments on quiet days. Duration of the fluctuations was typically from one to four hours. They occured between 180 km and at least 700 km and had amplitudes as large as 100%. They were strongest at the latitudes of Puerto Rico and much weaker to the north and south. During the fluctuations, the electron densities were observed to change inversely to the electron temperatures.

Mechanisms for causing the fluctuations were investigated by examining electron density and temperature instabilities, variations of solar ionizing radiation, motions of the neutral atmosphere in the forms of gravity waves and winds, electrodynamic drifts associated with the dynamo current system, local drifting irregularities, and large traveling disturbances.

Model computations of separate density and temperature profiles indicated that instabilities of the coupled density-temperature system were not responsible for these fluctuations. Local drifting irregularities and solar flux variations were shown to be not responsible by data from a network of spaced ionosondes. Electrodynamic drifts associated with the dynamo current system were shown to be at variance with vertical transport velocities computed from the experimental backscatter data. Data on one day indicated possible internal gravity wave induced fluctuations, but other

fluctuations were not due to waves.

It was suggested that the fluctuations could be explained by a low latitude system of neutral winds. However, there are large differences between the required winds and current global wind models.

CHAPTER 1 STATEMENT OF THE PROBLEM

1.1 General Statement

Observations of electron density and temperature at the Arecibo Ionospheric Observatory in Puerto Rico during solar minimum have revealed the existance of large amplitude fluctuations. Almost all the observations were during quiet geomagnetic and solar conditions and are believed to be indicative of the normal quiet ionosphere. Attention is centered on the F2 region because the density fluctuations appeared to occur mainly above the transition altitude of the F1 to the F2 region. Duration of the fluctuations was typically from one to four hours. They occurred between 180 km to an observational limit of 700 km, and had amplitudes as large as 100%. Consequently, we are not concerned with fine structure variations with scales as small as a few kilometers and a few minutes. In addition, the fluctuations do not necessarily correspond to mean monthly or seasonal behavior.

Most previous studies regarding the behavior of the F region have used electron density profiles either from ionograms or from rocket probes. Ionograms limit the data to either above or below the F2 peak and do not measure plasma temperatures directly. Rocket probes perform high resolution measurements of both electron density and temperature throughout the ionosphere but only for a short time interval. The results reported here are based largely on direct incoherent backscatter measurements of electron density and temperature and ion temperature above and below the F2 peak throughout the day. Thus, the time dependent structure of the F region as a whole can be studied.

1.2 Specific Statement of the Problem

a) Large electron density and temperature fluctuations are observed in the F region during the day. Can the changes in either density or temperature be explained as due to a variation of the other? Is the system of coupled electron density and temperature equations stable with respect to perturbations?

b) Is it necessary to invoke motion of the neutral atmosphere to explain the fluctuations? If so, then what types of neutral motion can be expected and what would be consistent with the experimental results?

c) The solar energy flux is variable. To what extent can this be ruled out as a source for the fluctuations?

d) To what extent can plasma drifts caused by electric fields be used to explain the fluctuations?

e) How are the fluctuations correlated at different ionospheric sounding stations and how are they related to traveling ionospheric disturbances?

f) Are the fluctuations due to local changes of density and temperature or are they due to regions of enhanced density drifting over the station?

CHAPTER 2 INTRODUCTION AND REVIEW

2.1 Introduction

There are several physical mechanisms which could cause large changes of F region electron densities. They include atmospheric motion in the form of winds and waves pushing ionization mainly along geomagnetic field lines, electric fields transporting ionization across field lines, and solar ultraviolet flux variations modifying the electron densities in situ. The theories for each of these mechanisms are reviewed, and some relevant experimental data are summarized. Theoretical calculations for model F regions are also discussed.

2.2 Atmospheric Winds

Neutral atmospheric winds in the F region are nearly horizontal, and change the electron density distribution by forcing ionization up or down field lines. Thus, the important wind components for ionization transport are those directed along field lines; i.e., meridional winds. Equatorialward winds lift ionization, and poleward winds depress it. Ionization transport across field lines is strongly inhibited in the F2 region because the electron-neutral and ion-neutral collision frequencies are smaller than their gyrofrequencies.

Kohl and King (1966) have calculated model wind systems for the F2 region. The driving force was the horizontal variation of atmospheric pressure due to solar heating. The neutral gas models were those of hydrostatic equilibrium fitted to global distributions of exospheric temperatures, and the driving force was sinusoidal in

time. Molecular viscosity and the Coriolis effect were included in the equation of motion while fixed electron density models were used for the ion drag effects.

Their computed wind speeds were relatively constant over the globe throughout the day. Two solar conditions were considered both at equinox. At solar minimum, with a peak electron density of 3×10^5 cm^{-3} at 300 km, the wind speed was about 150 m/s at 300 km while the direction changed from anti-solar at the north pole at 1300 hours LMT to due westward at the equator at the same time. For medium solar condition, with a peak electron density of 10^6 cm^{-3} at 300 km, the speed at 300 km was of the order 40 m/s. The direction was northward at 1500 hours LMT at nearly all latitudes in the northern hemisphere.

Geisler (1966) extended this work to non-equinox condition as well but with the same basic assumption as Kohl and King. His wind speeds in a north-south plane at 45° latitude during solar minimum were of the order 100 to 150 m/s at 200 km with a diurnal oscillation. They were directed toward the poles during the day and toward the equator at night. A prevailing wind of about 100 m/s toward the equator was superimposed on the summer 100 to 150 m/s diurnal variation. Time dependent electron density profiles were employed, but they were specified independently of the winds. There was little altitude dependence of the calculated wind velocities throughout the F2 region.

2.3 Atmospheric Waves

The atmosphere is able to sustain wave motion in addition to

the winds. The important characteristic for the electron density distribution is the neutral motion along lines of force.

Hines (1960) has developed a theory for the propagation of internal gravity waves in the neutral atmosphere from linearized equations of motion, adiabatic state, and mass conservation. For periods greater than an hour energy flow is mainly horizontal and neutral particle motion is oscillatory along the same direction. The oscillation amplitude grows exponentially with altitude, and plasma disturbances appear to progress downward due to the downward progression of phase. Periods range from a minimum of 15 minutes to about a day. The vertical wavelengths in the F region for periods longer than an hour are greater than 100 km and are largely independent of frequency and horizontal wavelengths. The horizontal wavelength, however, is directly related to the period and is about 0.9 cτ, where c is the adiabatic speed of sound, about 800 m/s in the F region, and τ is the period. Consequently, the phase velocity, ω/k, is about 700 m/s (0.9 c) there.

Hines (1960) has suggested that the lower atmosphere may be a source of the waves, and the mesopause temperature minimum would tend to filter out the smaller scale and shorter period components.

Friedman (1966) considered characteristics of gravity waves essentially ducted by the mesopause and tropopause and leaking energy into the F region.

Volland (1967) has derived a theory of atmospheric waves for which thermal conduction is important; he calls them heat

conduction waves. The basic equations are the same as those of Hines (1960) but heat conduction is now included.

These waves are almost vertically propagating in both energy and phase so that neutral particle motion is mainly vertical. The neutral motion projected along the field line is then reduced to the total velocity times the sine of the dip angle. Volland states that solar wind compression of the magnetospheric boundary may be a source of the waves, and that they then propagate toward the ground with exponentially decreasing phase and group velocity. About 10 hours are required to reach 200 km from the exosphere and 2 days to reach 120 km thus accounting for delayed ionospheric storm effects. In the F region between 200 and 400 km group and phase velocities of 10 to 100 m/s are predicted. The refractive index in the long period regime (greater than 10^{+3} sec) decreases from about 50 at 200 km to about 3 at 400 km so that the wavelength of one hour wave changes from about 100 km to 1600 km there.

Thome (1966) detected F region electron density fluctuations at Arecibo using a unique beam swinging backscatter experiment whereby the velocity vector of the traveling disturbance could be measured. In addition, critical frequencies from a number of ground based ionosondes, a spaced ionosonde technique, were used to verify the existance and velocity of the traveling disturbance.

Thome detected several cycles of the disturbances and found that their periods were between two and four hours with a horizontal velocity which decreased from about 700 ± 100 m/s for the first cycle to about 125 ± 25 m/s for the fourth cycle. The

direction was generally north to south and the horizontal wavelength was of the order 4000 km. A phase reversal between 250 km (near the peak) and about 350 km was detected. Only high amplitude waves and generally only the first cycle were evident on the spaced ionosonde records. Wave passage was seen as about a 1 mc decrease of critical frequency lasting for about an hour although 50% variation of electron density were noted at Arecibo.

The conclusion of this work was that the disturbances are boundary or surface waves propagated in the neutral atmosphere and are ducted from the auroral zone in the 100 km altitude region. Their existence was closely associated with the onset of geomagnetic storms, and heating of the neutral atmosphere by dumped particles was suggested as the source.

Hines (1967) has published an interesting application of gravity waves to the fluctuations of F2 peak plasma frequency, f_oF2, following a nuclear explosion. The strength, duration, time of arrival, and period increased roughly linearly with distance from the explosion. The dominant periods were 40 minutes at 1300 km range to 130 minutes at 4400 km range. Hines has interpreted the data as being indicative of the ray paths followed by different modes into the F2 region, i.e. longer period modes traveling at smaller elevation angles and hence reaching the F2 region only at larger ranges. The horizontal component of the centroid of the group velocity was estimated to be 200-400 m/s.

2.4 Electric Fields

The effect of slowly varying electric fields in the F region

on electrons and ions is almost entirely to cause an ambipolar drift perpendicular to both the electric field $\overline{E}$ and the geomagnetic field $\overline{B}$ with a time averaged velocity $\overline{v}$ given by

$$\overline{v} = \frac{\overline{E} \times \overline{B}}{B^2} \quad \text{meters/second.}$$

The relaxation time needed to attain this velocity, in the absence of collisions, is only a few ion gyroperiods and hence a fraction of a second. The drift would be uniform throughout the F region, again without collisions, since the high electrical conductivity along field lines allows them to act as equipotential surfaces. In the northern hemisphere, where $\overline{B}$ is directed to the north and down, an eastward electric field would produce an upward drift with a vertical component of (E/B) cos I; I is the geomagnetic dip angle. For example, at a dip angle of 45° an electric field of 10^{-3} v/m with $B \simeq 5 \times 10^{-5}$ webers/m^2 a 14 m/s vertical drift would be expected. Collisions between the charged and neutral gas modify the drifts, however, and it is discussed later in this section.

Electric fields in the F2 region are predicted as a consequence of the dynamo theory (Chapman and Bartels, 1940) of current generation in the E and lower F1 regions. The dynamo theory states that the daily geomagnetic field variations measured at the ground are produced in large part directly by neutral atmospheric winds around 120 km pushing ions across field lines. Electrons are largely immobile because their gyrofrequency is much higher than their collision frequency with the neutral gas. Slight charge densities arise because the vortex type wind patterns tend to move one type of

charge to the center and the other to the rim of the vortices. Electro-static fields then result. The basic diurnal current sheet patterns have been computed by Chapman and Bartels (1940) from magnetogram data.

The method of computing the electric field can be outlined quickly from S. Kato (1956). The basic equations are Ohm's law and Maxwell's equations

$$\bar{J} = \bar{\bar{\sigma}} \cdot (\bar{E} + \bar{v}_n \times \bar{B})$$

$$\nabla \cdot \bar{J} = 0$$

$$\nabla \times \bar{E} = 0$$

where $\bar{J}$ is the current density inferred from magnetogram data

$\bar{\bar{\sigma}}$ is the tensor conductivity

E is the electric field

v_n is the neutral wind velocity assumed to be the same as the ion velocity

B is the total magnetic field, earth plus ionosphere

Since $\nabla \times \bar{E} = 0$, then E is electrostatic. Consequently

$$\nabla \times (\bar{\bar{\sigma}}^{-1} \cdot \bar{J}) = \nabla \times (\bar{v}_n \times \bar{B})$$

The neutral wind is assumed to arise from horizontal pressure variations, p', by

$$\frac{\partial \bar{v}_n}{\partial t} = 2 \bar{v}_n \times \bar{\omega} - \nabla \left(\frac{p'}{\rho_o}\right)$$

over the surface of the globe where $\bar{\omega}$ is the earth rotation vector and ρ_o is the mean atmospheric mass density in the dynamo regions. Spherical harmonic expansions are made for both $\nabla \times (\bar{\bar{\sigma}}^{-1} \cdot \bar{J})$ and p'/ρ_o with harmonic diurnal time variations, and they are matched

to determine p'/ρ_0. This gives $\bar{v}_n$, and $\bar{E}$ results as the remainder to satisfy

$$\bar{E} = \bar{\bar{\sigma}}^{-1} \cdot \bar{J} - \bar{v}_n \times \bar{B} \, .$$

For the Sq system Kato (1956) after some approximation has shown the pressure variations, p', to be centered at 55° N latitude with minimum pressure at 08 hours and maximum at 20 hours LMT. The electrostatic field is mainly eastward during the morning and westward after 15 hours with an amplitude ranging from nearly zero at the equator to about 10^{-3} v/m at 80° N. Vertical electrodynamic drift velocities in the F2 region computed from this data are sinusoidal, upward from 4 to 16 hours, and have a maximum value of 20 m/s near 09 hours. Maeda and Kato (1966) have reviewed the dynamo theory, and their electrodynamic drift velocities are essentially the same as Kato's above.

Electric fields could also be generated in the magnetosphere and could possibly generate the necessary currents by transmission of the fields to the E region along the geomagnetic field lines (Fejer, 1965). The necessary theory, however, has not been developed.

There is no direct experimental evidence of electric fields in the F region during the day. Haerendel, Lust, and Rieger (1967), however, have inferred F region fields during twilight from the motion of rocket released Ba and Ba^+ ion clouds. The fields were about $1 - 3 \times 10^{-3}$ v/m and had the same general direction and strength as those predicted by Maeda (1955) for the Sq system dynamo theory.

Dougherty (1961) has shown that collisions between drifting

charged particles and the neutral gas seriously modify the simple $\bar{E} \times \bar{B}/B^2$ drifts. Within 20 minutes to an hour the neutral gas could be set into motion by the horizontal component of the plasma drift. The neutral motion in turn suppresses the vertical component of plasma drift. Vertical motion of the neutral gas is inhibited by the resulting pressure gradient changes. He has shown consequently that in steady state the effective ambipolar diffusion coefficient is increased from one appropriate to diffusion along field lines to one without an effective geomagnetic field. It is to be noted that, in equilibrium, increasing the diffusion coefficient lowers both the altitude and electron density at the F2 peak.

2.5 Traveling Irregularities

There are two classes of irregularities of interest here, small scale ones (< 1 km) measured in the upper Fl region and large scale ones (> 1000 km) in the F2 region. The small irregularities measured near 200 km are most likely associated with local movements of the neutral atmosphere and can serve as an indication of neutral winds in the F region. The larger ones involve the F2 region and the conception of a volume of ionization being transported gives way to the more likely condition of propagation of a disturbance through the ionosphere.

Yerg (1955) summarized small scale drift measurements over Mayaguez, Puerto Rico for 1954 and 1955 made by the correlation of a 4.57 mc signal diffraction pattern measured at three closely spaced receivers. This frequency corresponds to reflection near 200 km. The true velocity of the irregularities was found to be

toward the southwest during the winter and toward the north during the summer with an average speed below 10 m/s. The direction was more variable in winter than in summer. If the irregularities were moving with a neutral wind and if the same wind were present in the upper F region, then we should expect a general lifting of the F2 region during winter and a depressing during summer.

Chan and Villard (1962) have discussed a much larger class of traveling disturbance. Changes in high frequency signals (18 mc and 20 mc) sent from Mayaguez, Puerto Rico and Washington, D. C. to Palo Alto and Seattle were analyzed to determine the approximate speed, period, and length of the irregularities. Typical values are periods of 30 to 90 minutes, speeds of 1450 to 2750 km/hr, and lengths of 1300 to 2200 km. Their directions were mainly, within 25°, from north to south. A drawing of nighttime virtual height from ionograms during the passage of a 50 minute period disturbance indicates that a feature seen at 0015 hours UT at Boulder appears at 0045 UT at White Sands, 0030 UT at Washington, and 0115 UT at Puerto Rico.

Many of the traveling irregularities discussed by Chan and Villard occurred within an hour after the sudden commencement of geomagnetic storms or sudden impulses. Thome (1966) found the same relation. The irregularities are regarded by Thome and by Chan and Villard as the redistribution of ionization due to traveling waves in the neutral atmosphere.

Heisler (1963) summarized his studies of traveling disturbances revealed by the occurances of complex echoes from a network of

widely spaced ionosondes. The complexities or multiple echoes are due to small irregular structures in the electron density distribution which accompany the larger density perturbation. The characteristics of the large traveling irregularities are as large as 1800 km across, traversing more than 3000 km with one case having a period of about one hour and causing an 85% change in daytime peak electron density. Downward progression of the disturbance is generally noticed.

In another paper Heisler (1966) discussed fluctuations of peak electron density occurring at the same universal time for a number of ionosonde stations in and around Australia. The fluctuations occurred during local daytime and during relatively quiet magnetic conditions and amounted to two or three megacycle changes of the peak plasma frequency over periods of one or two hours. No firm conclusions were presented. The author did think however that these fluctuations were different from the frontal type which produced sudden ionogram complex echoes. The day to day variability of F region densities was thought to be due in part to the addition of local time and these universal time effects.

Cummack (1966) computed auto and cross-correlation functions of F2 peak critical frequency deviations about the mean diurnal variations from ionograms at Taipei and four Japanese stations. The data were for several days in January and April, 1964. Power spectra of the individual stations showed large fluctuations with periods of two days to about six hours. The longer period components were strongest at the lower latitude stations. Two classes of disturbances were detected from interstation correlations. The first was traveling

disturbances having Fourier components with periods of two to about
twelve hours and sizes of about 900 to 6000 km. Their velocity was
about 10 - 20 km/min in an equatorial direction. The second class
had components with periods of 45 to 90 hours and velocities of
2 - 3 km/min generally toward the southeast (toward the equator).
Their size was of the order 4000 km, and their amplitudes were about
ten times greater at low latitudes (13.6° N geomagnetic) compared
with high latitudes (35.3° N geomagnetic). These larger disturbances
were believed to be associated with large scale atmospheric ir-
regularities and not electrodynamic or acoustic perturbations.

In an interesting and extensive paper King, Eccles, Legg,
et al (1964) have developed a theory of two global drifting ionization
maxima in the F region. The theory was developed mainly for the
summer hemisphere but the general features were believed to
apply in lesser strength to the winter hemisphere as well. The low
latitude maximum develops at about 08 hours Local Mean Time on
the magnetic equator, moves poleward at about 65 m/s, and reaches
a position of 15° geomagnetic latitude about 13 hours LMT. After
15 hours it divides with one part returning toward the equator and
the other, the high latitude maximum, continuing outward. The
high latitude maximum reaches to 55° from the magnetic equator
by 03 hours LMT and reverses its direction; the speed is about
85 m/s at the higher latitudes. The widths of the maxima are about
30°. During the winter the movements are more symmetrical about
local noon rather than 15 hours as in the summer and their strengths

are weaker in the winter. No definite mechanism was proposed for causing the movements.

2.6 Solar Flux

Electron-ion pairs in the F region are produced by solar ultraviolet radiation mainly in the range 1025 $\overset{o}{A}$ to about 100 $\overset{o}{A}$ ionizing the neutral gases of molecular oxygen and nitrogen and of atomic oxygen. Below 100 $\overset{o}{A}$ the ionization cross sections and the solar flux both become small (Hintregger, Hall, and Schmidtke, 1964). Over a typical eleven year solar cycle, from minimum to maximum sunspot activity, Nicolet (1963) estimates the flux in this wavelength range changes by ± 60% or less from mean activity levels. Disturbed activity is reflected as flux changes below 10 $\overset{o}{A}$ whose contributions to F region ionization are small compared to longer wave lengths.

To examine the effect of production rate on an equilibrium ionosphere it is convenient to discuss the F1 region (110 to 180 km) separately from the F2 region (above 180 km) since the aeronomical problems are different. In the F1 region electron and ion diffusion rates are small, and chemical equilibrium is quickly established after sunrise. The chemical process is balancing of production and recombination rates

$$P \simeq \alpha N_e^2$$

where P is the production rate, N_e is the electron density, and α is the effective recombination rate coefficient. The major ion in this region is nitric oxide, and Donahue (1966) has found its recombination coefficient, α, to depend roughly on $T_e^{-3/2}$ where T_e is the electron temperature.

If the temperature were constant, then doubling the production rate would increase the electron density by $\sqrt{2}$. If the temperature also increased, then the density increase would be somewhat larger.

In the F2 region the loss rate becomes proportional to the product of the electron density with the densities of molecular oxygen and nitrogen, and diffusion becomes important. It can be shown that for an equilibrium ionosphere with this linear loss rate that the electron densities are directly proportional to the production rate. There would be no change in the altitude of the peak. When an F1 region is added as a lower boundary, the variation of F2 region electron densities with production rate is expected to be only slightly different than linear.

For changes of solar flux to account for the observed peak electron density variations, ignoring changes of peak altitude, we should expect the following consequences.

a) The flux should exhibit 25% to 100% increases over periods of one or two hours in local winter.

b) The increases should be more regular in local summer with maximum values in the afternoon.

c) Similar variations would occur for a number of stations at the same universal time.

d) E and F1 electron densities would show variations similar to F2 region densities.

e) The measured solar flux at 10.7 cm should also change, based on the empirical correlation between the 10.7 cm measurements and solar activity.

Evans (1965) reported electron density and temperature data taken during the June 20, 1963 solar eclipse from the Millstone Hill, Massachusetts incoherent backscatter experiments. The eclipse there lasted from 1545 to 1750 hours EST; totality occurred at 1650 hours at 300 km, and 97% of totality existed between 150 km and 430 km at the same time. The data were averaged over 15 minute intervals. The altitude of the F2 peak increased by 20 - 30 km before totality and quickly returned to its normal value at totality. Electron densities at the F2 peak increased smoothly about totality; the maximum value was about 45% greater than the values before and after the eclipse. Above 450 km, however, the densities decreased during the event thus reflecting some redistribution of ionization from high altitudes to the F2 peak. At 180 km, the transition between F1 and F2 layers, during totality the electron densities dropped to about 25% of their normal values. Electron content in a vertical column below 750 km decreased from 10.29×10^{12} cm^{-2} at 1600 hours to 9.42×10^{12} cm^{-2} at 1650 hours to 7.83×10^{12} cm^{-2} at 1750 hours EST. Electron temperatures varied smoothly during the eclipse with temperatures decreased by about 1000° K at all altitudes above 250 km at totality. Evans found the uniform electron temperature variations to be a consequence of high electron thermal conductivity. Due to the symmetrical pattern of isotherms about the time of totality Evans suggested that the electron temperatures closely followed the variation of incident solar radiation. Ion temperatures also decreased during the eclipse but with amplitudes which increased with altitude, e.g. a 100° K change at 350 km and 300° K at 650 km compared with control days.

Comparing Evan's data with what we expected from solar flux changes it is clear that the electron density at the F2 peak does not necessarily follow the quick flux changes. Instead of decreasing with solar obscuration the peak density increased because the F layer became cooler and the ionization moved down from above. Below the F2 region, however, the densities decreased through totality. The altitude of the peak did not change very much. Variations of electron content due to the eclipse are not easily estimated from Evan's data because the eclipse occurred shortly before sunset, but the content clearly did decrease.

Experimental data presented here, however, show that during non-eclipse conditions electron density fluctuations do not occur at the same time at all locations and do not occur at all at some locations. Consequently, variations of the solar ultraviolet flux is not responsible for these fluctuations.

2.7 Model Studies of F Region Electron Densities

A number of F2 region electron density models have been developed for both time dependent and equilibrium states. The studies considered here pertain to quiet daytime conditions and, with one exception, to middle latitudes.

The basic equation employed in all the models is the electron density continuity equation

$$\frac{\partial N_e}{\partial t} = P - L - \nabla \cdot (N_e \, \overline{v})$$

with essentially the same boundary conditions. The variables are electron density N_e, effective production rate P of electron-ion pairs,

their loss rate L, and the ambipolar transport velocity $\bar{v}$. In the F2 region production is normally proportional to the atomic oxygen number density while the loss is proportional to the product of electron density and the densities of either molecular oxygen or nitrogen or both.

The transport velocity $\bar{v}$ has received most attention. It consists of two parts, ambipolar diffusion along geomagnetic field lines through an immobile neutral atmosphere and an additional effective drift velocity due to motion of the neutral gas or electric fields. At middle latitudes horizontal gradients are normally neglected compared to vertical ones so that the diffusion velocity is

$$- D \left[\frac{1}{N_e} \frac{\partial N_e}{\partial z} + \frac{m_i g}{k(T_e + T_i)} \right] \sin \ I$$

where z is the altitude. D is the ambipolar diffusion coefficient and is inversely proportional to the neutral gas density, principally atomic oxygen. The parameter $k(T_e + T_i)/m_i g$ is sometimes called the plasma scale height where k is Boltzmann's constant, T_e and T_i are the electron and ion temperatures, m_i is the ion mass, and g is the acceleration of gravity. Field lines are inclined at an angle I with respect to the horizontal. Near the equator, $\partial N_e/\partial z$ must be replaced by the full spherical coordinate gradient operator with sin I included.

Boundary conditions are equality of production and loss at a lower boundary and vanishing of N_e at infinite height. The latter condition is usually restricted to mean that the diffusion velocity vanishes also. Field lines at middle latitudes are considered to be rectilinear so that sin I is not altitude dependent.

Yonezawa (1958) found equilibrium solutions for uniform drift velocities by employing perturbation expansions in terms of integral Green's functions. Plasma temperatures were equal to an isothermal neutral temperature. He found that the altitude of the F2 peak was almost linearly proportional to the drift velocity and that the peak density increased exponentially with the peak altitude. A layer at 49.1° latitude with an undisturbed peak at 300 km would be shifted upward to 340 km by a 13 m/s upward drift and the peak density would be doubled. An equal downward drift lowered the peak to 275 km and then decreased the peak density by one third.

Rishbeth and Barron (1960) considered the dependence of equilibrium density profiles both on the ratio of loss to diffusion coefficients and on uniform drift velocities. Equal and isothermal temperatures were assumed. For the cases when the loss rate coefficient β (Loss $= \beta N_e$) involves just molecular oxygen and the diffusion coefficient D and the production rate P depend on atomic oxygen they found the following results. When the drift velocity v_d was zero then the ratio of loss to production at the peak was constant at about 0.7 while $H^2\beta/D$ at a given altitude was changed over four orders of magnitude. H is the atomic oxygen scale height $kT_n/m_o g$. Under the same condition, the altitude of the peak was linearly proportional to Log_{10} (β/D) at a given altitude. Under the action of a uniform drift velocity, v_d, the altitude of the peak z_p and the electron density there N_p were found to change from their undisturbed values according to

$$\Delta (Log_{10} N_p) \propto v_d/(D_o)$$

$$\Delta z_p \propto v_d/(D_o)$$

where D_o is the diffusion coefficient at the undisturbed peak altitude. Again, these relations held under wide ranges of the ratio $(H^2 \beta/D)$ at a given altitude.

Nisbet (1963) computed equilibrium models allowing for the electron temperature to exceed the ion temperature. Solutions were obtained above and just below the peak as a set of exponential series for a number of combinations of production and loss rate coefficients and of temperatures. Helium and hydrogen ions were included in the upper F region. Tornatore (1964) extended this work to include uniform drift velocities. The profiles were similar to those of Yonezawa and of Rishbeth and Barron for comparable conditions.

Rishbeth (1964) obtained time dependent solutions of F2 region electron densities by an analog computer. The procedure was to compute electron densities for a static neutral atmosphere throughout the day and night and then to scale the results in proportion to a time dependent neutral atmosphere. Electron, ion, and neutral temperatures were equal. The results pertinent here are those relating to the value of the diffusion rate coefficient under low sunspot conditions. The "fast diffusion" model peak density was nearly constant during the daytime. Below the peak, densities slowly decreased by about 50% after midmorning while the reverse was true above the peak. "Slow diffusion" was achieved by reducing the diffusion coefficient one order of magnitude. Slower diffusion resulted in larger densities and a peak density which increased throughout the day until sunset.

Density variations above and below the peak were similar to the fast model but slightly larger. No drifts were considered.

L. Thomas (1966) computed equilibrium electron density models without drifts but with altitude dependent and unequal electron and ion temperatures. When electron and ion temperatures were equal in a large region about the peak the peak density was about 25% smaller for $T_e = 2.8\ T_n$ than for $T_e = T_n$; T_n is the isothermal neutral temperature. This reduction was only 10% when $T_i = T_n$ about the peak. There was little change in the altitude of the peak. A reduction of up to one third of a neutral scale height could occur though if there existed a large height gradient of ion temperature; the peak density showed a slight decrease also.

Rishbeth (1967) repeated some of his previous (1964) time dependent model calculations with the inclusion of Geisler's (1966) time dependent neutral winds as uniform drifts. During the daytime Geisler's summer solar minimum winds produced larger early morning peak densities than the no wind model and ones which after 09 hours continuously dropped below the no wind model. The winter winds resulted in a peak density which steadily decreased after sunrise to very small values at sunset.

Cummings (1966) obtained eigenvalue solutions to the homogeneous continuity equation under the conditions of no drift and of thermal equality. The normal lower altitude boundary condition that production equals loss was replaced by a requirement that the electron density remain finite at infinite distances below the reference height. The eigenvalues λ are then

$$\lambda = \beta_o (4\beta_o H^2/D_o)^{-\alpha/(\alpha + 1)} \Lambda, \quad \Lambda = 1.04, 6.94, 14.63, \text{ etc. for}$$

$\alpha = 1.75$ and $\Lambda = 1.06$, 7.46, 16.26, etc. for $\alpha = 2.0$. The variables have the following meaning: β_0 is the loss rate coefficient with a neutral species whose scale height is the scale height of atomic oxygen, H, divided by α; D_0 is the diffusion coefficient. Subscripts o indicate evaluation at a given altitude. The parameter α corresponds to loss with different neutral species; $\alpha = 1.75$ with molecular nitrogen, and $\alpha = 2.0$ with molecular oxygen.

Although Puerto Rico is generally regarded as being in the middle latitude region rather than the equatorial or auroral ones, it is 30 geographic and geomagnetic degrees from the magnetic equator. Hanson and Moffett (1966) have computed electron density models of the daytime equatorial zone under the influence of electrodynamic drift velocities. Plasma induced motion of the neutral atmosphere was assumed to be zero. The equilibrium models indicate that the centers of enhanced ionization ridges of the Appleton anomaly move 15° to 20° away from the equator under the action of upward drifts of the order 10 - 15 m/s. Several hours, however, were needed to accomplish the transport.

2.8 Model Studies of F Region Electron Temperatures

The electron temperature in the F region is determined by the balancing of energy gained from energetic photoelectrons, of the energy lost by collisions with both the neutral and ion gases, and of the energy transported by thermal conduction and ionization movements. The term electron temperature, T_e, refers to the ambient electron gas which has a Maxwellian velocity distribution of

a temperature T_e. Electrons in the high energy tail of the distribution (1 ev or more) in excess of the Maxwellian distribution are sources of energy for the ambient electron gas, and they are generated by photoionization of all available neutral gases.

Hanson and Johnson (1961) computed equilibrium electron temperatures based on equality of production and loss. Photoelectrons were assumed to lose their energy locally, and almost all of it would be transferred to the neutral gas rather than to the ambient electrons. Ion temperatures were equated to the neutral temperature.

Hanson (1963) expanded on this work with better estimates of the photoelectron heating efficiency and with consideration of their migration. Due to inelastic collisions with molecular nitrogen each photoelectron would have about 1.3 ev at 200 km to 5 ev at 300 km available for transfer to the ambient electrons. Above 300 km, many photoelectrons could escape along field lines to the opposite hemisphere. Electron thermal conduction and departure of ion temperatures from neutral temperatures were discussed.

More detailed photoelectron energy calculations were made by Dalgarno, McElory, and Moffett (1963) by considering the solar flux in a number of wavelength intervals and the various ionization thresholds of the neutral gases. Consideration was given to the average energy each photoelectron could give to the ambient electron gas assuming that no migration occurred. This energy at solar minimum ranged from 1.5 ev at 150 km to 40 ev at 500 km. Electron temperatures were computed for equality of production and loss.

Geisler (1965) and Geisler and Bowhill (1965) considered the

problem of photoelectron migration and developed an expression for their non-local heating of the ambient electron gas. Equilibrium electron and ion temperatures were computed, with coefficient of electron thermal conductivity appropriate to a fully ionized gas, by an iterative numerical method. F region electron temperatures were nearly isothermal for small F2 peak densities and developed an inflection near the peak for larger densities.

Time dependent electron temperatures were obtained by daRosa (1966) for the sunrise period. The time dependent temperature equation was linearized in electron temperature and solved numerically by a version of the implicit method. Solutions were begun before sunrise with a static electron density model, and as the sun rose the peak density was increased at a given rate while the density scale height above the peak was determined by the temperatures. A temporal maximum of electron temperature was found about one hour after sunrise as the heat capacity and energy loss of the electron gas balanced the energy production rate. Thermal conduction was included and Geisler's (1965) non-local heating rate factor was used above 300 km. daRosa found that the electron temperature was in quasi-equilibrium during sunrise so that equilibrium temperature solutions would be sufficient for many problems.

In a series of papers Banks (1966 a-e, 1967 a, b) examined the problems of energy transfer rates between electron, ion, and neutral gases, and he computed equilibrium temperatures of the plasma. Non-local heating of the electron gas by migrating photoelectrons was approached differently than Geisler (1965), and the numerical heating

rates are similar. As a consequence of frequent electron-neutral collisions in the lower F region Banks was able to show that the electron thermal conduction coefficient was reduced from that of a fully ionized gas by a factor depending on the ratio of electron to neutral densities. During the day, the reduction could be a factor of 5 or 10 at some altitudes. Equilibrium electron temperature profiles were computed by a version of the implicit method. Ion temperatures were found by equating energy gains and losses at each time step. Thermal conduction through the ion gas was shown to alter the ion temperature by less than 100° K below 600 km.

CHAPTER 3 EXPERIMENTAL DATA

3.1 Description of the Experiment

Gordon (1958) proposed the basic theory for the incoherent backscattering experiment based on Thomson scattering of radio waves by ionospheric free electrons. Subsequent investigations by a number of authors (Salpeter (1960), Buneman (1961), Bowles (1961), Fejer (1961), Hagfors (1961), Renau et al (1961), Dougherty and Farley (1963), Moorecroft (1963), and Salpeter (1963)) have shown that the scattering involves both electrons and ions and that the total back-scattering cross section is

$$\sigma_T = \frac{\sigma_o N_e^2}{R^2 (1 + T_e/T_i)}$$

where σ_o is the cross section for a single electron, N_e is the electron (and ion) density, R is the range to the observer, T_e and T_i are the electron and ion temperatures. Doppler broadening of the returned signal occurs because of the charged particle thermal motions. The frequency spectrum of the backscattered power depends on T_e, T_i, and the masses of the various ionic species present.

The Arecibo Ionospheric Observatory, where these data were obtained, employs a 1000 foot diameter reflector to transmit a 1/6 degree wide beam pulse at 430 mc through the ionosphere and to receive the backscattered signals. A high speed digital computer controls the signal sampling and processing.

Long pulse lengths were used for temperature measurements so that the Doppler broadening is not obscured by convolution with a

wide transmitted pulse spectrum. Normally, a 500 µs pulse is employed so that the temperatures reflect a weighted average over a 75 km height interval. Temperatures are obtained from comparison of experimental with theoretical autocorrelation functions on a least squares basis. Perkins and Wand (1965) have described the measurement techniques and the temperature errors; the latter are about $\pm 100^{\circ}$ K.

Temperatures were measured at mean altitudes of 175, 250, 325, 400, 475, 550, and 600 km. The auto-correlation functions are dependent on ion mass so that the data at 175 km and 600 km were not used because the mixture ratios of NO^+ and O^+ ions at 175 km and of H^+, H_e^+ and O^+ ions at 600 km could not be estimated with confidence. Instead, T_e/T_i at 175 km was assumed to be the same value as at 250 km and to decrease linearly to unity at 100 km. At 600 km, T_e/T_i was taken to be unity. Mahajan (1967) indicates that at sometimes a linear law below 250 km may be appropriate. It is not clear which method is best.

Electron densities were obtained from the power profiles after corrections for range, T_e/T_i, and receiver recovery effects. Density data presented here were measured with 100 µs pulses representing a weighted average over 15 km. Density and temperature experiments were alternated, and the ratios of T_e/T_i needed to correct the power profiles were interpolated at the appropriate times. The final density profiles were normalized at the F2 peak to the maximum electron densities scaled from Arecibo ionograms.

Typical averaging times were 10 - 15 minutes for densities and 15 - 20 minutes for temperatures.

3.2 Experimental Conditions

Parameters of solar and geomagnetic activity during the experiments were obtained from the Solar-Geophysical Data of the Space Disturbances Laboratory, U. S. Department of Commerce, Environmental Scientific Services Administration and are listed in Table 1. Intensity of solar radiation at the monitored 10.7 cm wavelength (2800 mc) is given by $S_{10.7}$ in units of 10^{-22} watts/m^2. R_z is the final Zurich sunspot number. Magnetic activity at Fredricksburg, Virginia, is recorded as K_{FR} on a scale of 0 - 9, 0 represents no activity and 9 extreme activity, over three hour intervals beginning at midnight UT.

3.3 Incoherent Backscatter Measurements

Electron density, electron temperature, and ion temperature data from six incoherent backscatter experiments at Arecibo, Puerto Rico, are summarized in Figures 1 through 18. The six experiments were performed on December 15, 22, 29, 1965; July 22, 30, 1966; and August 17, 1966. Electron densities at four fixed altitudes are shown in Figures 1, 4, 7, 10, 13, and 16 together with the density at the F2 peak and the altitude of the peak. Central times of each measurement are indicated by symbols and straight lines join the points. Representative electron density versus altitude profiles are shown in Figures 2, 5, 8, 11, 14, and 17 at three times during each experiment. Electron and ion temperatures measured during the day are plotted in Figures 3, 6, 9, 12, 15, and 18. Temperatures at 475 km were omitted near sunrise and sunset because the power spectra indicated the presence of hydrogen and helium ions in addition to the normal oxygen ions.

Table 1 Solar and Geomagnetic Parameters during the Experiments

Date	$S_{10.7}$	K_{FR}		R_z
December 14, 1965	74.7	0100	0001	0
15	76.8	0000	0001	14
21	74.1	0210	0100	10
22	72.3	1222	2212	11
28	83.8	3333	2323	64
29	84.7	1212	1221	64
July 21, 1966	100.5	4333	2232	55
22	103.2	4200	1232	66
29	128.9	2211	0021	76
30	124.2	1340	0122	59
August 16	92.8	3120	1011	40
17	94.4	1100	0000	41
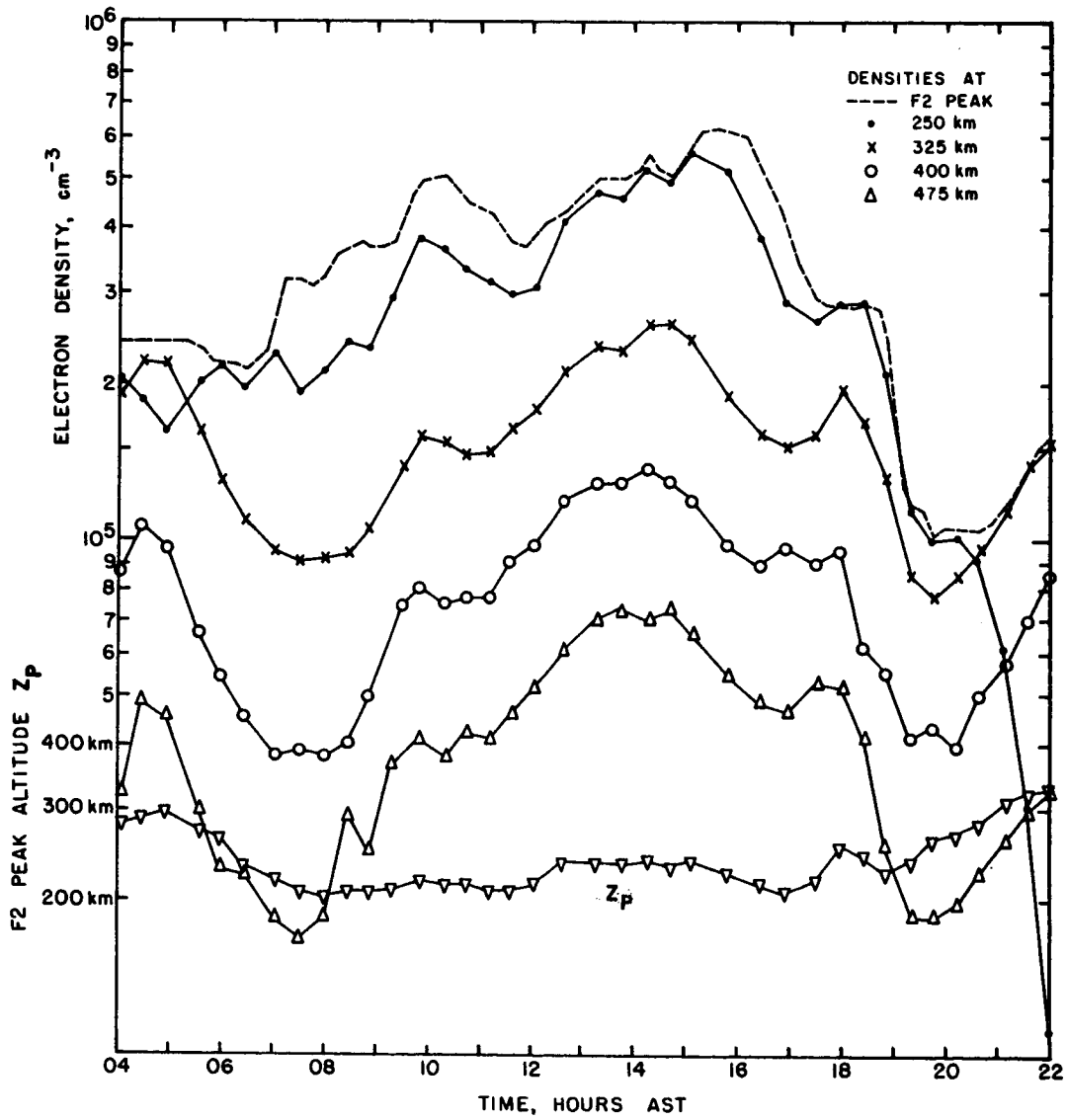
FIGURE I.   ARECIBO ELECTRON DENSITIES ON
DECEMBER 15, 1965.
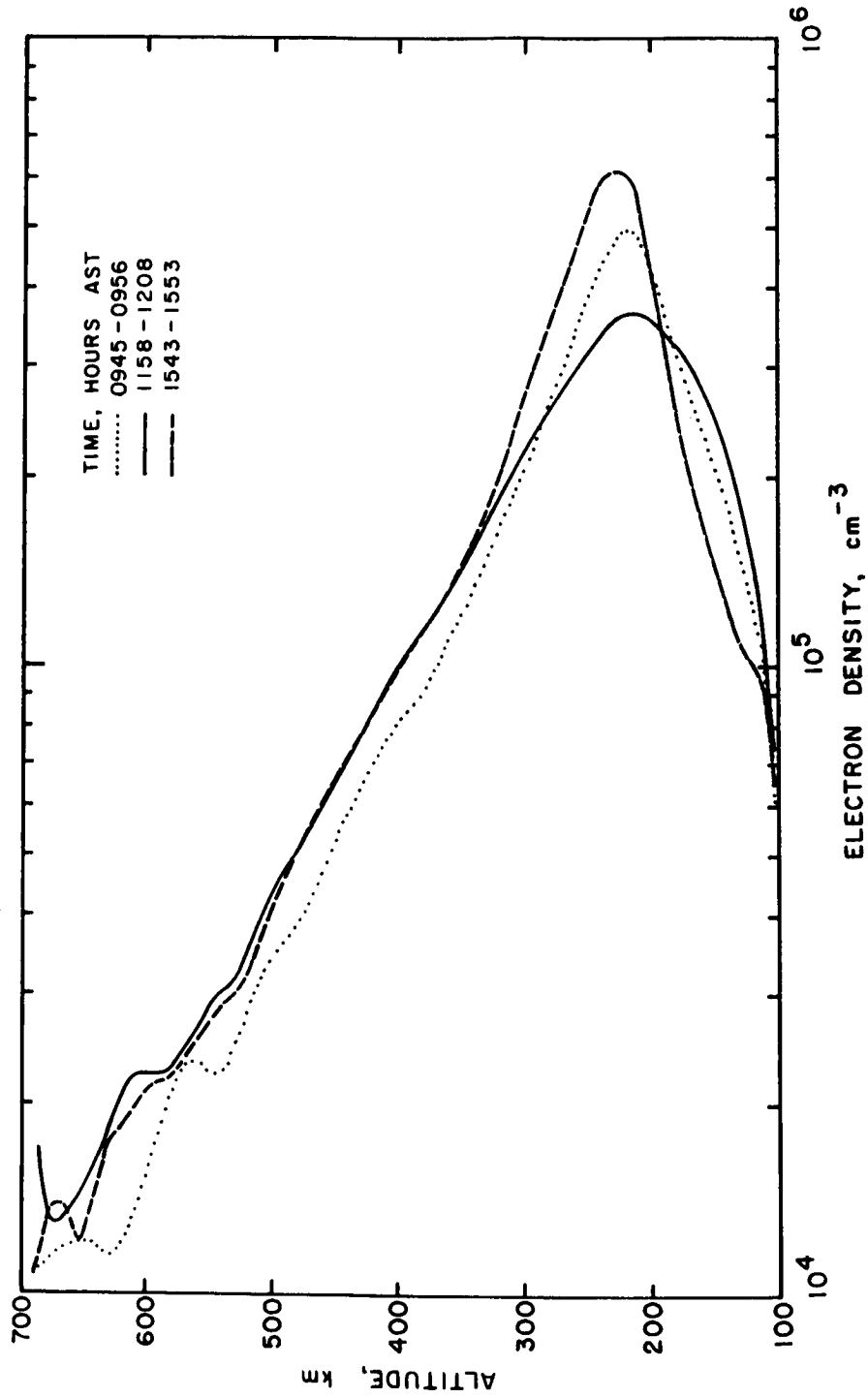
FIGURE 2. ELECTRON DENSITY PROFILES AT ARECIBO ON
DECEMBER 15, 1965.
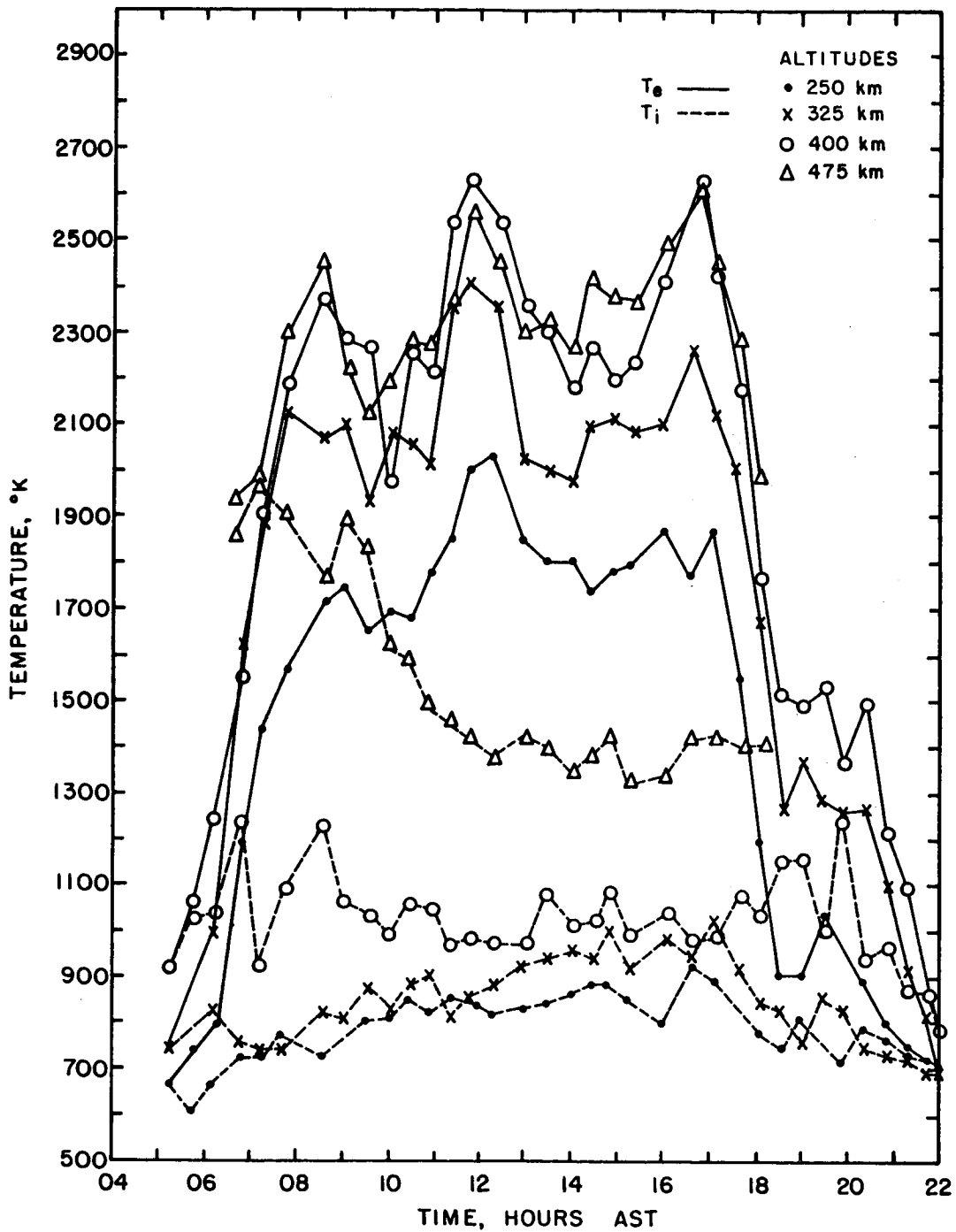
FIGURE 3. ELECTRON AND ION TEMPERATURES AT ARECIBO ON DECEMBER 15, 1965.
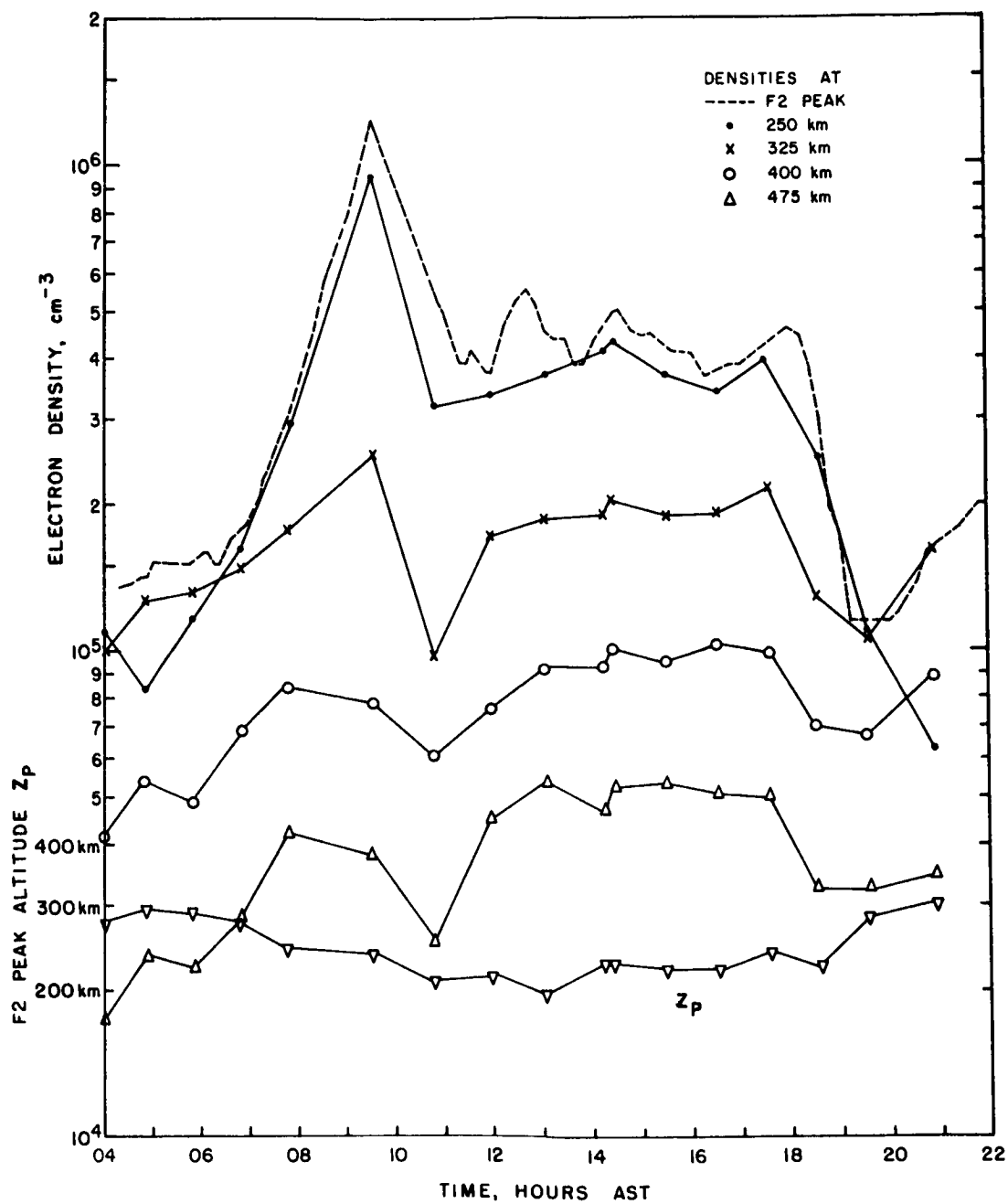
FIGURE 4.   ARECIBO   ELECTRON   DENSITIES   ON
DECEMBER 22, 1965.
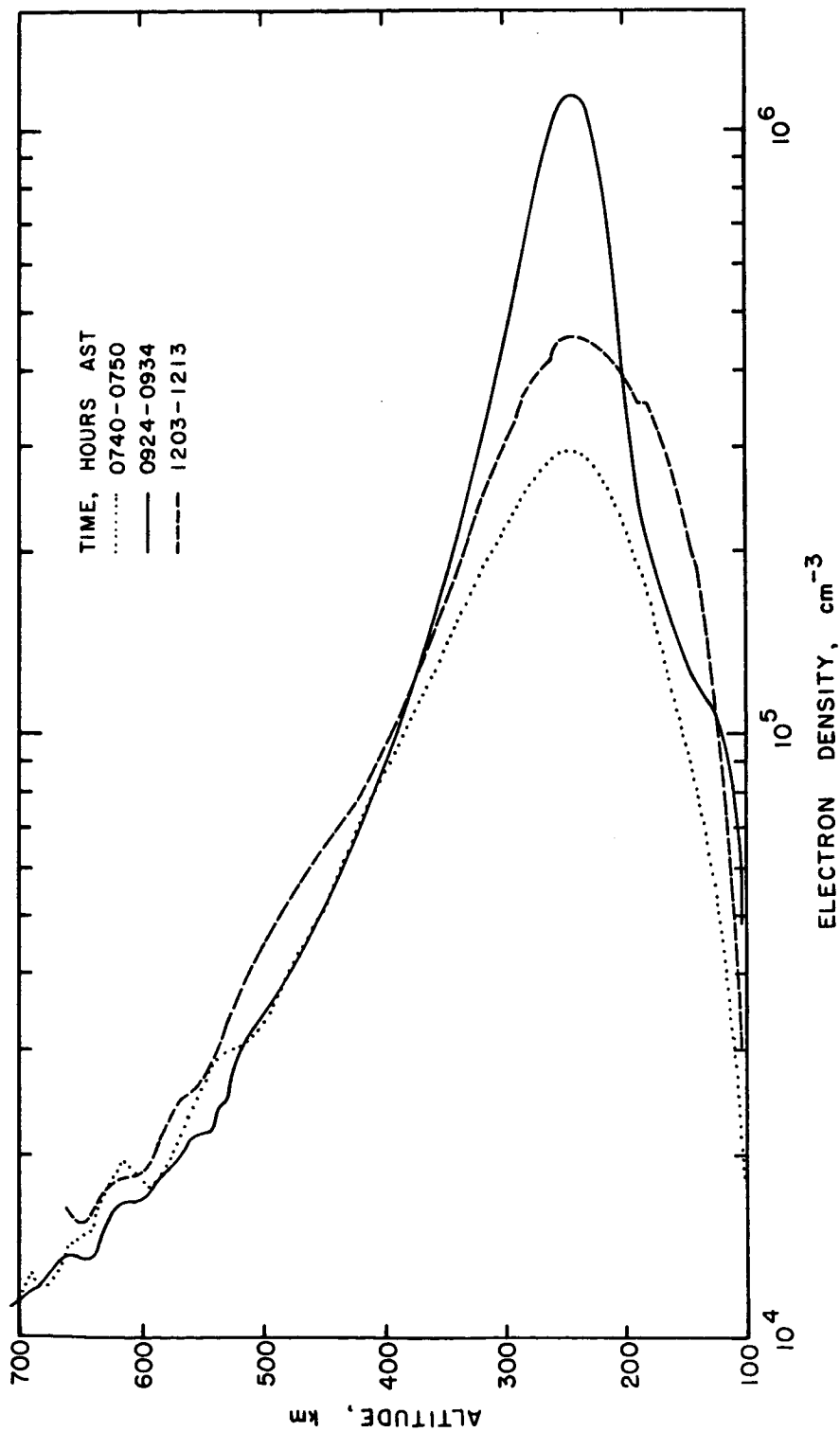
FIGURE 5. ELECTRON DENSITY PROFILES AT ARECIBO ON
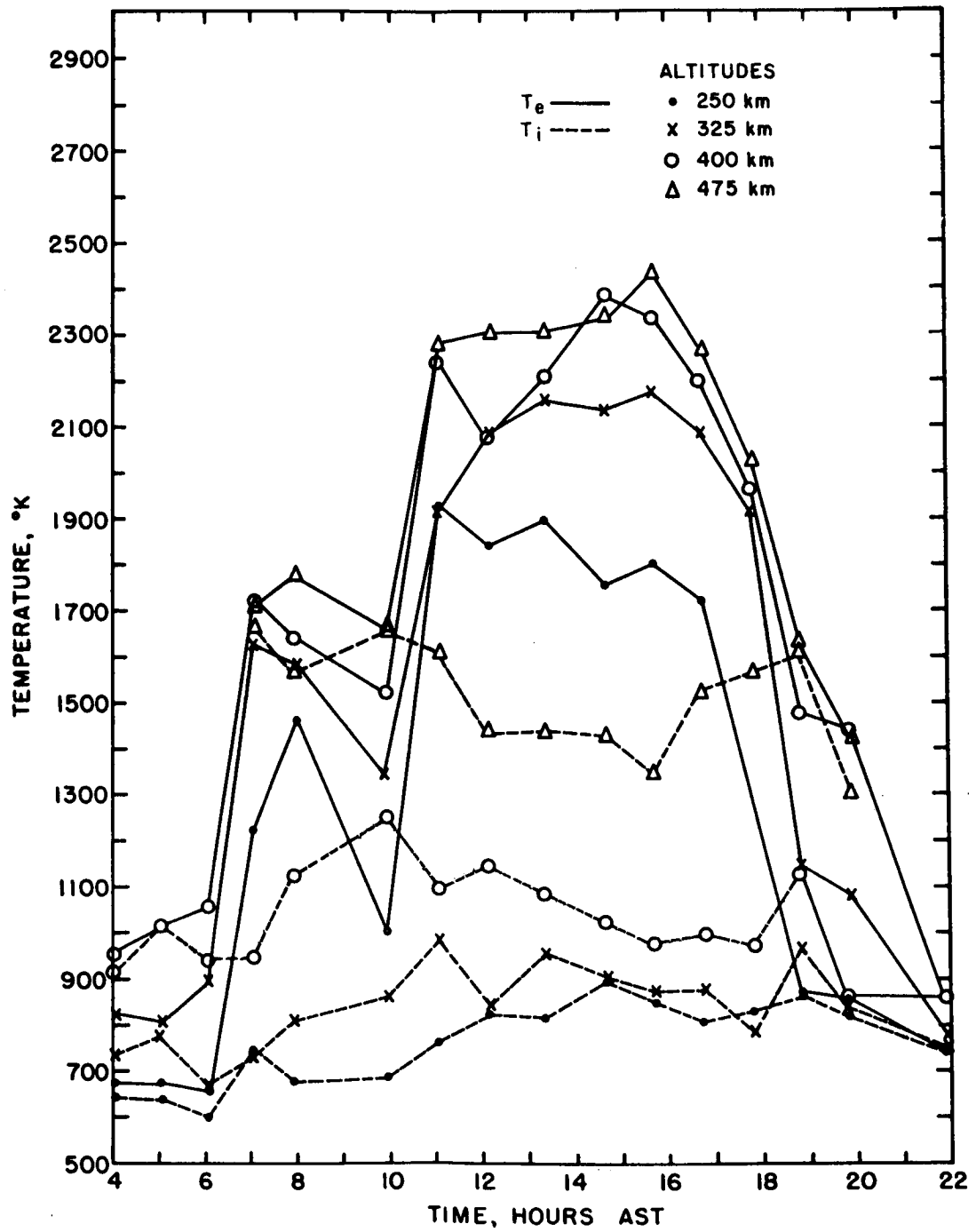
DECEMBER 22, 1965.

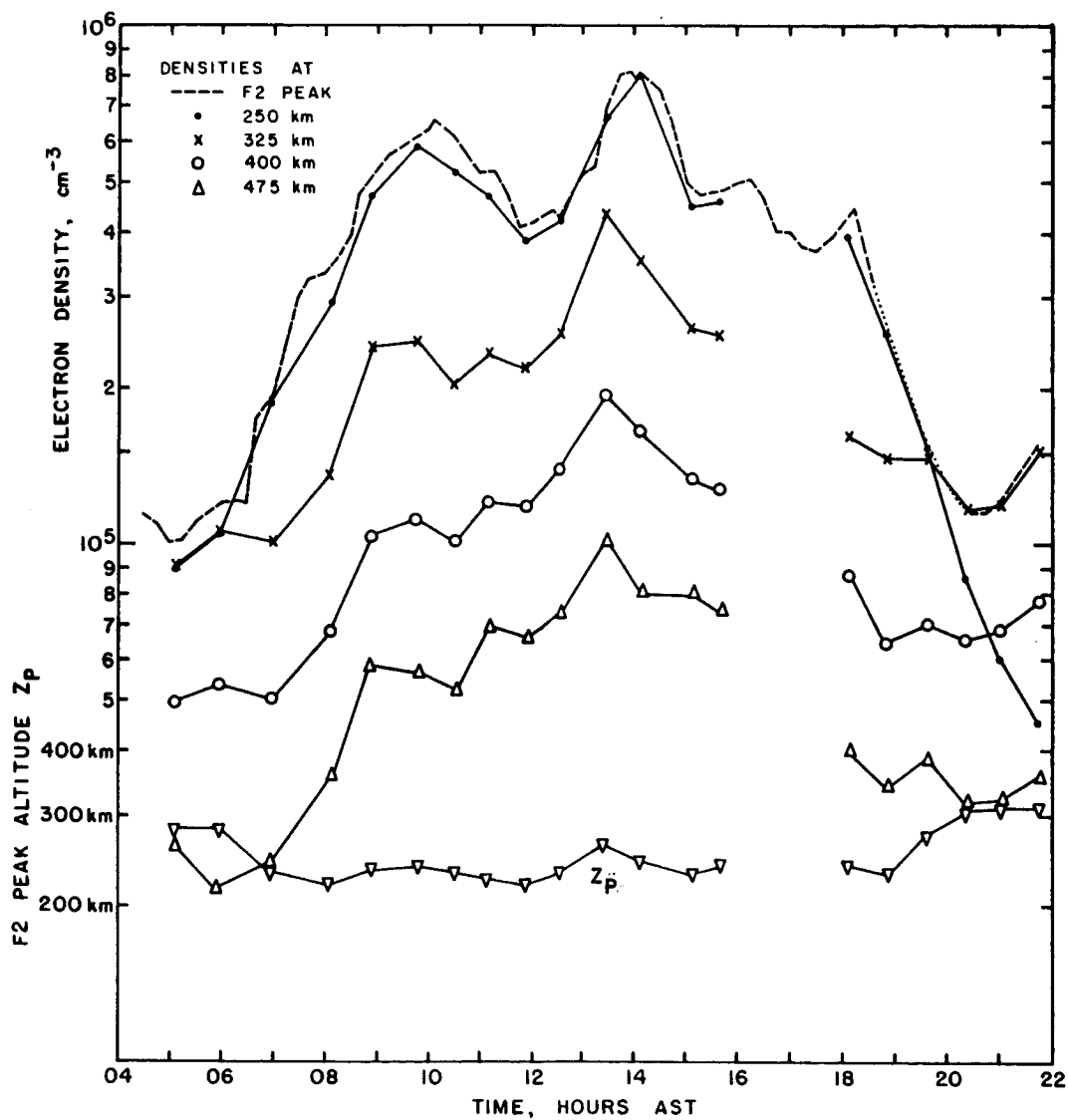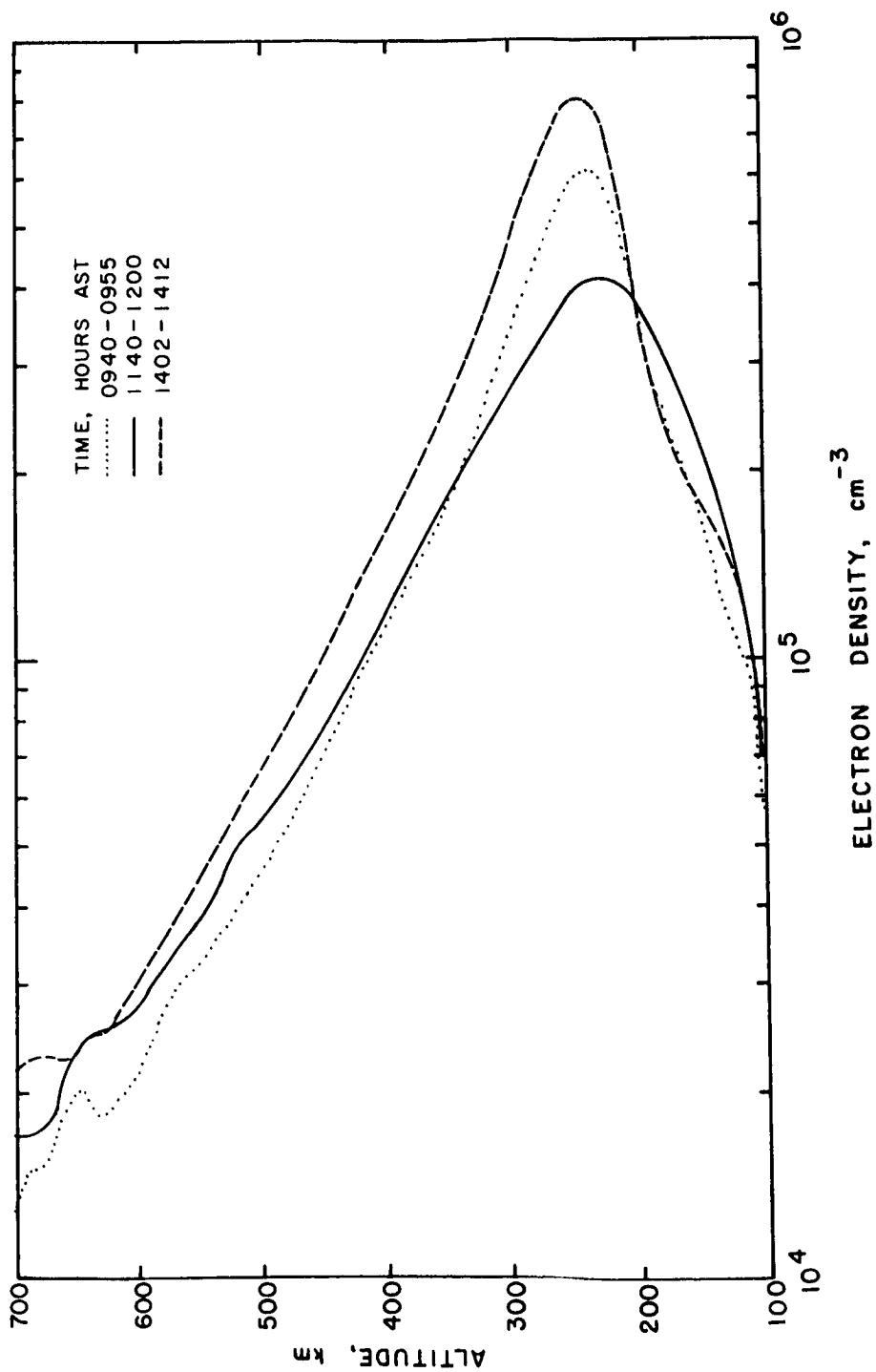FIGURE 6. ELECTRON AND ION TEMPERATURES AT ARECIBO ON DECEMBER 22, 1965.

FIGURE 7.   ARECIBO ELECTRON DENSITIES ON
DECEMBER 29, 1965.

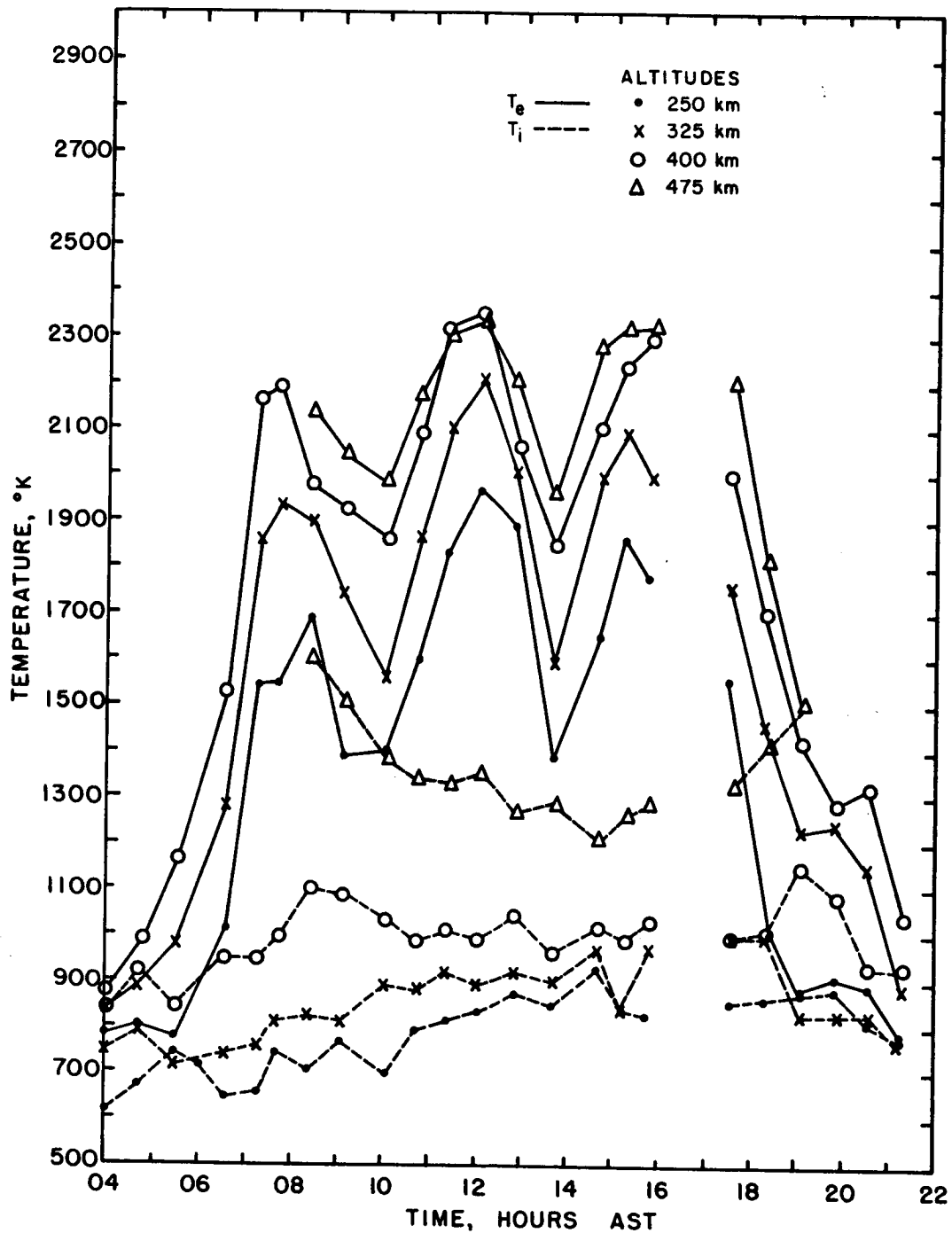FIGURE 8. ELECTRON DENSITY PROFILE AT ARECIBO ON
DECEMBER 29, 1965.

FIGURE 9.   ELECTRON AND ION TEMPERATURES AT
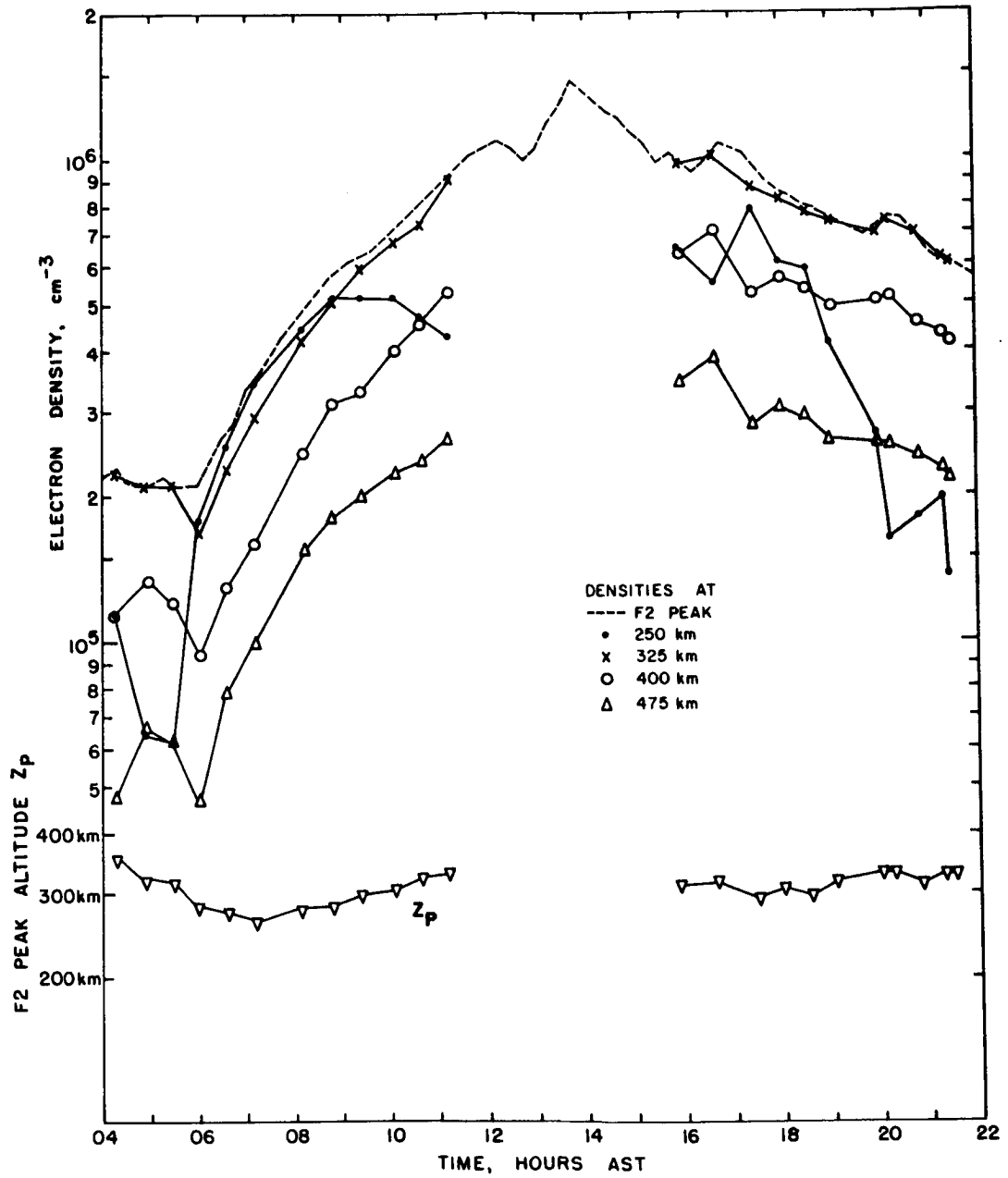ARECIBO   ON   DECEMBER   29, 1965.

FIGURE 10.   ARECIBO   ELECTRON   DENSITIES   ON
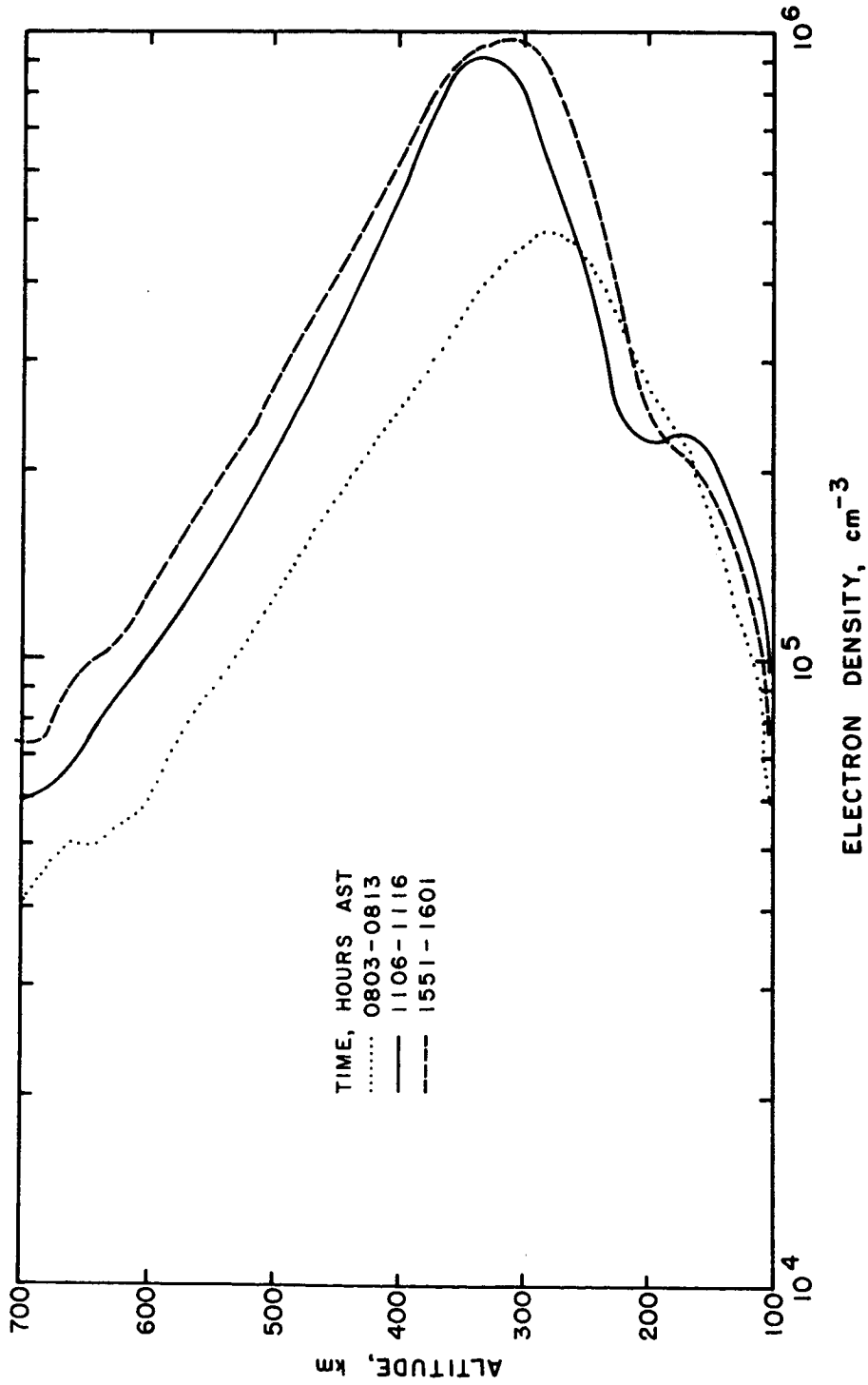JULY   22,   1966.

-41-

FIGURE II.   ELECTRON DENSITY PROFILES AT ARECIBO ON
JULY 22, 1965.
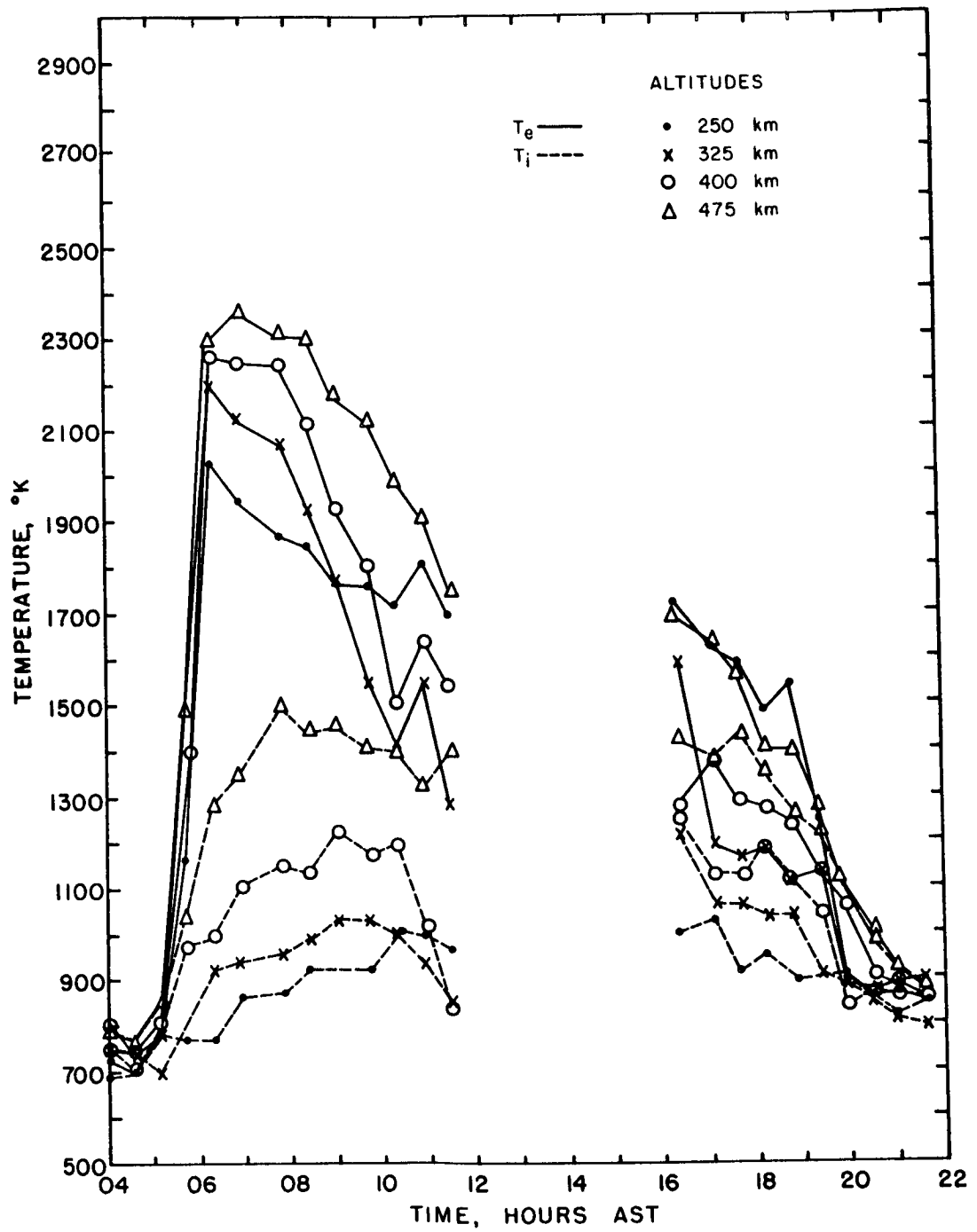
FIGURE 12.   ELECTRON   AND   ION   TEMPERATURES   AT
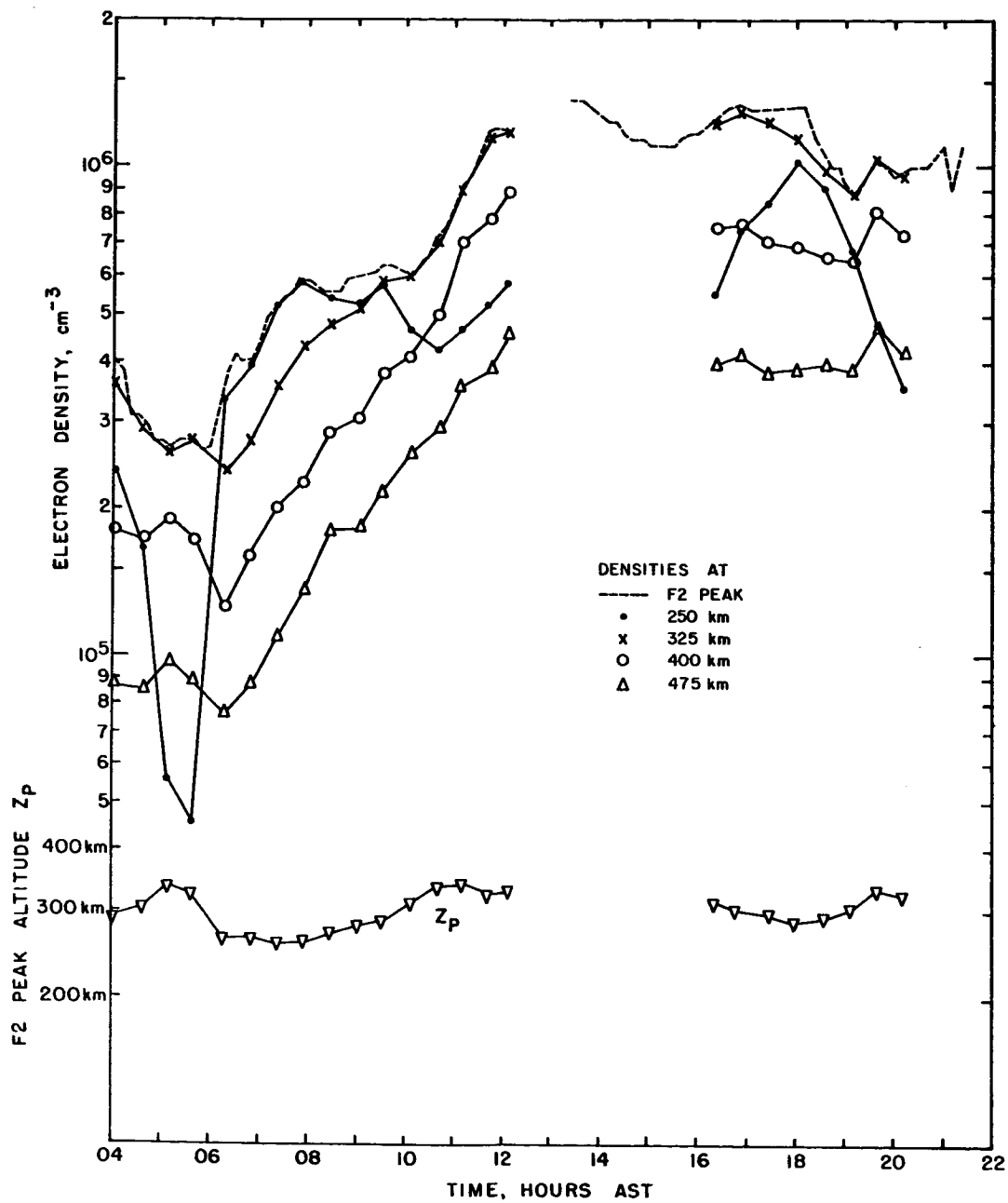   ARECIBO   ON   JULY   22,   1966.

FIGURE 13. ARECIBO ELECTRON DENSITIES ON JULY 30, 1966.
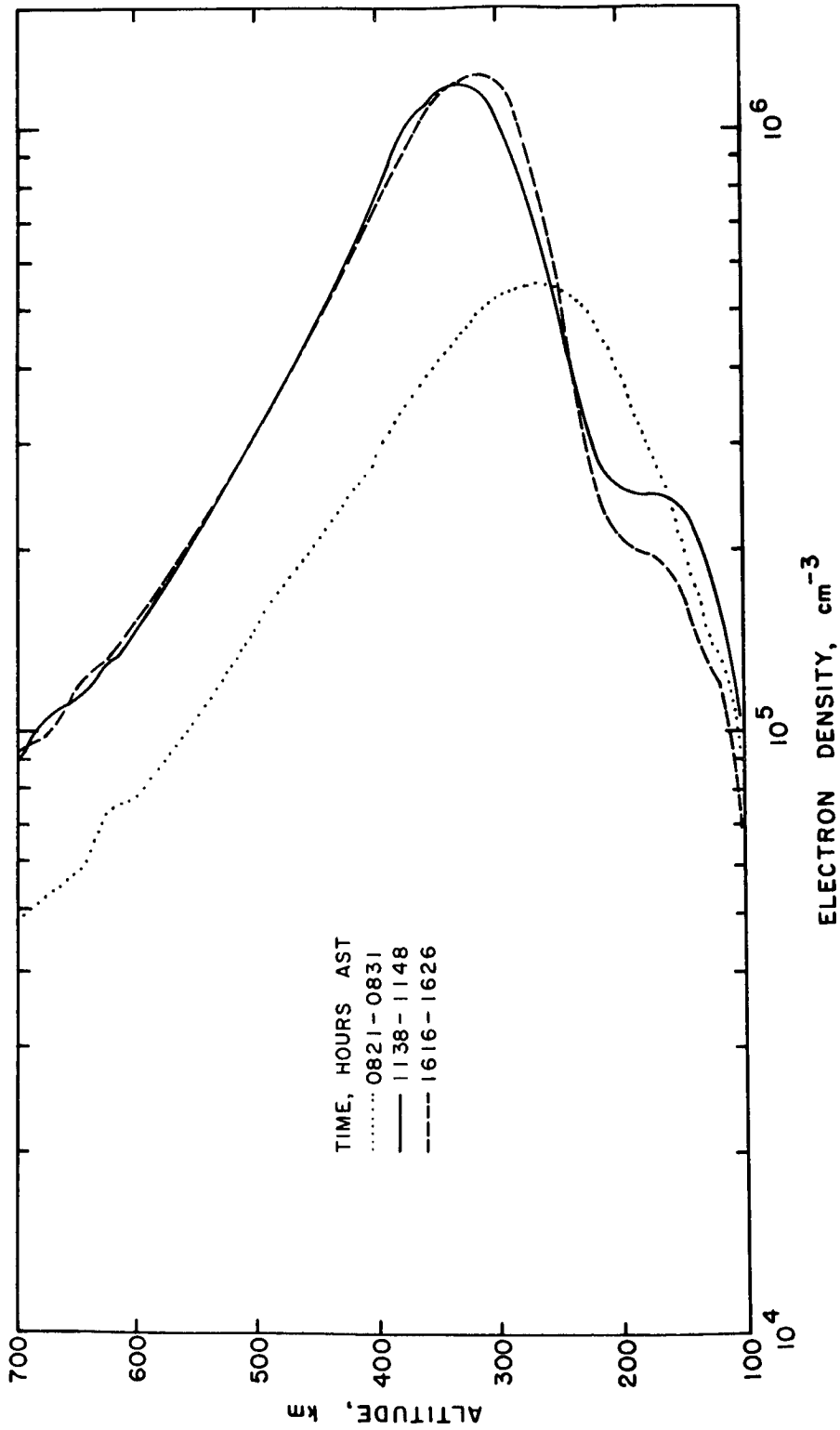
FIGURE 14. ELECTRON DENSITY PROFILES AT ARECIBO ON
JULY 30, 1965.
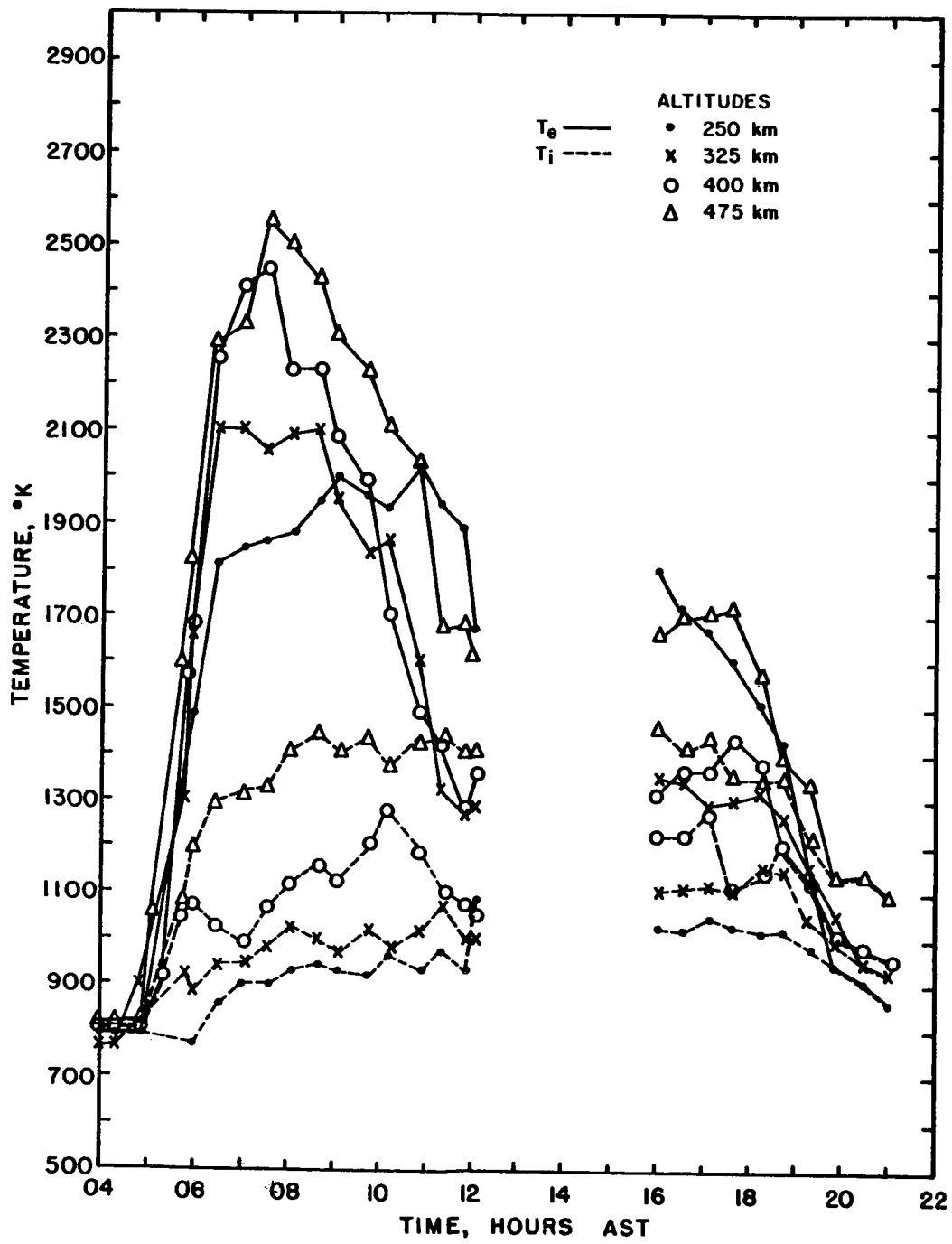
FIGURE I5.   ELECTRON   AND   ION   TEMPERATURES   AT
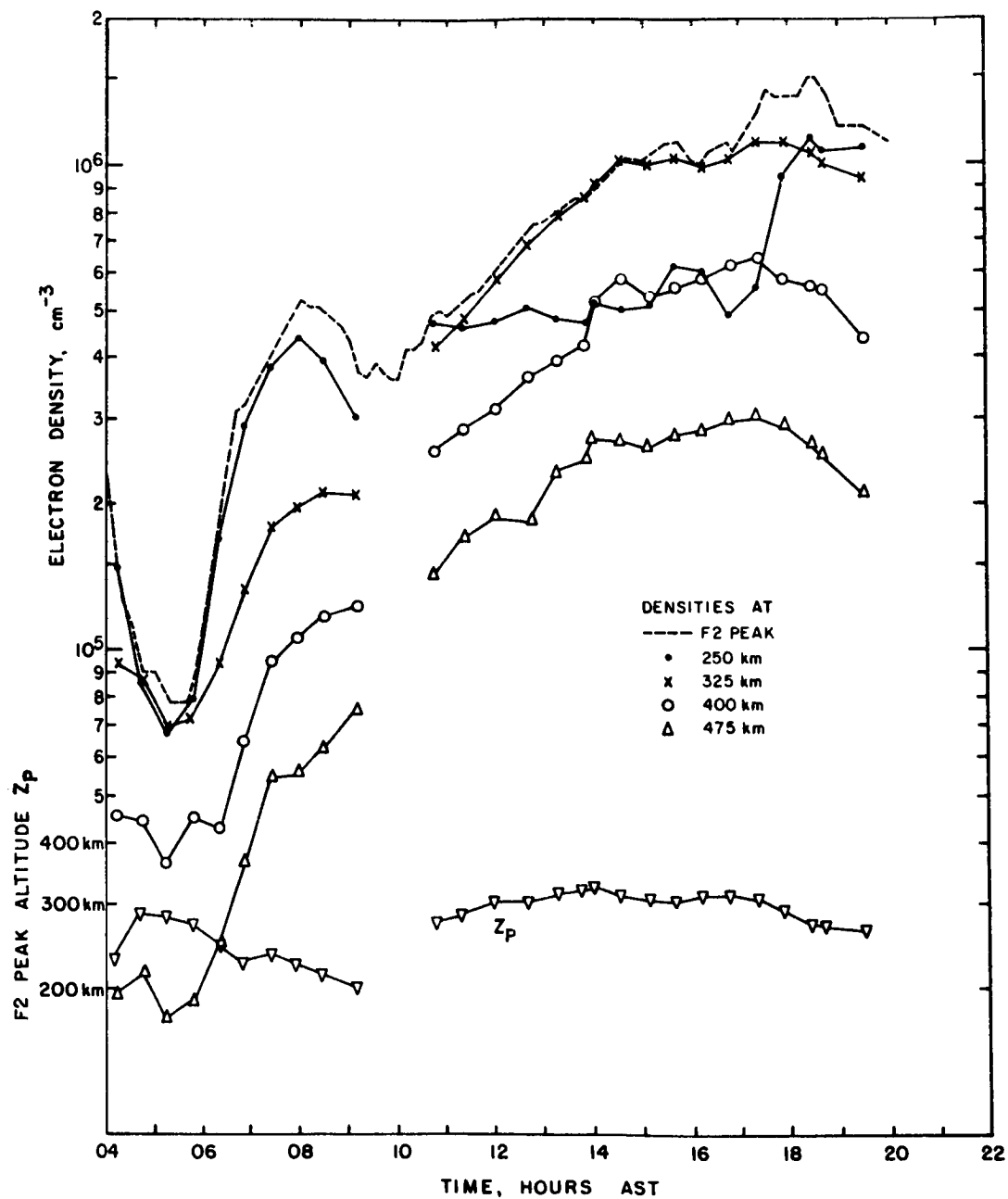   ARECIBO   ON   JULY   30, 1966.

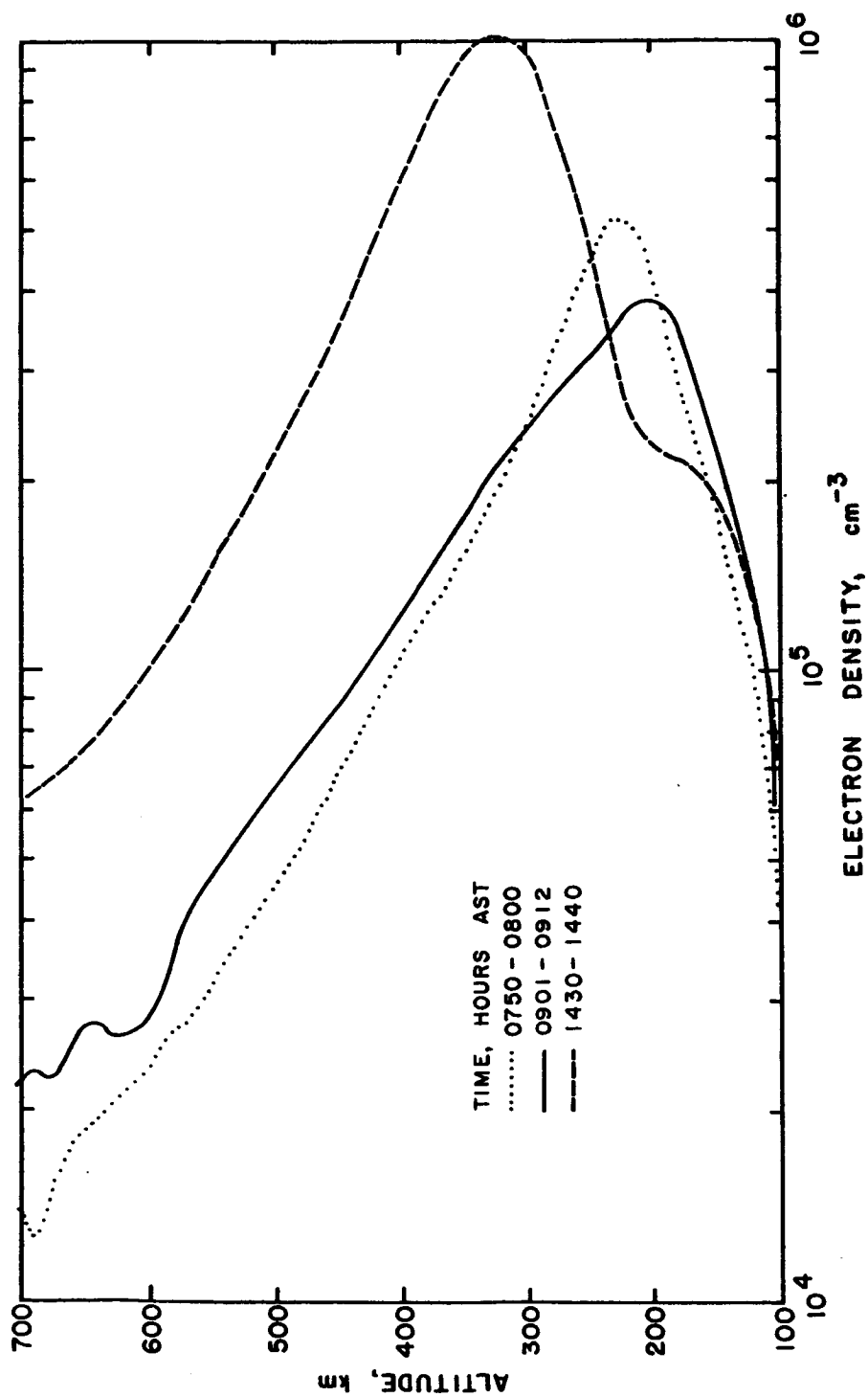FIGURE 16. ARECIBO ELECTRON DENSITIES ON
AUGUST 17, 1966.

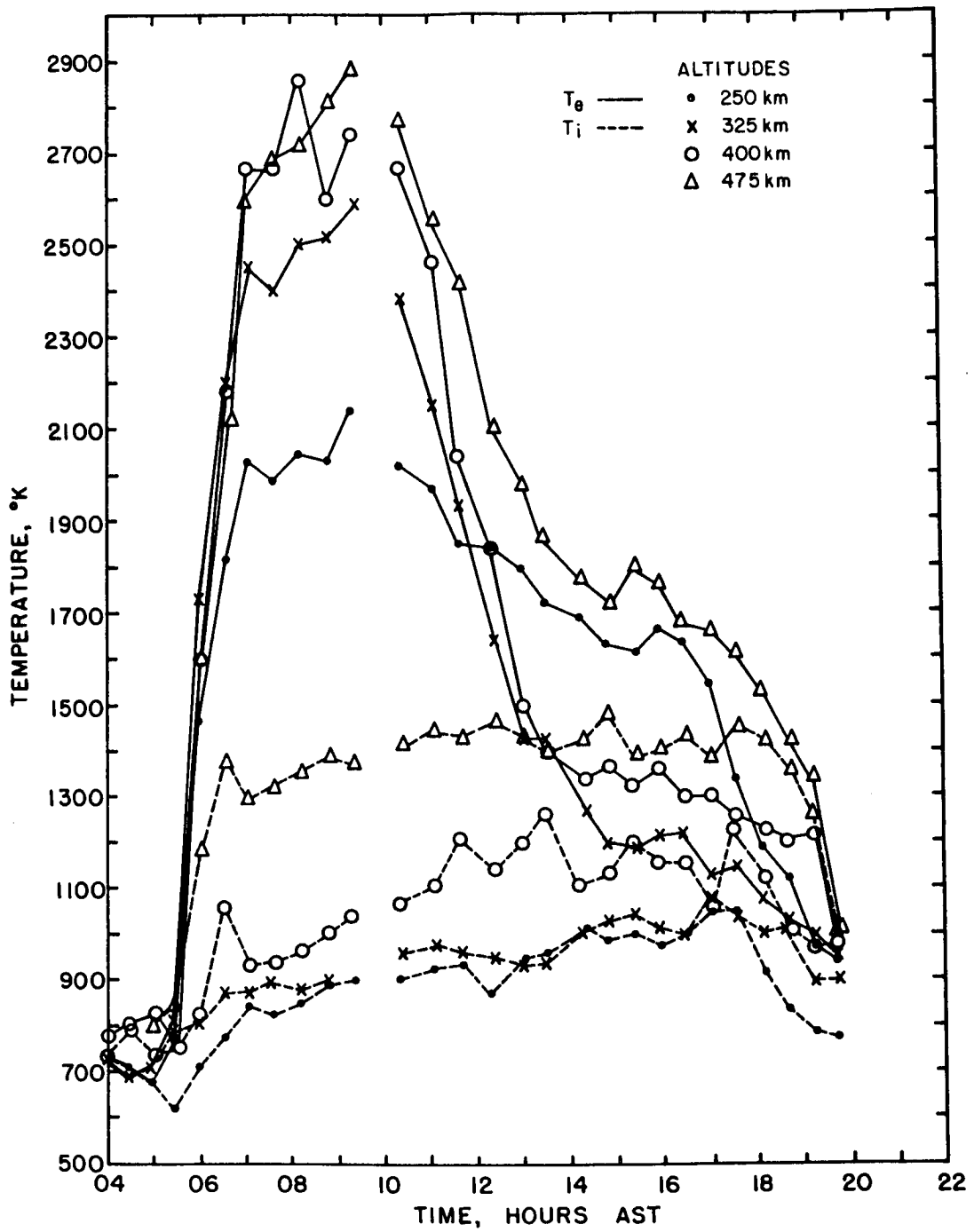FIGURE 17.   ELECTRON DENSITY PROFILES AT ARECIBO ON

AUGUST 17, 1965.

FIGURE 18. ELECTRON AND ION TEMPERATURES AT ARECIBO ON AUGUST 17, 1966.

3.4 Supporting Data

3.4.1 San Juan Magnetograms

The horizontal, H, and declination, D, components of the geomagnetic field at San Juan, Puerto Rico were scaled from magnetograms and redrawn in Figures 19 through 23. Several days about each experimental period are plotted together, except for the missing July 21 and 22 data. Increasing H is northward, and increasing D is westward. The units are gammas where one gamma equals 10^{-5} gauss or 10^{-9} webers/m^2.

The current system responsible for the daytime geomagnetic field fluctuations is an elliptical shaped counterclockwise flow pattern whose focus passes slightly to the north of Puerto Rico. Since an eastward current increases H and a northward one increases D, we should expect a positive increase in H symmetrical about midday and a decrease of D followed an increase sinusoidal about midday.

December 14 and 15 were magnetically quiet days, and these data can be used as a standard for the other winter days. The general pattern is seen to be an increase of H centered near 08 to 09 hours AST and a smaller decrease at 14 to 15 hours. D is a minimum near 10 to 11 hours AST and a maximum near 14 to 15 hours. On December 21 and 22, however, the field shows departures from this description, particularly H on December 22. On December 28 and 29, H decreases sharply after 12 hours AST. The phase of the variations differs by one or two hours from day to day on all the magnetograms.

During the summer of 1966, excursions of D were generally larger than those of the previous winter, especially on July 30.

FIGURE 19. VALUES OF HORIZONTAL, H, AND WESTWARD, D, COMPONENTS ABOVE THEIR REFERENCE LINES OF THE GEOMAGNETIC FIELD FROM SAN JUAN MAGNETO-GRAMS.

FIGURE 20. VALUES OF HORIZONTAL, H, AND WESTWARD, D, COMPONENTS ABOVE THEIR REFERENCE LINES OF THE GEOMAGNETIC FIELD FROM SAN JUAN MAGNETO-GRAMS.

FIGURE 21. VALUES OF HORIZONTAL, H, AND WESTWARD, D, COMPONENTS ABOVE THEIR REFERENCE LINES OF THE GEOMAGNETIC FIELD FROM SAN JUAN MAGNETO-GRAMS.
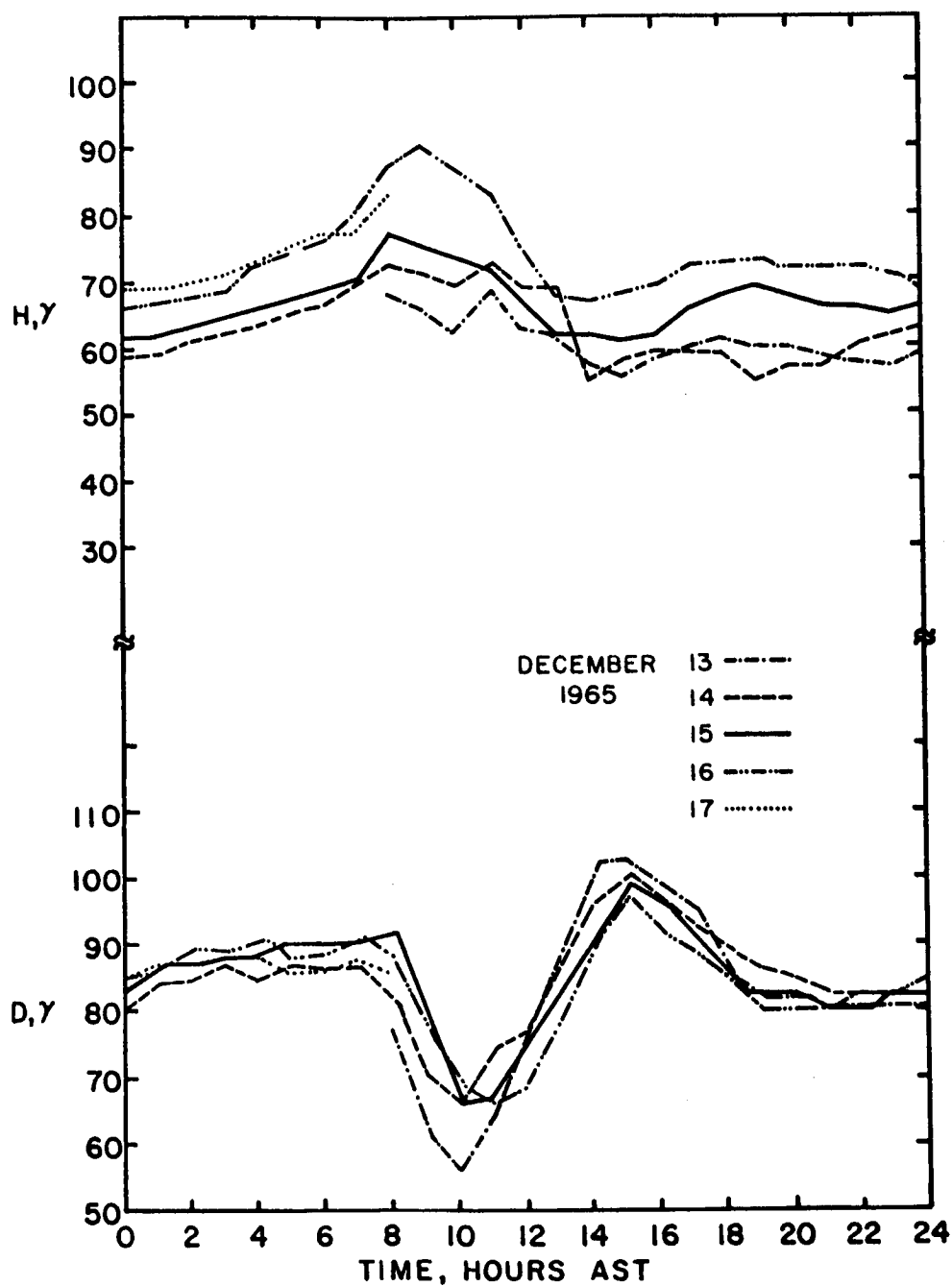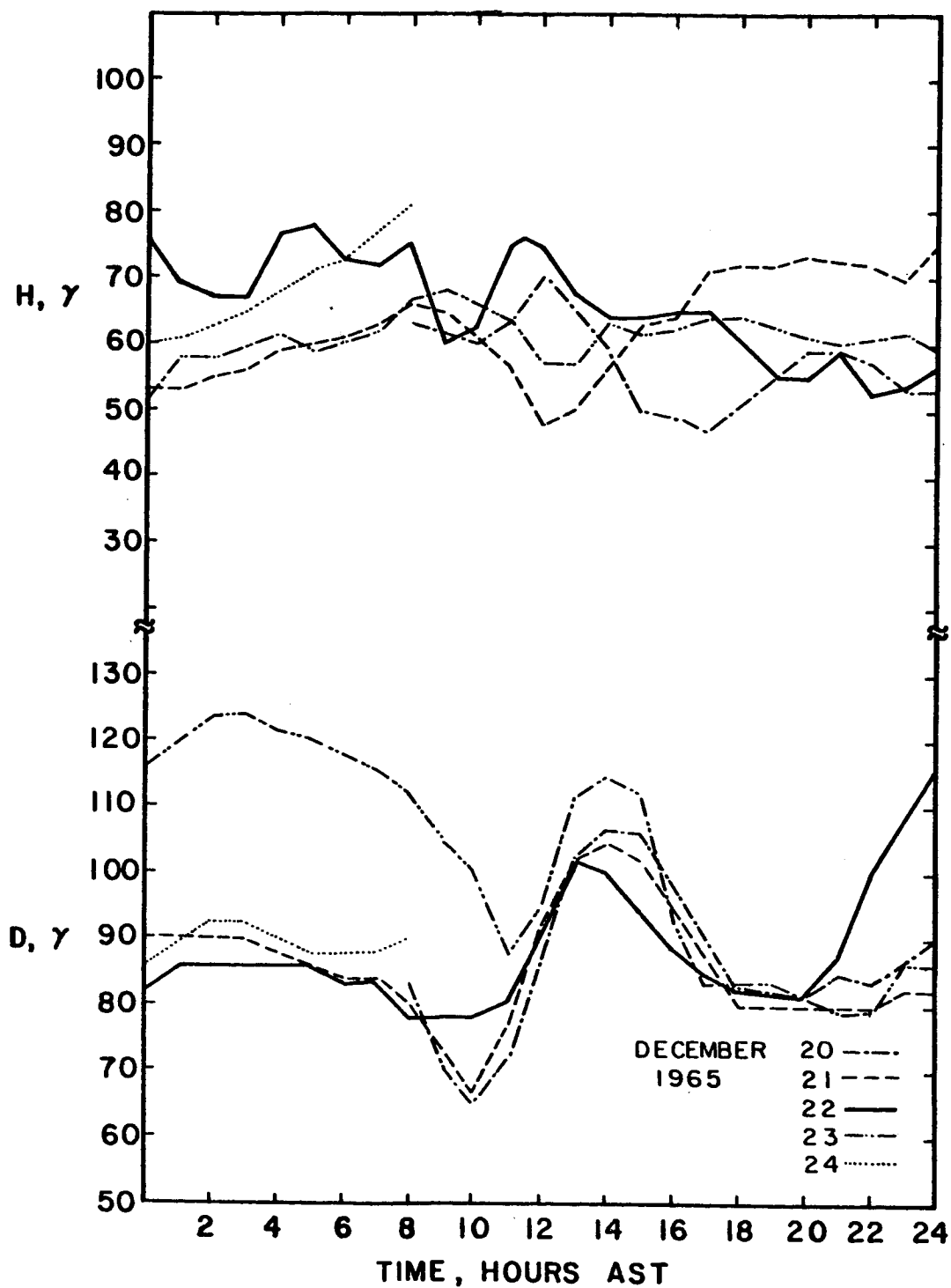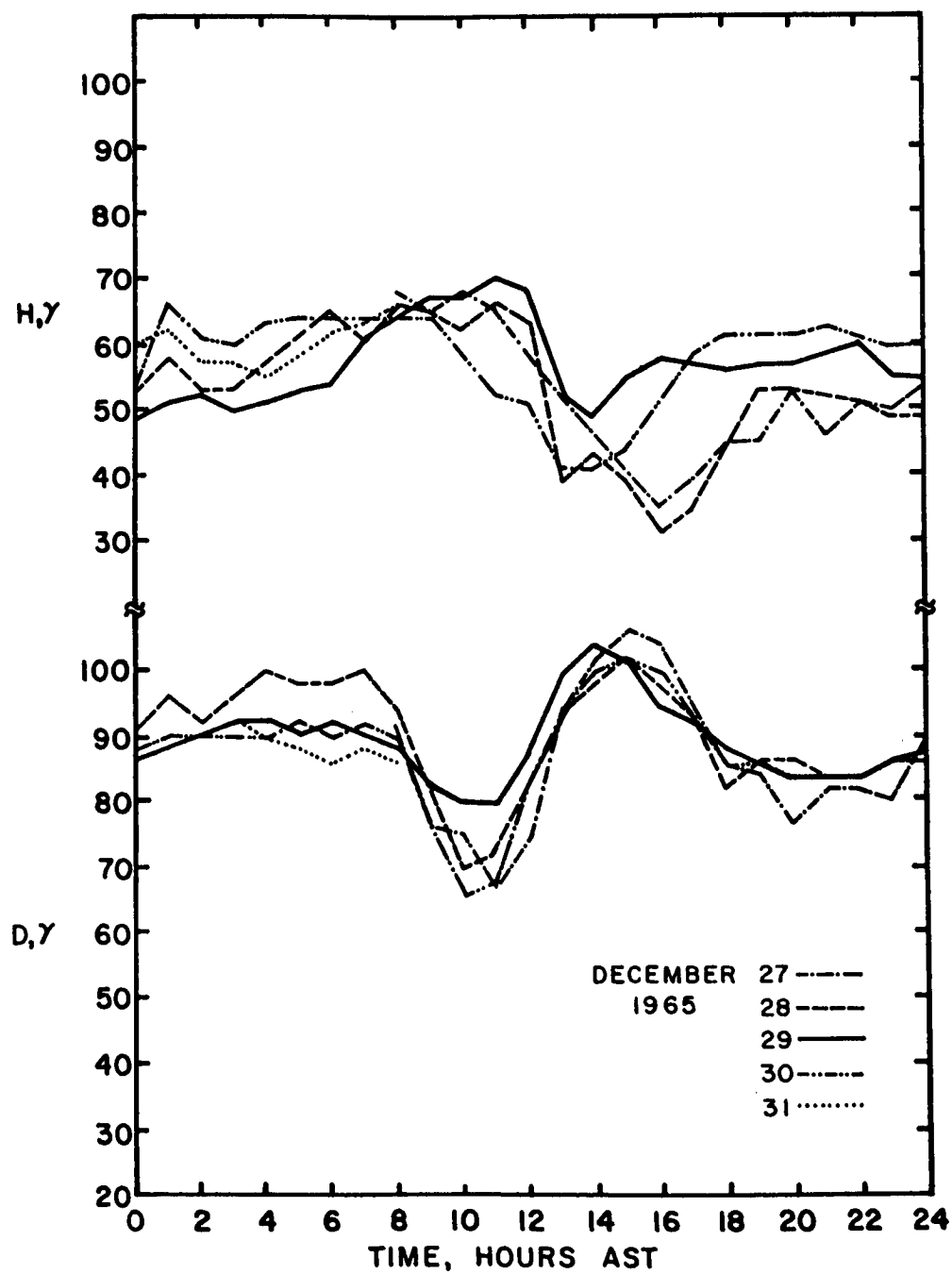
FIGURE 22. VALUES OF HORIZONTAL, H, AND WESTWARD, D, COMPONENTS ABOVE THEIR REFERENCE LINES OF THE GEOMAGNETIC FIELD FROM SAN JUAN MAGNETO-GRAMS.
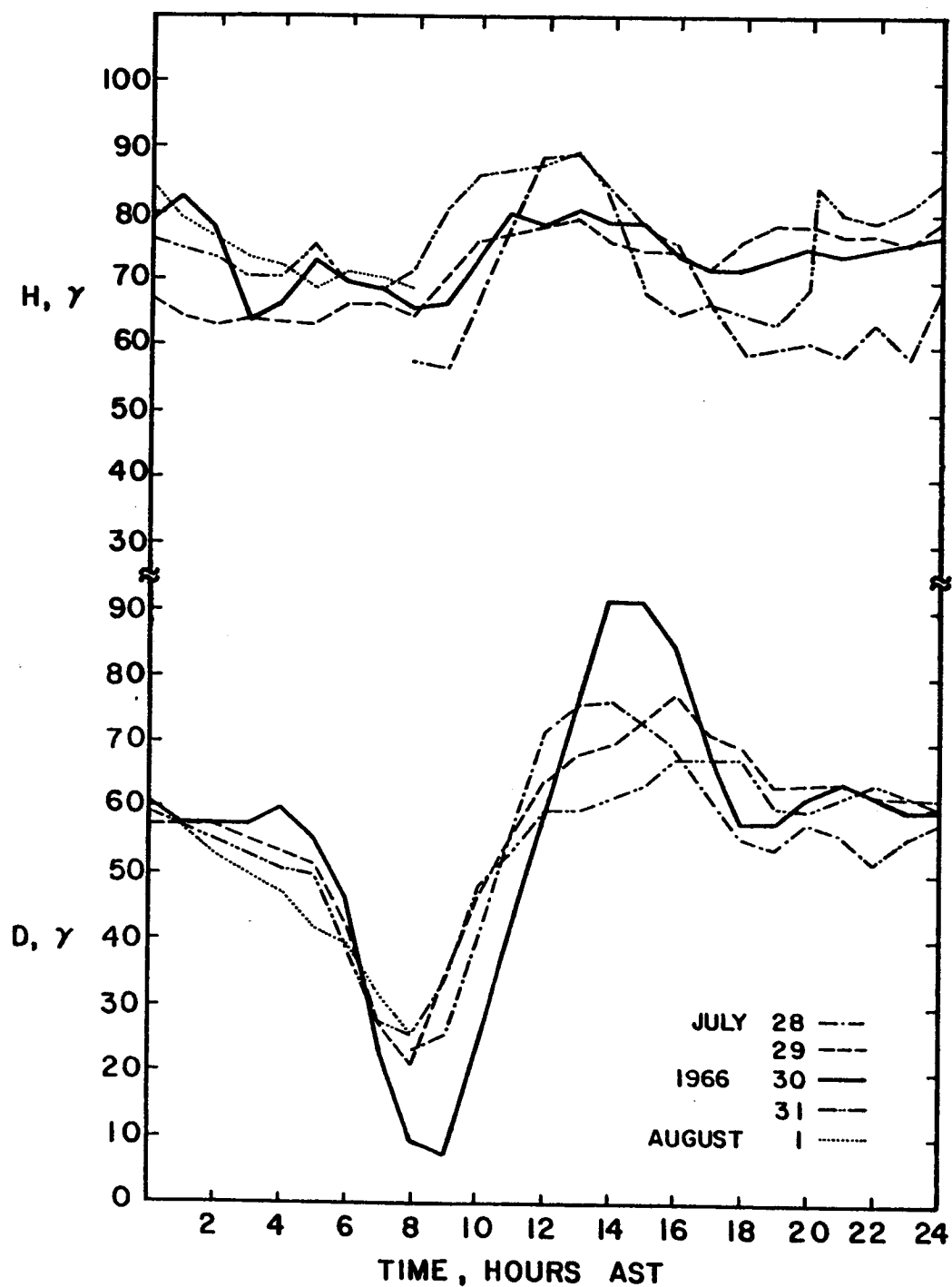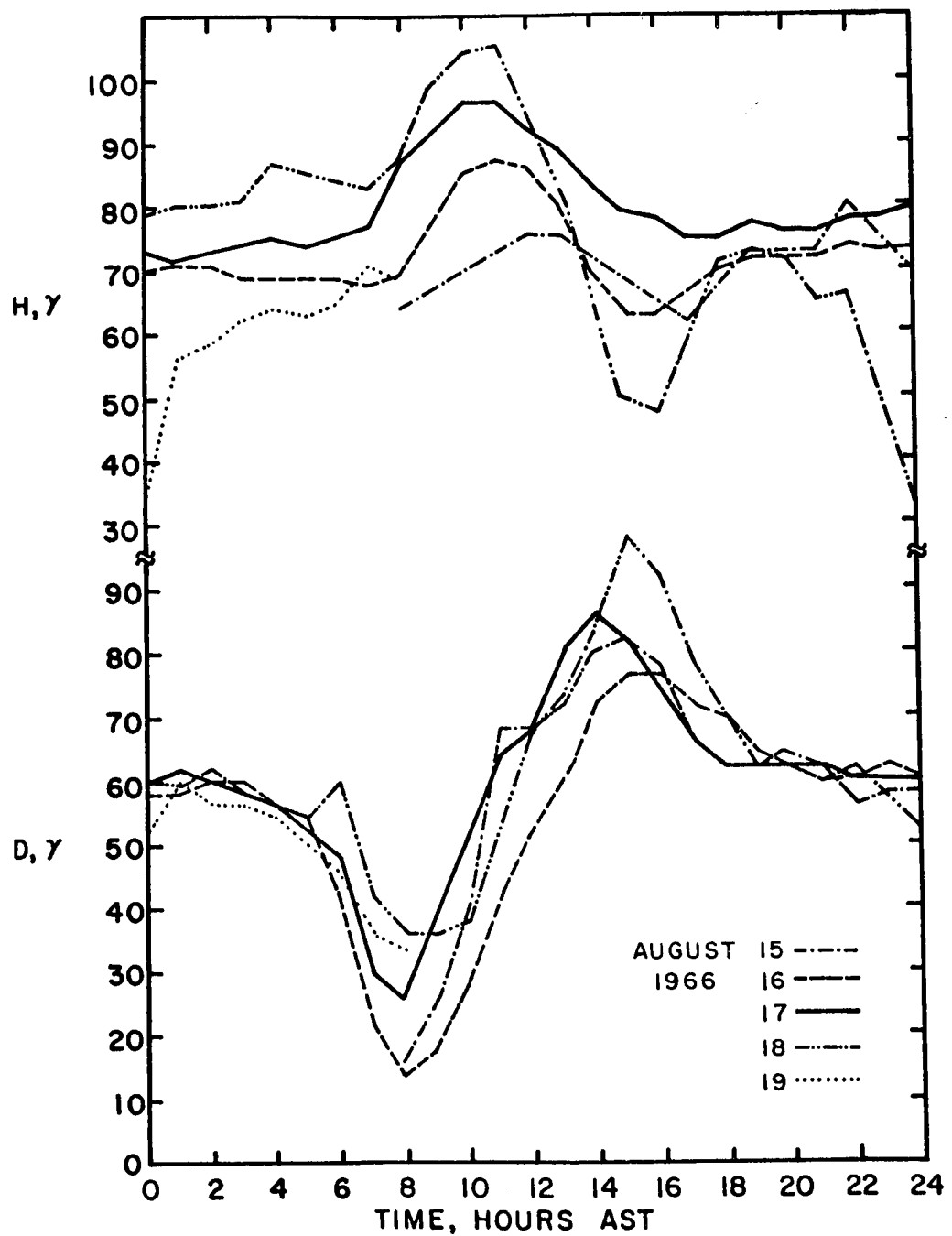
FIGURE 23. VALUES OF HORIZONTAL, H, AND WESTWARD, D, COMPONENTS ABOVE THEIR REFERENCE LINES OF THE GEOMAGNETIC FIELD FROM SAN JUAN MAGNET-OGRAMS.

H changes were small on July 29 and 30 and were larger on August 16 and 17. The phase of D in summer seems to be more variable from day to day than in winter, and the morning increase of H occurs about four hours later in summer.

3.4.2 Spaced Ionosondes

Plasma frequencies at the F2 peak were scaled from ionosondes at Arecibo and eight other stations listed in Table 2 on the day and preceding day of each experiment. These data are shown in Figures 24 through 39. The F2 region peak plasma frequency, f_oF2, is related to the peak electron density, N_{max}, by

$$N_{max} = 1.24 \times 10^4 \left[f_o F2 \ (mc) \right]^2 \ \text{electrons/cm}^3 .$$

Arecibo, Jamaica, and Mexico City are all approximately at the same geographic latitude (18° N) and geomagnetic latitude (30° N) so that they are useful in separating fluctuations occuring at local times from those at universal times. Grand Bahama Island, Cape Kennedy, Wallops Island, and Ottawa lie near the 75th meridian slightly to the west of Arecibo and are useful in detecting possible traveling disturbances propagating north or south. White Sands is at the same magnetic latitude as Cape Kennedy and Grand Bahama Island (40° N), and Huancayo is on the magnetic equator. These stations form a grid of spaced ionosondes similar to Thome's (1966).

Judging from the fluctuations of f_oF2, the stations can be loosely separated into three groups according to magnetic latitude. The low latitude group consists of Arecibo, Jamaica, Mexico City and Huancayo. Grand Bahama Island, Cape Kennedy, and White Sands form the middle latitude group with magnetic latitudes about 40° N.

Table 2 Stations Forming Spaced Ionsonde Network

Station	Geographic Coordinates	Geomagnetic Latitude	Approximate Distance to Arecibo
Ottawa	45.4 N, 75.4 W	61.8 N	3240 km
Wallops Island	37.9 N, 75.5 W	53.6 N	2430 km
White Sands	32.3 N, 106.5 W	41.0 N	4770 km
Cape Kennedy	28.4 N, 80.6 W	42.4 N	1920 km
Grand Bahama Island	26.7 N, 78.4 W	40.6 N	1600 km
Mexico City	19.3 N, 99.5 W	27.6 N	3730 km
Arecibo	18.5 N, 67.2 W	31.7 N	---
Jamaica	17.0 N, 76.8 W	30.0 N	1120 km
Huancayo	12.0 S, 75.3 W	0.5 N	3635 km
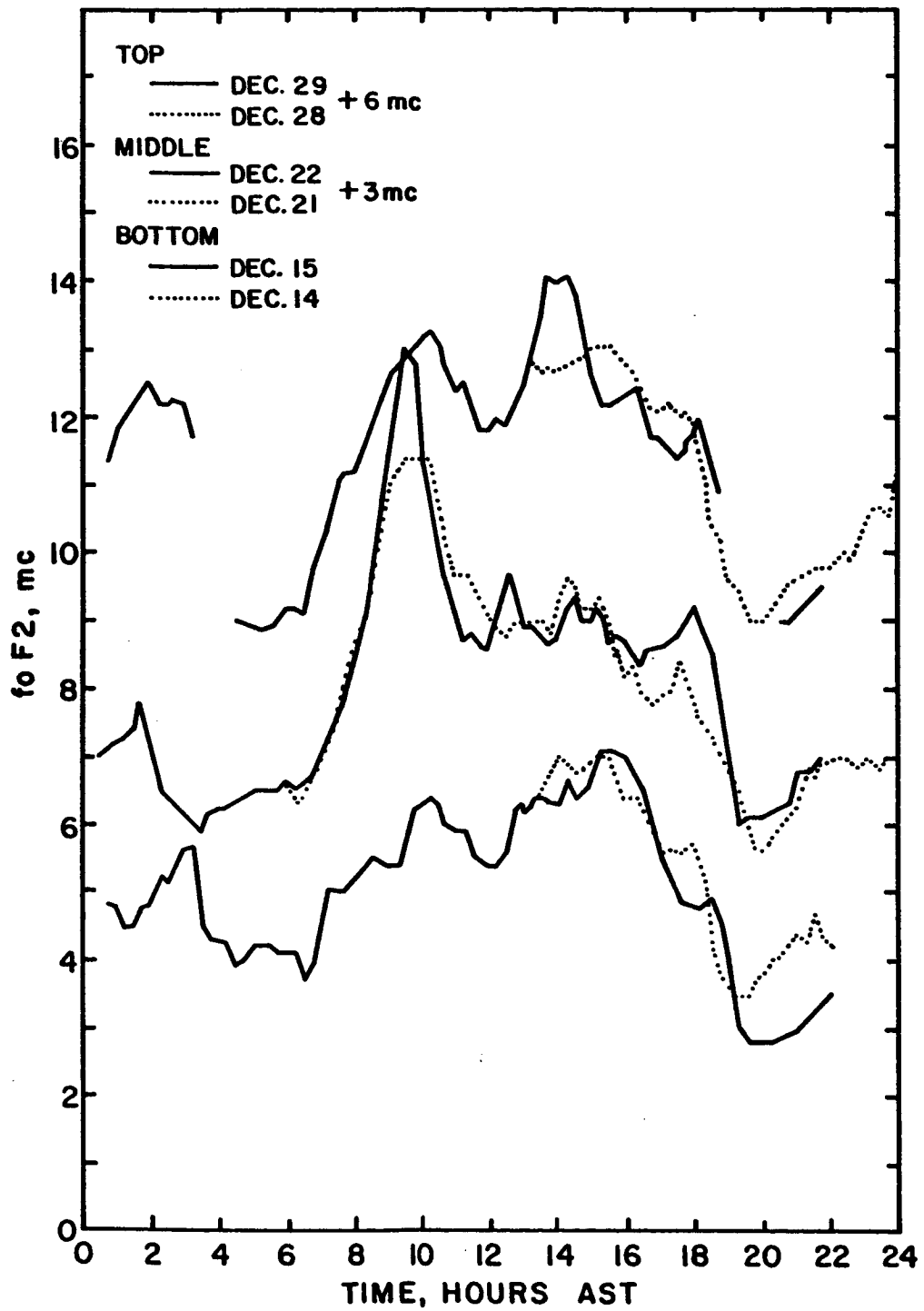
FIGURE 24. F2 PEAK PLASMA FREQUENCIES AT ARECIBO FOR WINTER, 1965.

FIGURE 25. F2 PEAK PLASMA FREQUENCIES AT
ARECIBO FOR SUMMER, 1966.
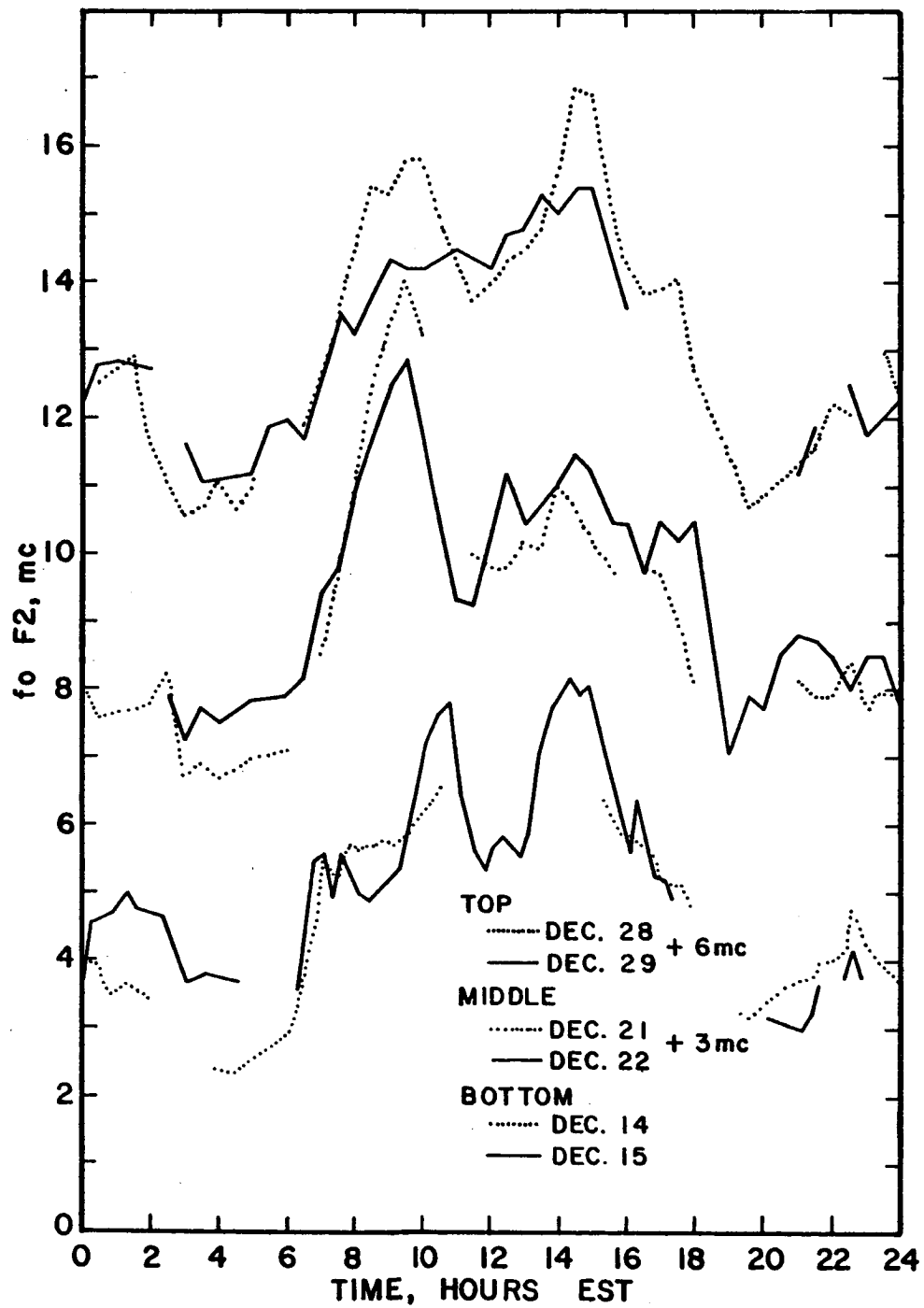
FIGURE 26. F2 PEAK PLASMA FREQUENCIES AT
JAMAICA   FOR   WINTER, 1965.

FIGURE 27. F2 PEAK PLASMA FREQUENCIES AT
JAMAICA FOR SUMMER, 1966
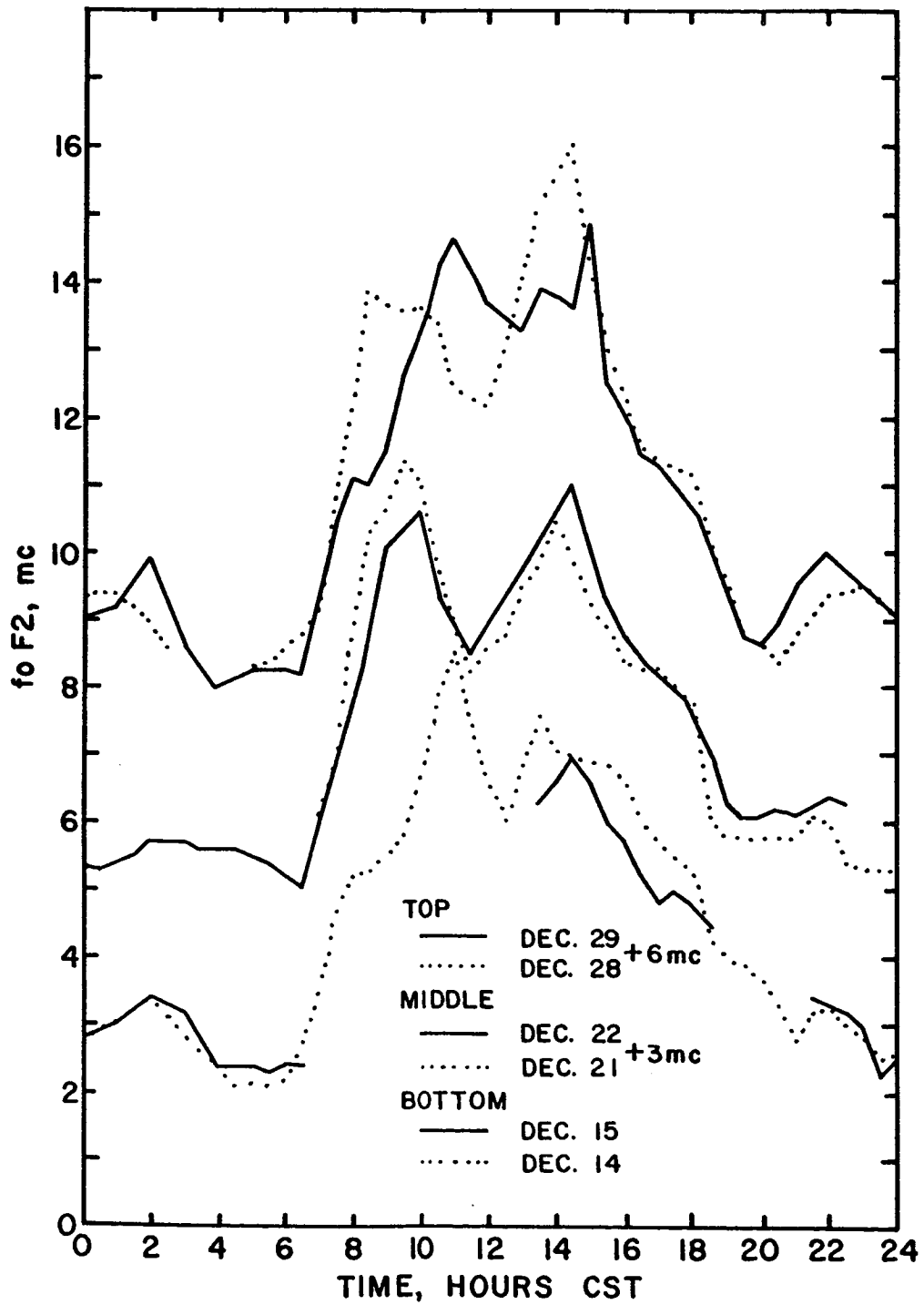
FIGURE 28. F2 PEAK PLASMA FREQUENCIES AT MEXICO FOR WINTER, 1965
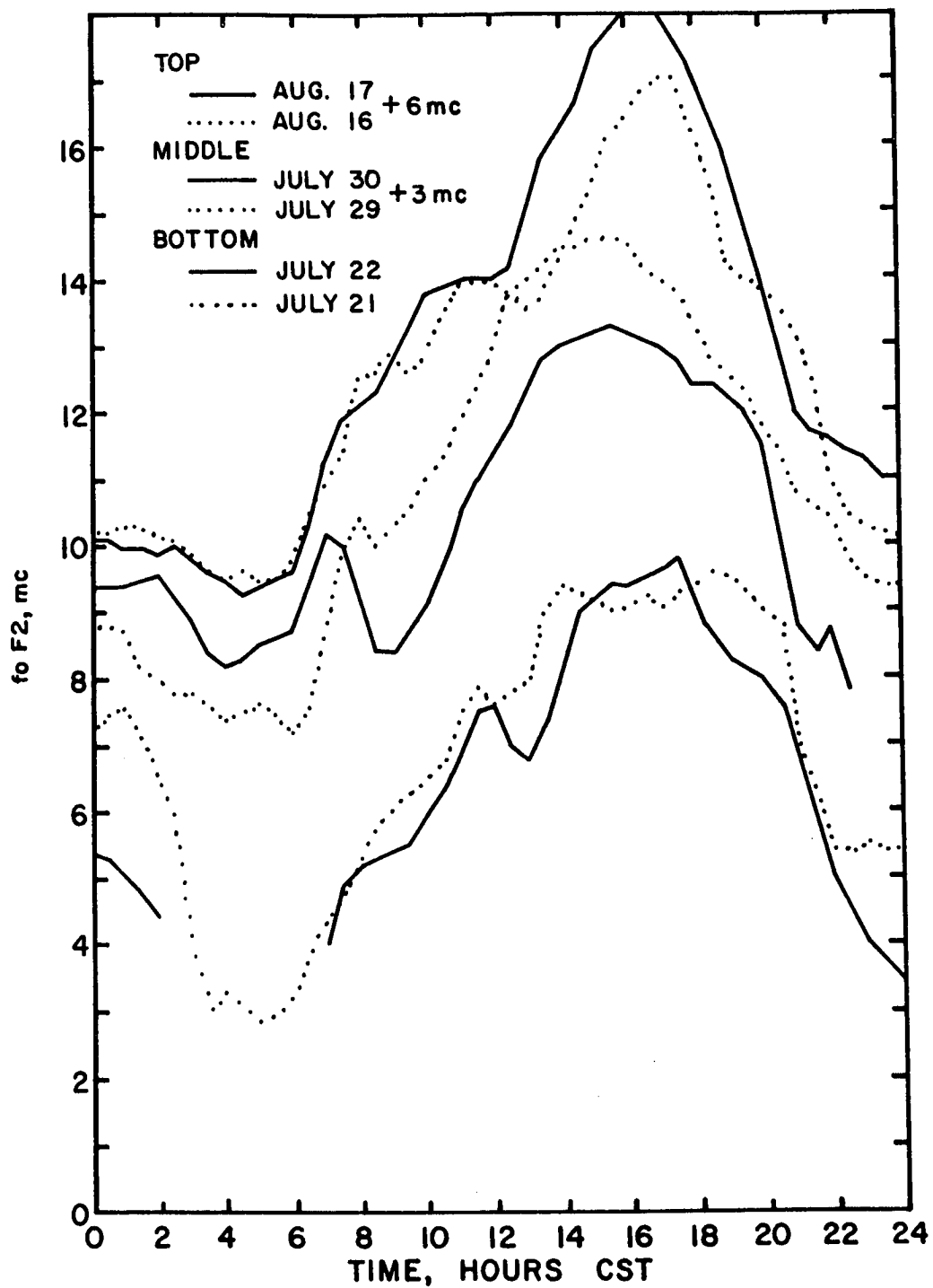
FIGURE 29. F2 PEAK PLASMA FREQUENCIES AT
MEXICO CITY FOR SUMMER, 1966
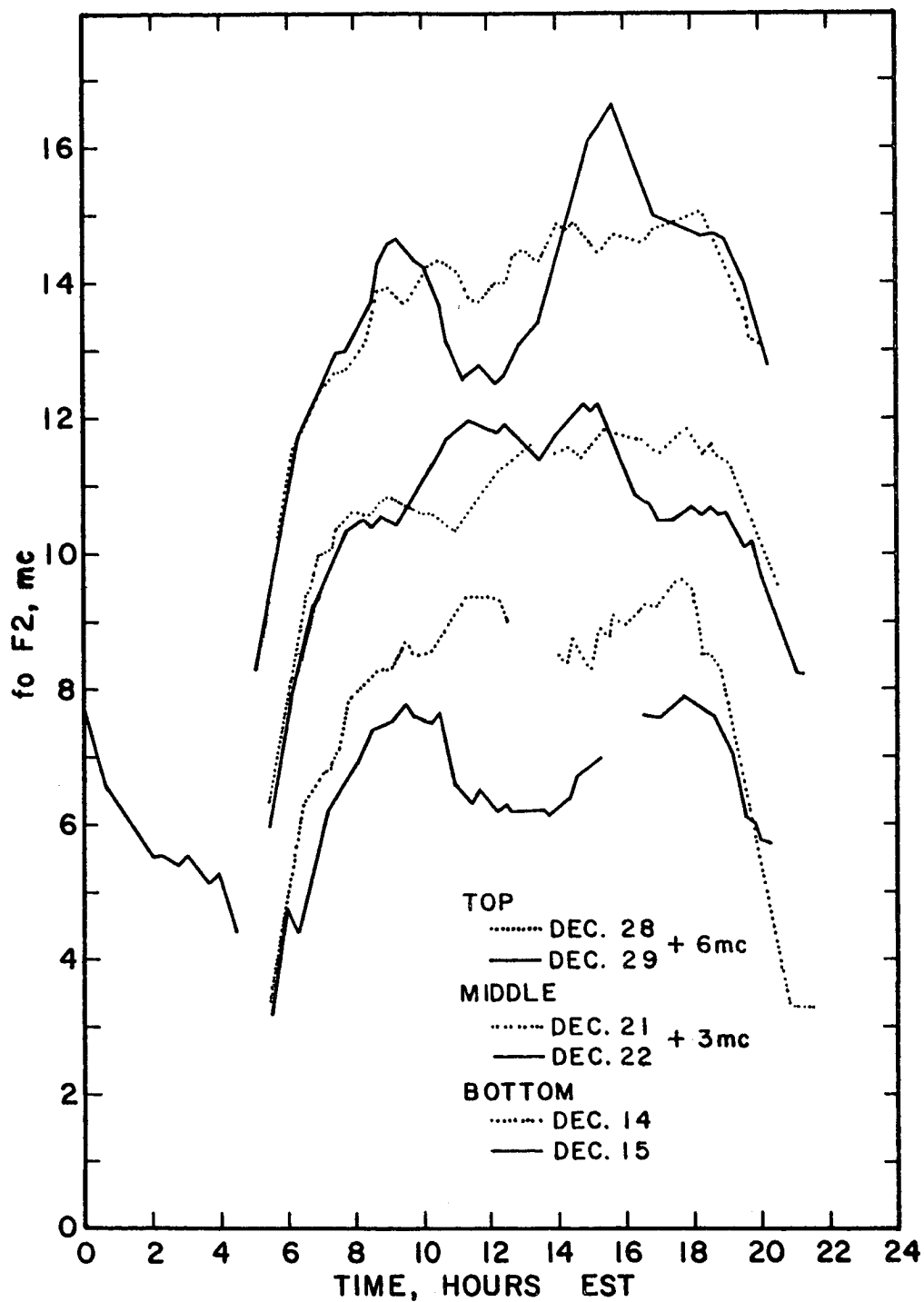
FIGURE 30. F2 PEAK PLASMA FREQUENCIES AT HUANCAYO FOR WINTER, 1965.
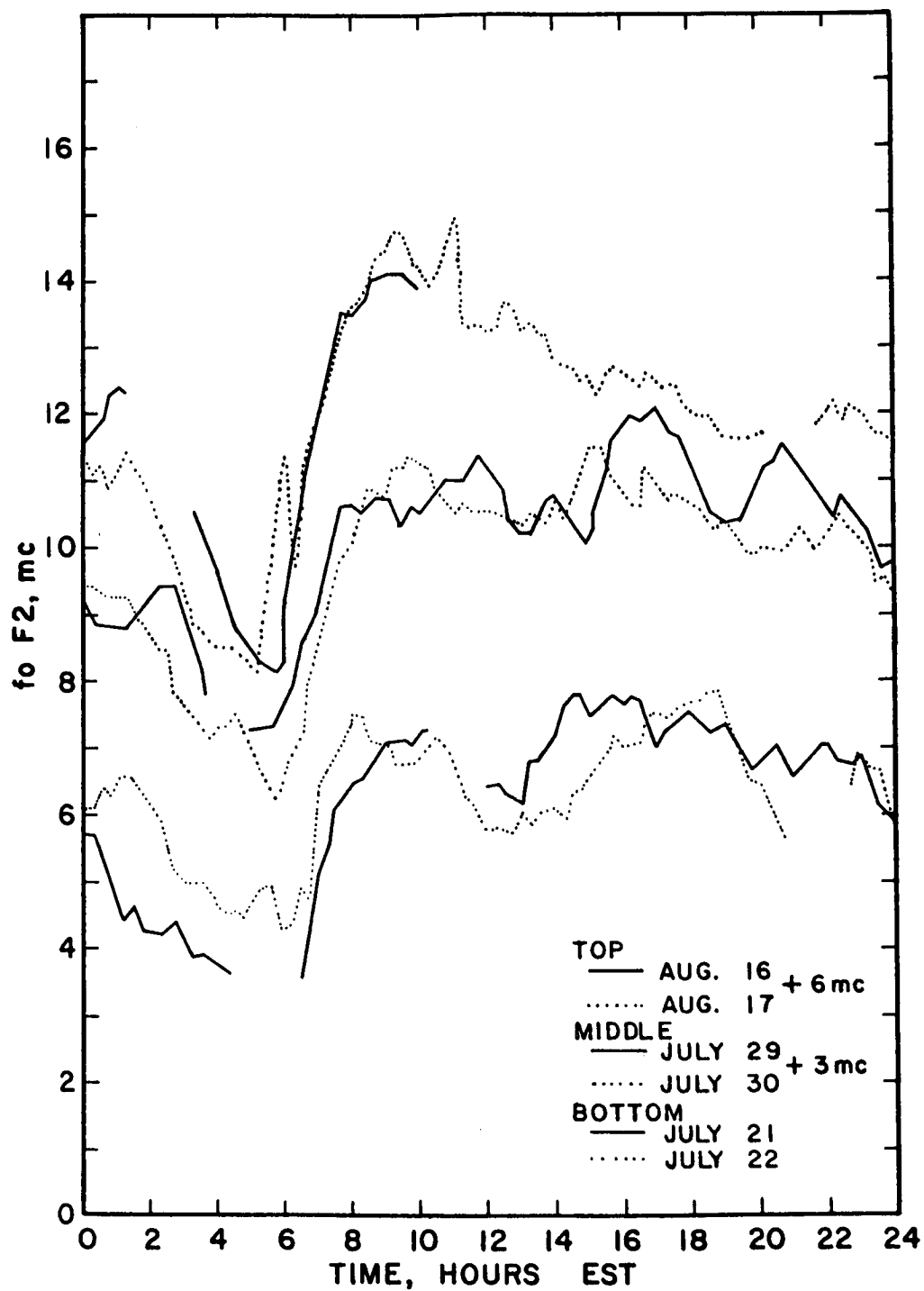
FIGURE 31. F2 PEAK PLASMA FREQUENCIES AT HUANCAYO FOR SUMMER, 1966.
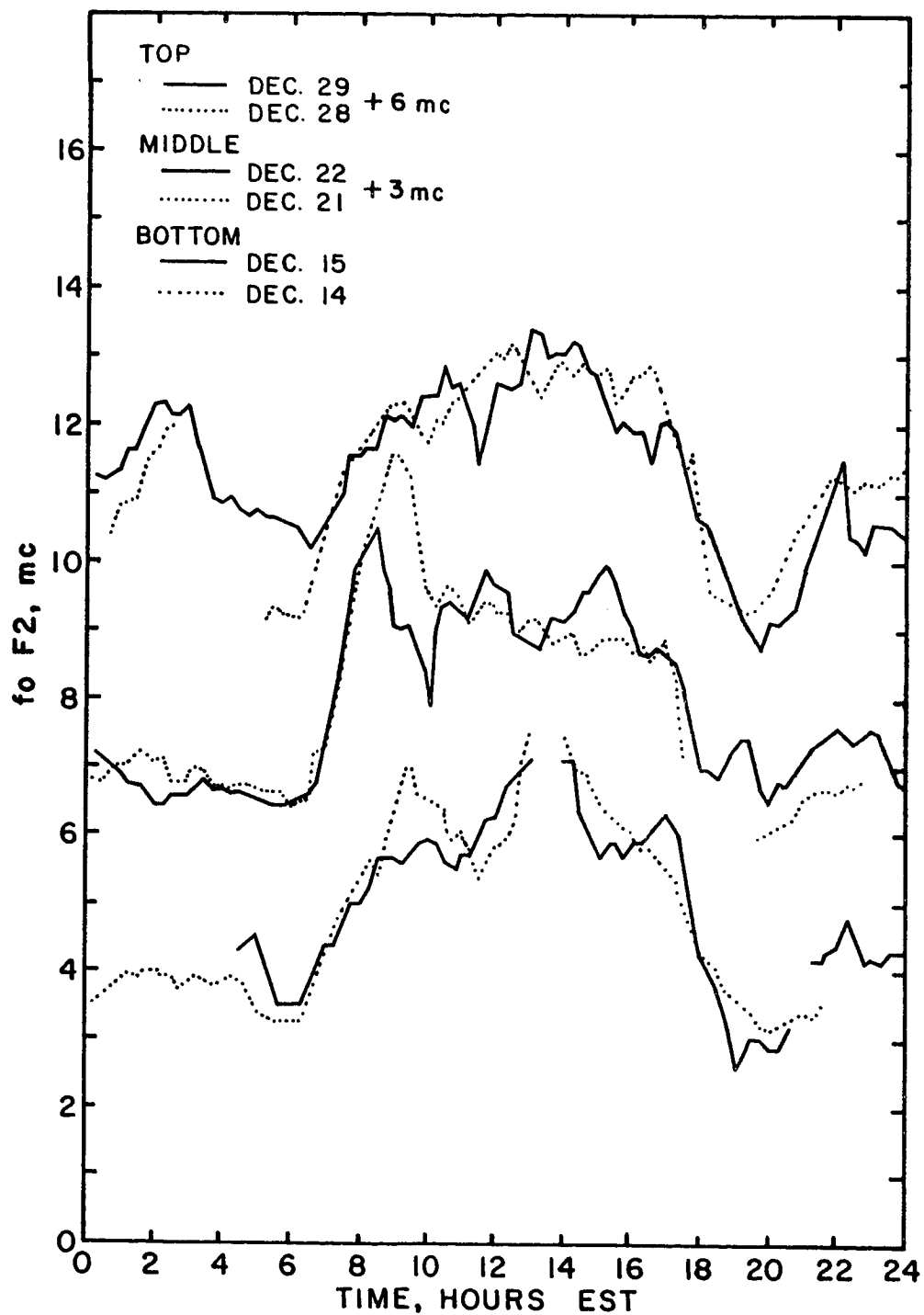
FIGURE 32. F2 PEAK PLASMA FREQUENCIES AT GRAND BAHAMA ISLAND FOR WINTER, 1965
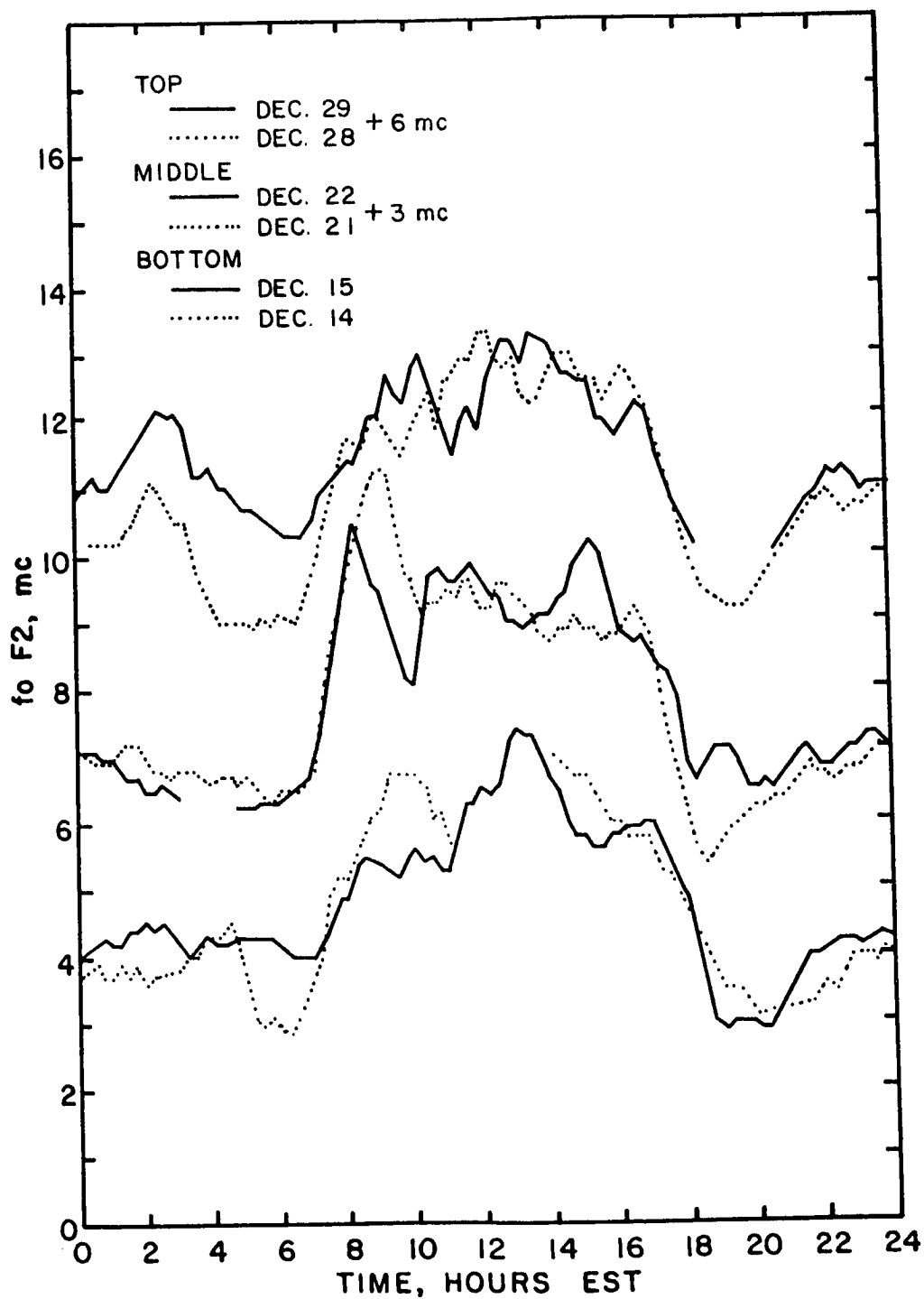
FIGURE 33. F2 PEAK PLASMA FREQUENCIES AT CAPE KENNEDY FOR WINTER, 1965
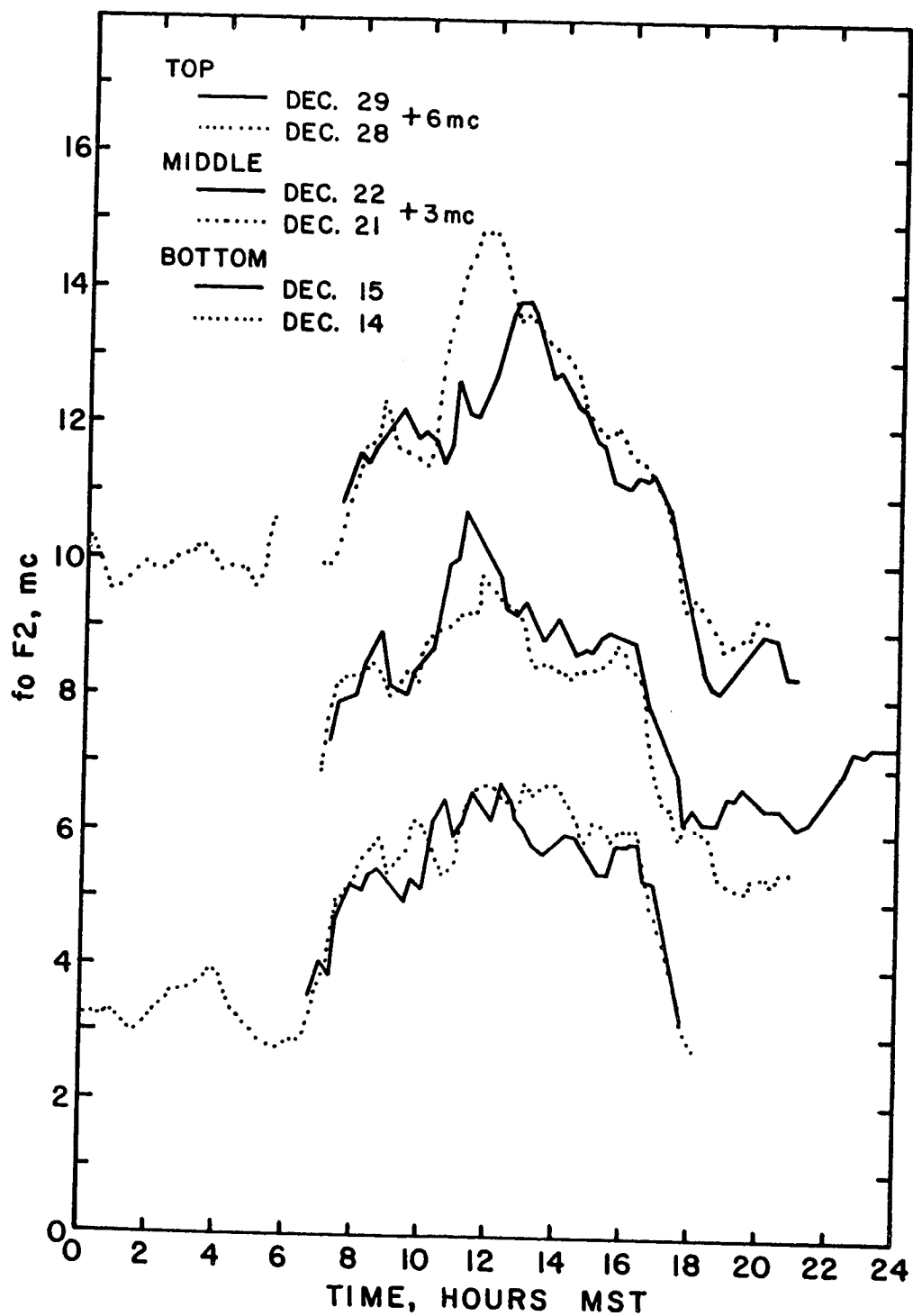
FIGURE 34. F2 PEAK PLASMA FREQUENCIES AT
WHITE SANDS FOR WINTER, 1965
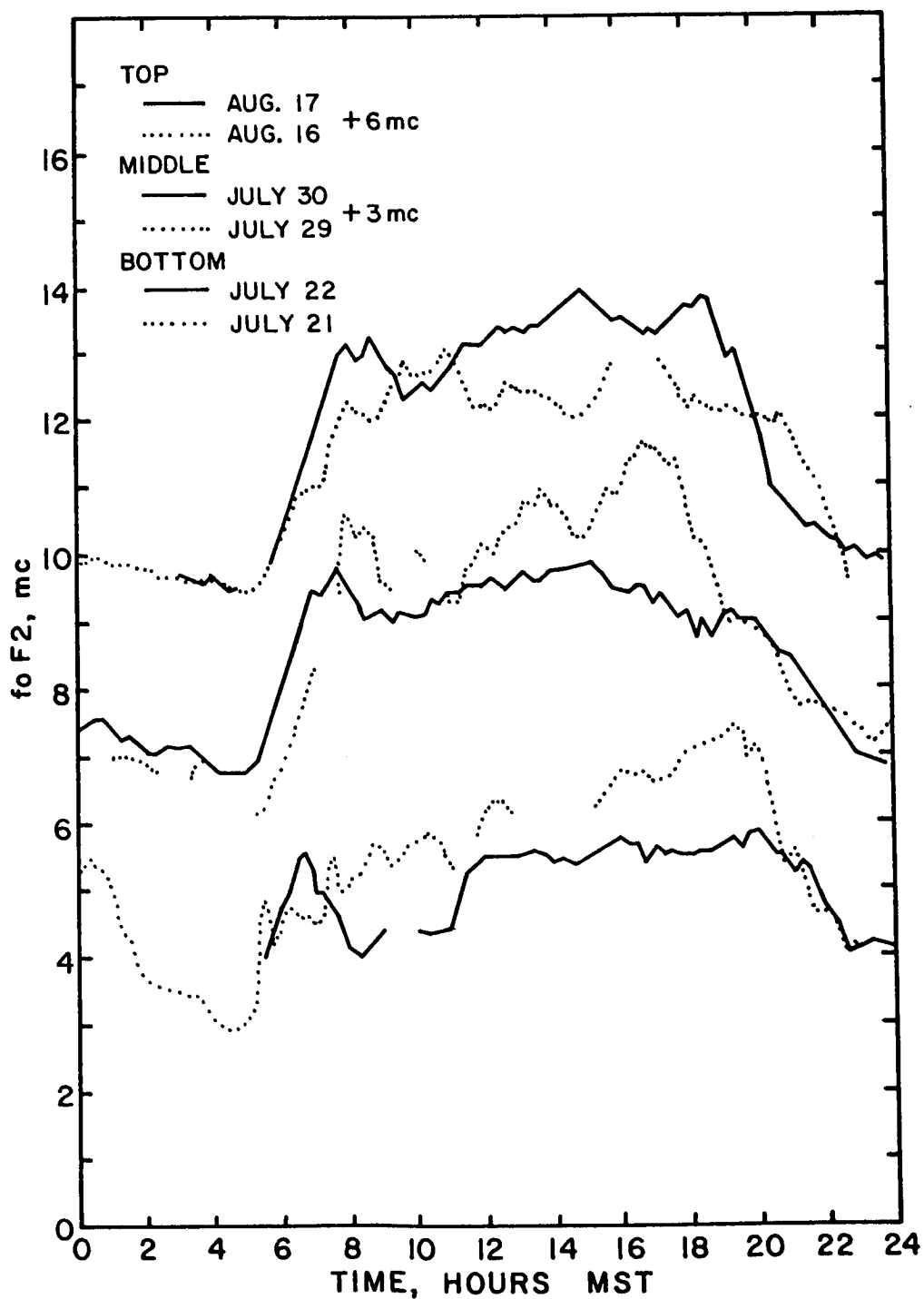
FIGURE 35. F2 PEAK PLASMA FREQUENCIES AT
WHITE SANDS FOR SUMMER, 1966
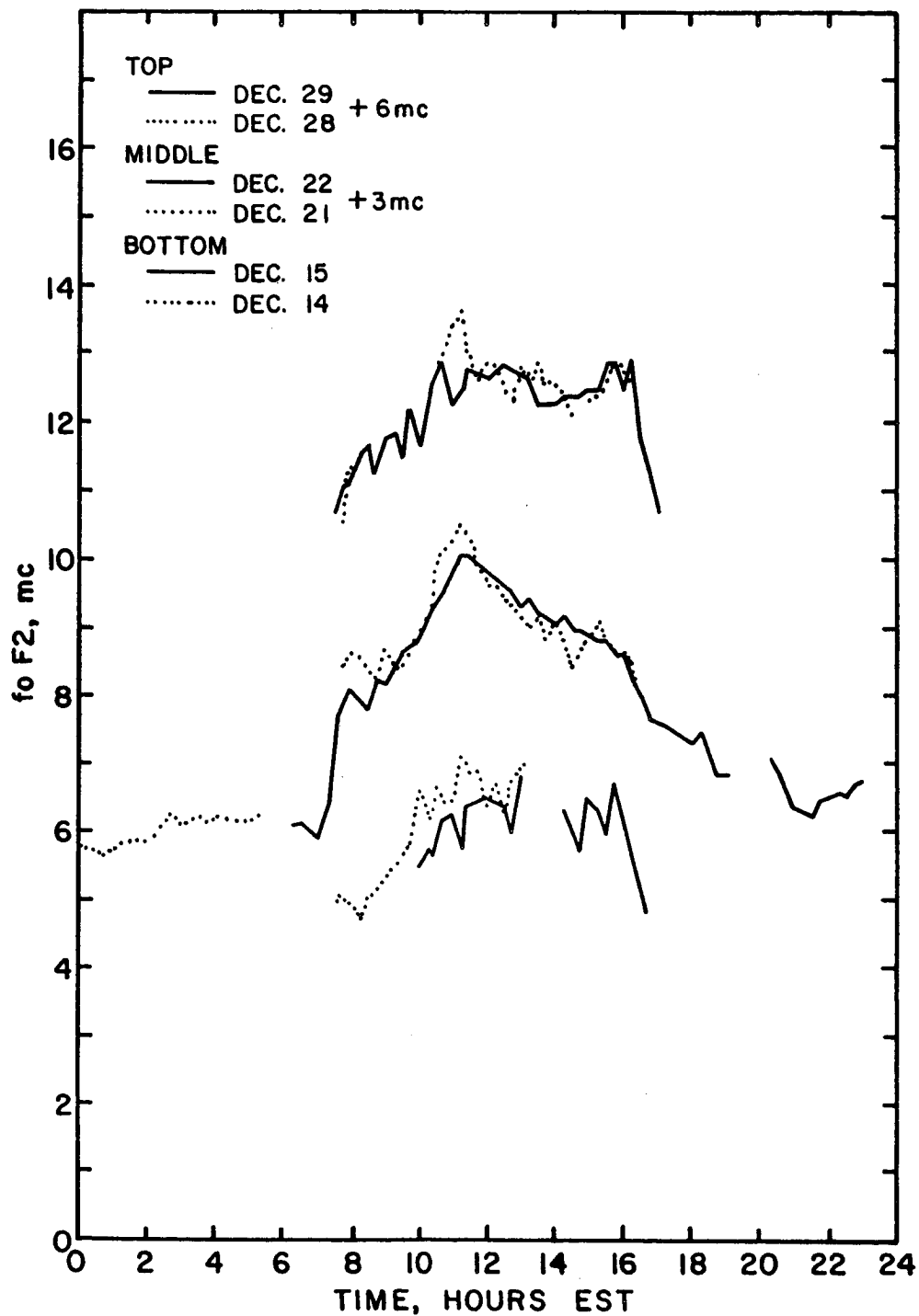
FIGURE 36. F2 PEAK PLASMA FREQUENCIES AT
WALLOPS ISLAND FOR WINTER, 1965
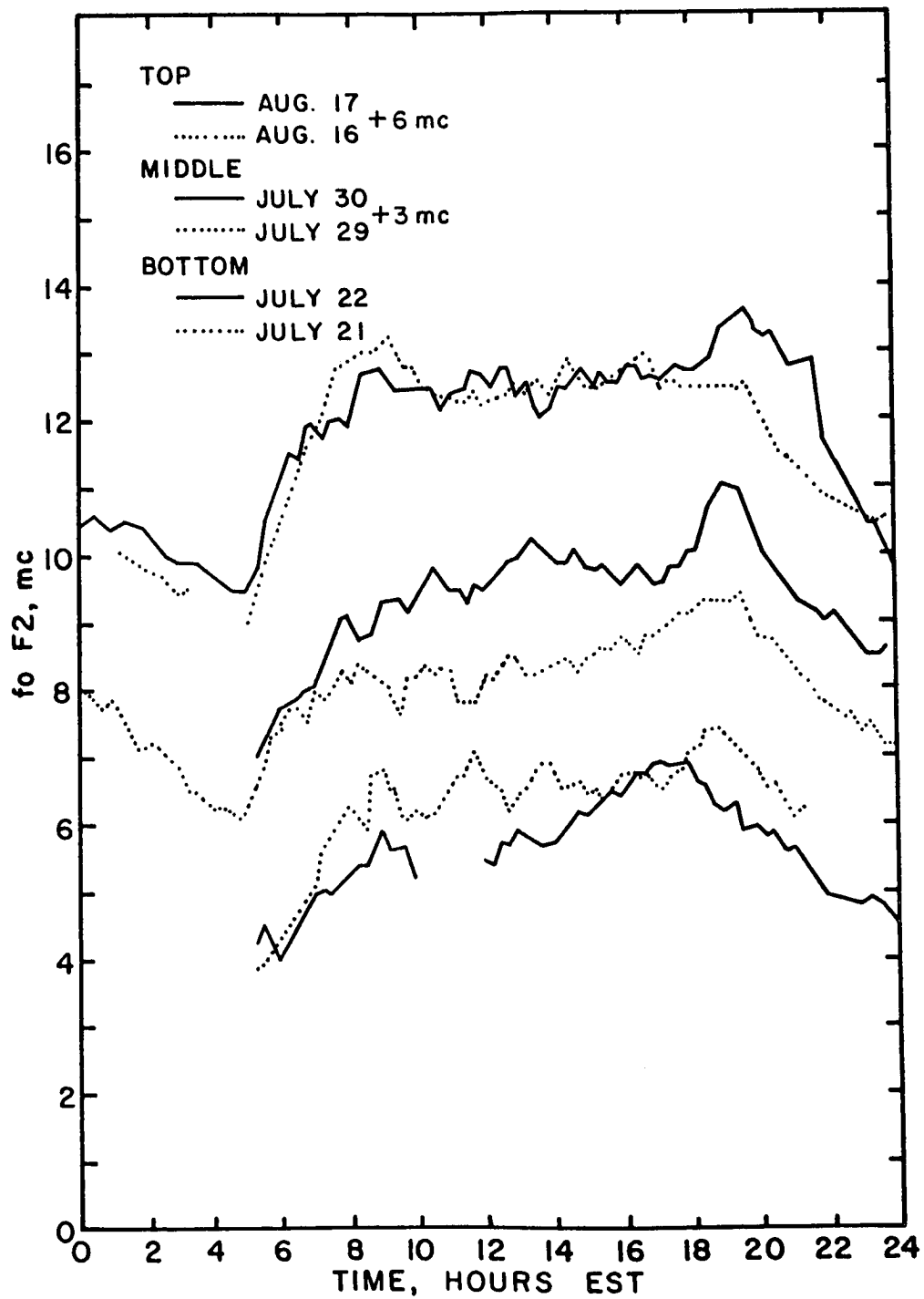
FIGURE 37. F2 PEAK PLASMA FREQUENCIES AT
WALLOPS ISLAND FOR SUMMER, 1966
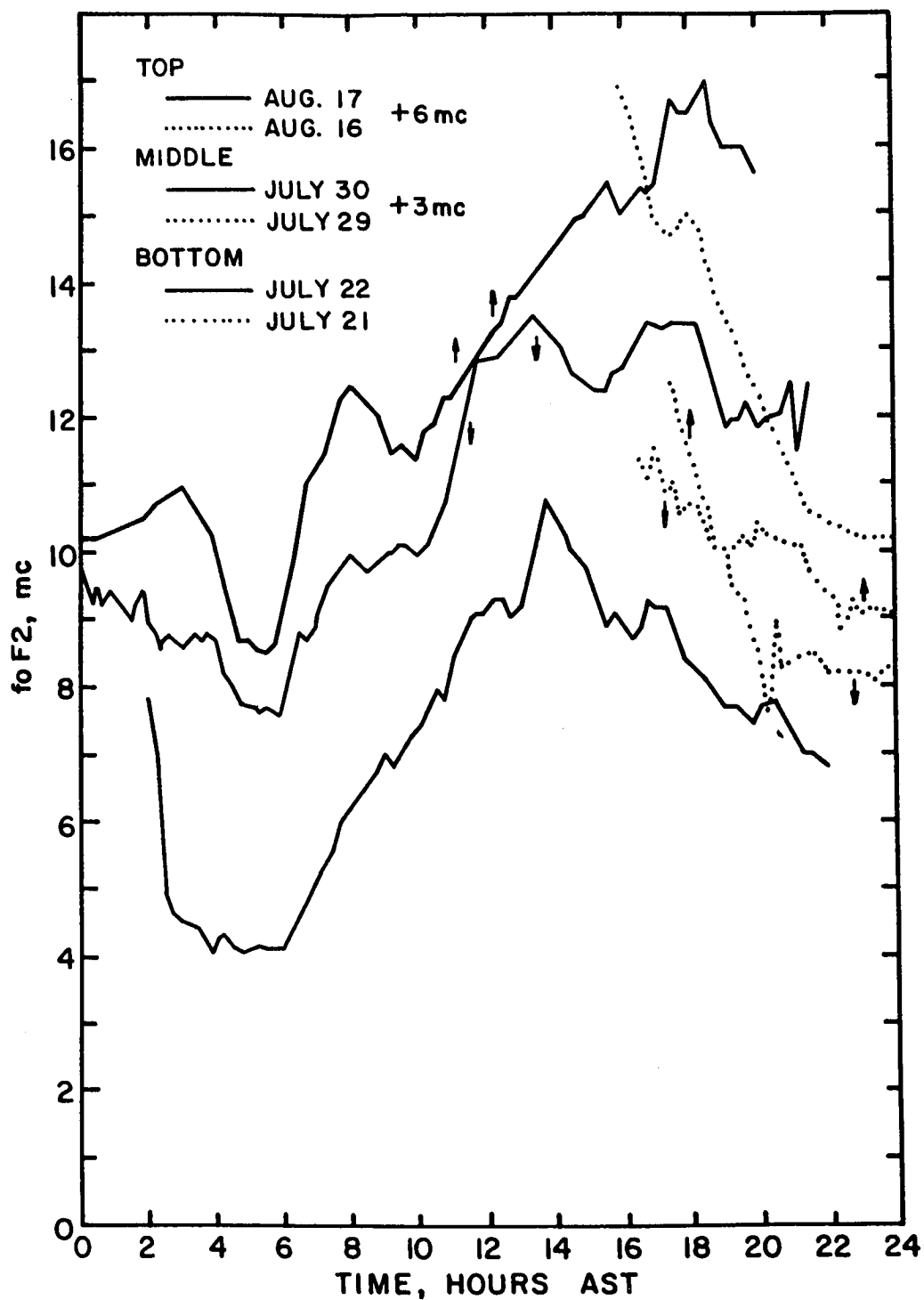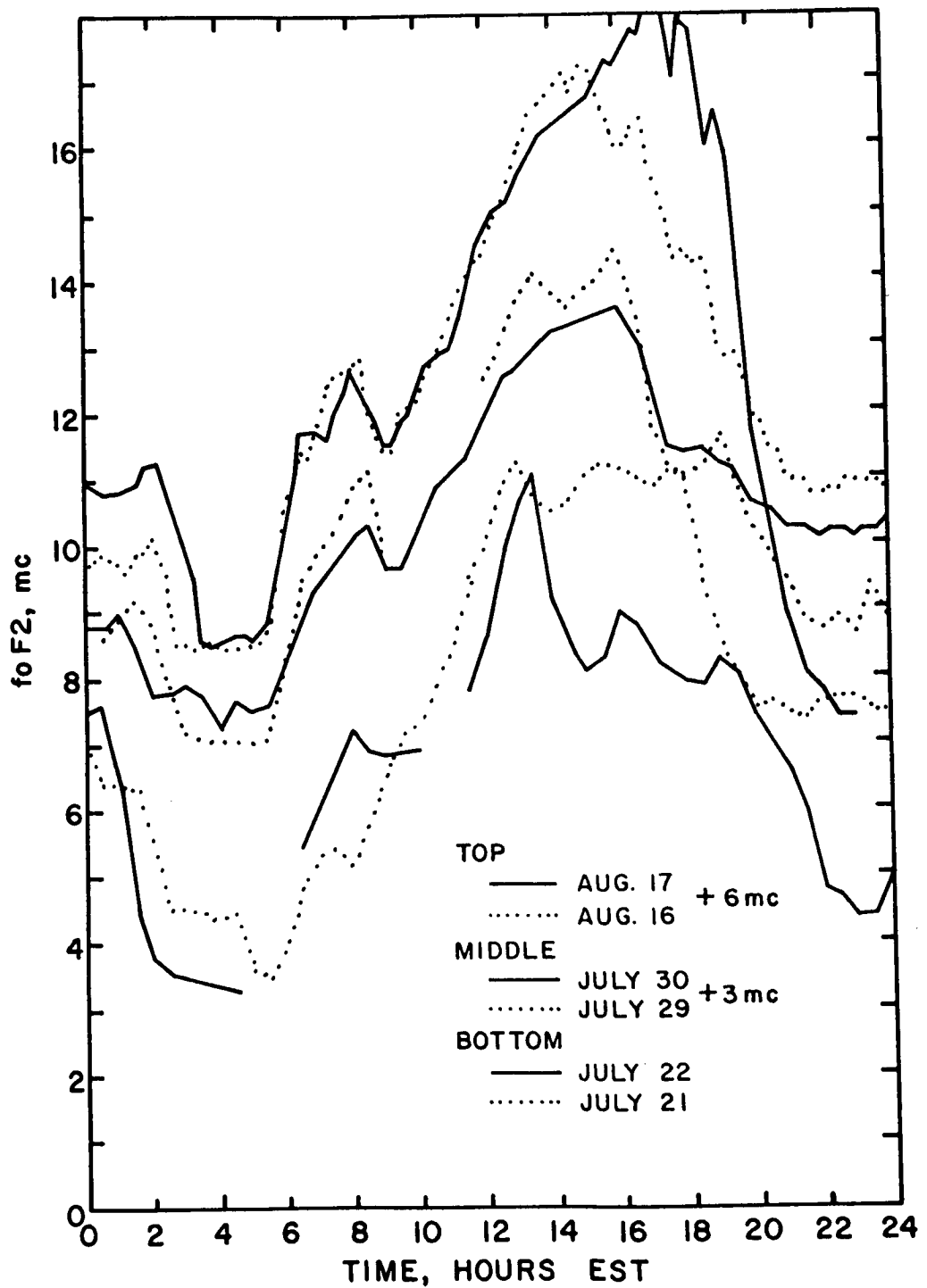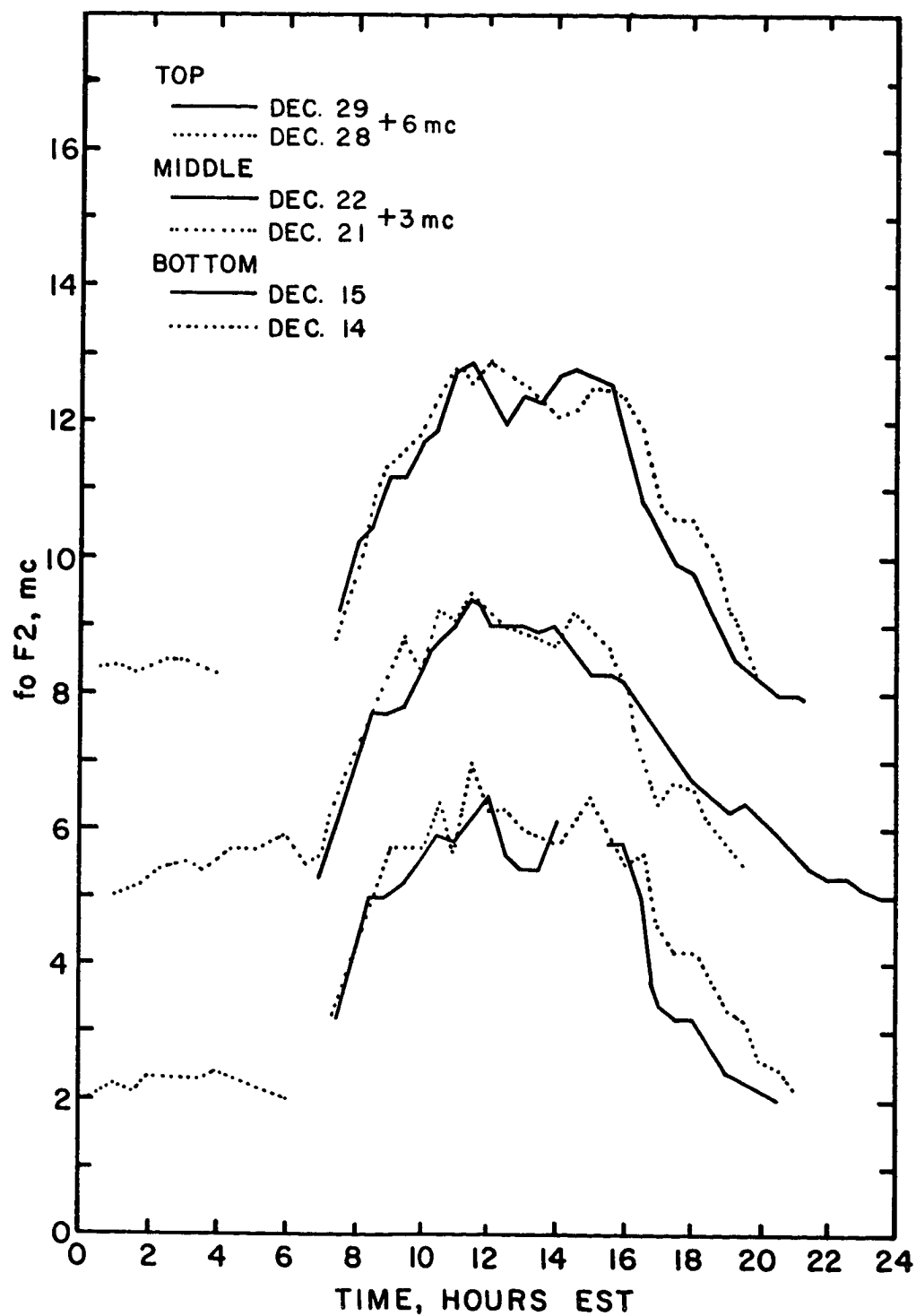
FIGURE 38. F2 PEAK PLASMA FREQUENCIES AT
OTTAWA FOR WINTER, 1965
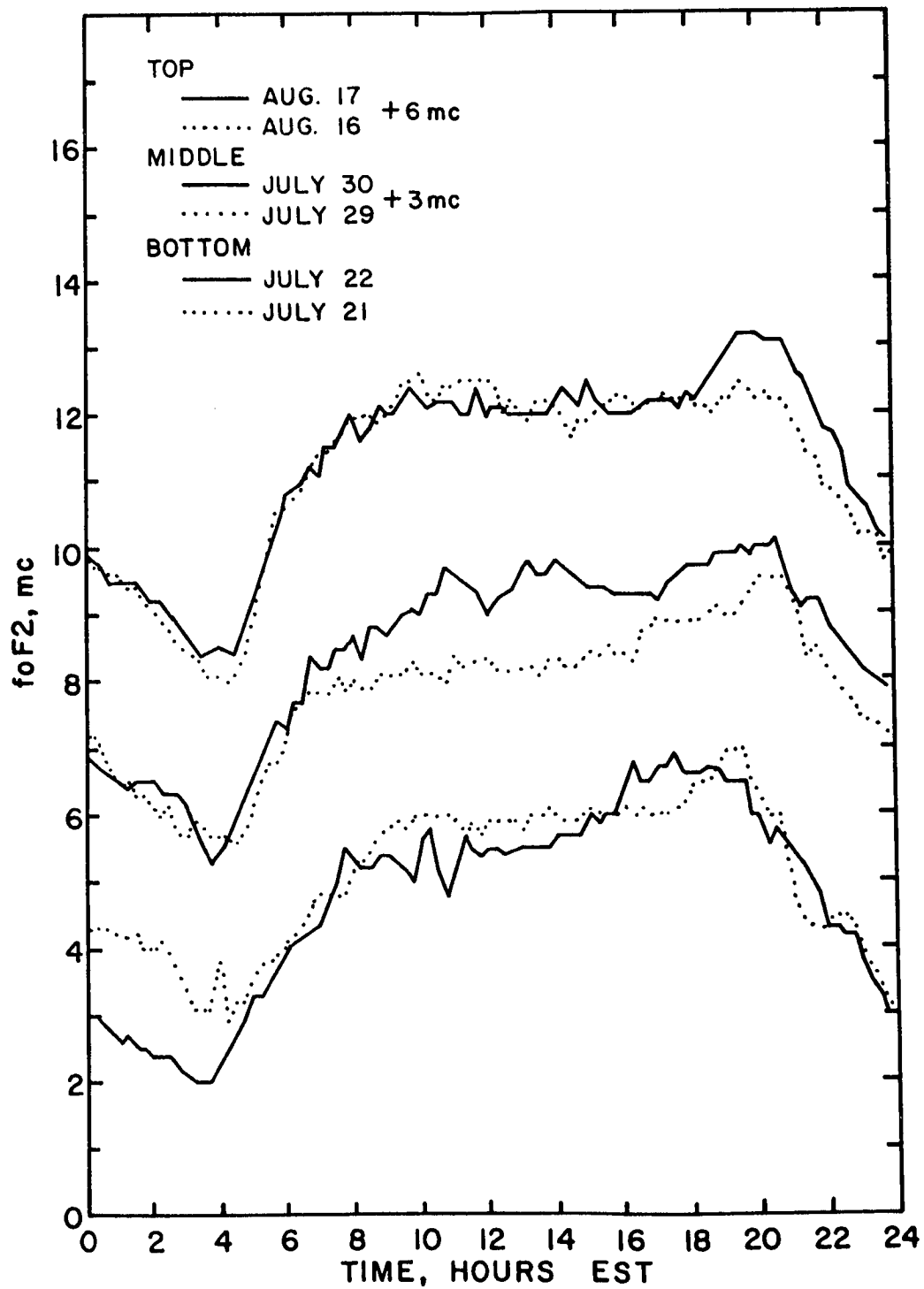
FIGURE 39. F2 PEAK PLASMA FREQUENCIES AT OTTAWA FOR SUMMER, 1966

The high latitude group consists of Ottawa and Wallops Island. The distinguishing features between groups are roughly large fluctuations at low latitudes, small fluctuations at high latitudes, and, somewhat arbitrarily, intermediate size ones at middle latitudes. This grouping does not imply that the stations are necessarily located in the conventional equatorial, middle latitude, and auroral zones.

Data from Wallops Island ionograms were difficult to scale because oblique propagation path echoes and disturbed echoes of the types described by Heisler (1963) were frequently present. The more prominant disturbances appeared to move from the F2 region down through the F1 region. In addition, data for Huancayo on August 16, 1966 between 1115 and 2000 hours EST are smaller than the true values because the ionogram traces went beyond the recording film borders before reaching the F2 peak.

CHAPTER 4 THEORETICAL CALCULATIONS

4.1 Purpose

We are interested in knowing how electron densities in the F region change in response to drift velocities or changes in electron temperature and how the temperature depends on the densities. The time constants of relaxation are important to decide if the observed density and temperature fluctuations are either following an external perturbation or are recovering from a much shorter perturbation. If the time constants of density or temperature fluctuations are widely different then it might be possible to treat one of the quantities (density or temperature) as being parasitic on the other. Further, we wish to consider the possibility that the electron densities and temperatures might form an unstable system which could generate fluctuations internally in response to a small perturbation.

4.2 Governing Equations

The ionospheric electron and ion gases will be treated as fluids in a predominantly neutral atmosphere permeated by a uniform geomagnetic field. Although above 500 km or 600 km the mean free paths of electrons become larger than typical electron density scale heights (200 km), the fluid concept will be extended above this altitude for the sake of simplicity. Only the Maxwellian, or ambient, electron and ion gases will be considered. Interactions between electrons, ions, and neutral particles are included; but the neutral

gas will be considered unaffected by them. The fluid equations describing conservation of electron and ion number density (or mass), transport velocity, and thermal energy are from Holt and Haskell (1965, Chapter 6) with somewhat different notation.

Conservation of mass or number density of electrons and ions is expressed in the continuity equation

$$\frac{\partial N_e}{\partial t} = P - L - \nabla \cdot (N_e \overline{v}) \tag{4-1}$$

where N_e is the electron or ion density since charge neutrality will be assumed, P and L are the effective production and loss rates of electron-ion pairs, and $\overline{v}$ is their transport velocity. Actually, both electron and ion gases obey separate continuity equations. If only one major ion is present, as will be assumed here, then P and L refer equally to either electrons or ions. Their transport velocities will be the same also when the reasonable restrictions below are imposed. Therefore, one continuity equation will suffice for both species in these F region model studies.

Transport velocities, $\overline{v}_e$ and $\overline{v}_i$, of electrons and ions with respect to a stationary observer depend on several factors. They are collisions between the charged species and the neutral gas, electric and magnetic fields, gravity $\overline{g}$ and pressure gradients. Writing the pressures as $N_e k T_e$ for electrons and as $N_e k T_i$ for ions, the transport velocities obey equations 4-2 and 4-3:

$$m_e \frac{\partial (\overline{v}_e N_e)}{\partial t} + N_e \mu_{en} \nu_{en} (\overline{v}_e - \overline{v}_n) + N_e \mu_{ei} \nu_{ei} (\overline{v}_e - \overline{v}_i) + m_e N_e (\overline{v}_e \cdot \nabla) \overline{v}_e =$$

$$-N_e q [\overline{E} + \overline{v}_e \times \overline{B}] - m_e N_e \overline{g} - \nabla (N_e k T_e) + \overline{v}_e m_e (P - L) \tag{4-2}$$

$$m_i \frac{\partial(\overline{v}_i N_e)}{\partial t} + N_e \mu_{in} \nu_{in}(\overline{v}_i - \overline{v}_n) + N_e \mu_{ie} \nu_{ie}(\overline{v}_i - \overline{v}_e) + m_i N_e (\overline{v}_i \cdot \nabla) \overline{v}_i =$$

$$+ N_e q [\overline{E} + \overline{v}_i \times \overline{B}] - m_i N_e \overline{g} - \nabla(N_e k T_i) + \overline{v}_i m_i (P - L) \qquad (4-3)$$

where m_e and m_i are the electron and ion masses, μ_{jk} is the reduced mass $m_j m_k /(m_j + m_k)$ of two interacting species j and k, ν_{jk} are their respective collision frequencies for momentum transfer of a type j particle with all type k particles, and q is the electronic charge. $\overline{E}$ is an assumed electrostatic field due to both external sources and to slight gravatational charge separation, and $\overline{B}$ is the geomagnetic field. Electrons and ions are assumed to have separate temperatures T_e and T_i, to be found from the energy equations. The last term, vm(P - L), in these equations is an approximation to account for the momentum changes per unit volume due to the generation and loss of particles.

Equations 4-1, 4-2, and 4-3 can be simplified and combined if a number of reasonable assumptions are made. These are that:

a) no currents flow, implying that $\overline{v}_e = \overline{v}_i$

b) the time scales for bulk changes are much longer than the collision intervals so that accelerations are neglectable

c) $\mu_{en} \nu_{en} << \mu_{in} \nu_{in}$

d) the ion-neutral collision frequency ν_{in} is smaller than the ion gyrofrequency ($q B/m_i$, in M.K.S.A. units)

e) the external part of the electrostatic field $\overline{E}$ is transverse to $\overline{B}$

f) the neutral velocity $\overline{v}_n$ is horizontal

g) geomagnetic field lines are linear, have a dip angle I below the horizontal, and lie in a north-south plane

h) there are no horizontal gradients

Then equations 4-2 and 4-3 can be added to eliminate both E and B and to give the ambipolar transport velocity. Taking z as the altitude coordinate we have

$$\frac{\partial N_e}{\partial t} = P - L - \sin I \frac{\partial (N_e v_d)}{\partial z} - \frac{\partial (N_e W)}{\partial z} \qquad (4-4)$$

where the transport velocity has been separated into an ambipolar diffusion velocity v_d through a stationary neutral atmosphere,

$$v_d = - \sin I \frac{k(T_e + T_i)}{\mu_{in} \nu_{in}} \left[\frac{1}{N_e} \frac{\partial N_e}{\partial z} + \frac{m_i g}{k(T_e + T_i)} \right] \qquad (4-5)$$

and into an effective vertical drift velocity W

$$W = \frac{E_y}{B} \cos I + v_{nx} \sin I \cos I . \qquad (4-6)$$

A coordinate system was chosen with the x axis to the south, y to the east, z upward, and with B pointing northward in the x-z plane. Thus, an eastward electric field or a southward neutral velocity produce an upward effective drift velocity in the northern hemisphere.

The equations for thermal energy conservation from Holt and Haskell (1965) but in different notation are

$$\frac{\partial p_e}{\partial t} + \overline{v}_e \cdot \nabla p_e = - u_e (\nabla \cdot \overline{v}_e) - \nabla \cdot \overline{Q}_e - p_e \nabla \cdot \overline{v}_e + Pu_e - Lu_e$$

$$(4-7)$$

$$\frac{\partial p_i}{\partial t} + \overline{v}_i \cdot \nabla p_i = - u_i (\nabla \cdot \overline{v}_i) - \nabla \cdot \overline{Q}_i - p_i \nabla \cdot \overline{v}_i + Pu_i - Lu_i$$

$$(4-8)$$

where we have assumed isotropic electron and ion pressures $p_e = N_e k T_e$ and $p_i = N_i k T_i$. Also, u_e and u_i are the electron and ion energy densities $3/2 N_e k T_e$ and $3/2 N_e k T_i$ respectively, and

the transport velocities v_e and v_i were discussed before and assumed to be equal. Heat conduction is represented by the energy flux terms $Q_e = -K_{T_e} \nabla T_e$ for electrons and $Q_i = -K_{T_i} \nabla T_i$ for the ions with K being the appropriate conduction coefficients. Pu and Lu are the energy production and loss rates, and they include effects of electron-ion pair number density production and loss of values $3/2\ k\ T_e$ and $3/2\ k\ T_i$ per particle.

Banks (1966 e) found that below 600 km during solar minimum ion thermal conduction had little effect on the ion temperature. Therefore, Q_i will be omitted from the calculations. The terms $p\nabla \cdot \overline{v}$ in equations 4-7 and 4-8 represent work done under adiabatic compression and will be neglected here because the transport velocity gradients are small. The convective transport terms $3/2\ k\ N_e \overline{v} \cdot \nabla\ T$ are neglected here because thermal gradients are small, and these terms are usually much smaller than production, loss, and conduction in the F region.

Equations 4-7 and 4-8 are now

$$\frac{3}{2} N_e\ k\ \frac{\partial T_e}{\partial t} = Pu_e - Lu_e + \nabla \cdot (K_{T_e} \nabla T_e) - \frac{3}{2} k\ T_e\ [\frac{\partial N_e}{\partial t} + \nabla \cdot (N_e \overline{v})]$$

(4-9)

for the electrons and

$$\frac{3}{2} N_e\ k\ \frac{\partial T_i}{\partial t} = Pu_i - Lu_i - \frac{3}{2} k\ T_i\ [\frac{\partial N_e}{\partial t} + \nabla \cdot (N_e \overline{v})]$$

(4-10)

for the ions, with $\overline{v}$ being their common transport velocity.

Recalling equation 4-1

$$\frac{\partial N_e}{\partial t} + \nabla \cdot (N_e v) = P - L$$

the bracketed terms in equations 4-9 and 4-10 are just the thermal energy changes due to particle number density changes. In the regions where P and L are large, Pu and Lu are larger so that these bracketed terms will be neglected. Since the ion temperature Ti is nearly equal to the neutral temperature over most of the F region, the time derivative in equation 4-10 will be omitted, and the ion gas temperature will be determined from equality of its energy production and loss rates. Therefore, the temperature equations become

$$\frac{3}{2} k N_e \frac{\partial T_e}{\partial t} = Pu_e - Lu_e + \nabla \cdot (K_{T_e} \nabla T_e) \qquad (4-11)$$

and

$$Pu_i = Lu_i \qquad (4-12)$$

With a magnetic field, Sharofsky, Bernstein, and Robinson (1963) have shown that the coefficient of thermal conduction for conduction transverse to the magnetic field is reduced by a factor of $1/(1 + \omega_H/v)$ compared to conduction parallel to the field. The factors are electron gyrofrequency ω_H and electron collision frequency v. In the F region the electron gyrofrequency is about one megacycle while the collision frequency is several orders of magnitude smaller. Consequently, we shall use just the parallel conduction component and the equations become

$$\frac{3}{2} k N_e \frac{\partial T_e}{\partial t} = Pu_e - Lu_e + \sin^2 I \frac{\partial}{\partial z} (K_{T_e} \frac{\partial T_e}{\partial z}) \qquad (4-13)$$

and

$$Pu_i = Lu_i \qquad\qquad (4\text{-}14)$$

4.3 Model Studies

The electron densities are dependent on electron and ion temperatures in both diffusion coefficient, $k(T_e + T_i)/(\mu_{in} \, \nu_{in})$, and "scale height", $k(T_e + T_i)/(m_i g)$, terms of the diffusion velocity. Electron densities appear prominantly in the temperature equations also because the electron gas energy loss rates, Lu_e, and both the ion energy production and loss rates, Pu_i and Lu_i, depend directly on electron density.

We see, therefore, that the plasma density and temperature equations are coupled. No analytic solutions for the individual equations has been discovered for the F region. Numerical solution of the simultaneous equations has been prevented by inadequate computer storage space. Consequently, the temperatures and densities are computed separately for reasonable values of the conjugate variables in an attempt to assess the relative magnitude and time rates of change one would have on the other.

4.3.1 Electron Density Profiles

We are interested in knowing how equilibrium electron density profiles depend on electron temperature and drift velocity, and what are the time constants of density changes due to perturbations of temperature or drift velocity.

The continuity equation for electron densities was found in section 4.2 to be

$$\frac{\partial N_e}{\partial t} = P - L - \sin I \frac{\partial(N_e v_d)}{\partial t} - \frac{\partial(N_e W)}{\partial z} \tag{4-4}$$

with a diffusion velocity v_d with respect to a stationary observer

$$v_d = - \sin I \frac{K(T_e + T_i)}{\mu_{in} \nu_{in}} \left[\frac{1}{N_e} \frac{\partial N_e}{\partial z} + \frac{m_i g}{k(T_e + T_i)} \right] \tag{4-5}$$

and a drift velocity W due to an eastward electric E and an equatorial-ward neutral velocity v_n

$$W = \frac{E}{B} \cos I + v_n \sin I \cos I. \tag{4-6}$$

F region electron density production, P, above 180 km is due almost entirely to photoionization of atomic oxygen by ultraviolet radiation. In the F2 region the solar flux is essentially unattenuated so that the production rate P is the product of the solar flux, ionization cross sections, and atomic oxygen number density averaged over all wave lengths. We will assume that the production is a constant times the atomic oxygen density.

Although molecular nitrogen and molecular oxygen ions are being produced at rates comparable to that of atomic oxygen, they recombine with electrons so quickly that their average density is very small (Donahue (1965)). Atomic oxygen-electron pairs are lost through two parallel two step reactions of ion-atom interchange

$$O^+ + N_2 \rightarrow NO^+ + N \qquad \text{(rate } \gamma_1) \tag{4-15}$$

$$O^+ + O_2 \rightarrow O_2^+ + O \qquad \text{(rate } \gamma_2) \tag{4-16}$$

followed by dissociative recombination

$$NO^+ + e \rightarrow N + O \qquad\qquad (\text{rate } \alpha_1) \qquad\qquad (4\text{-}17)$$

$$O_2^+ + e \rightarrow O + O \qquad\qquad (\text{rate } \alpha_2) \qquad\qquad (4\text{-}18)$$

Under conditions of equilibrium and equality of production and loss rates

equations 4-15 through 4-18 can be solved to give the loss term L as

$$L = \frac{\alpha_1 \alpha_2 [\gamma_1 N(N_2) + \gamma_2 N(O_2)] N_e^2}{\alpha_1 \alpha_2 N_e + \alpha_2 \gamma_1 N(N_2) + \alpha_1 \gamma_2 N(O_2)} \qquad\qquad (4\text{-}19)$$

In the F2 region, the denominator of equation 4-19 is dominated by

$\alpha_1 \alpha_2 N_e$ so that the effective loss rate is

$$L \simeq [\gamma_1 N(N_2) + \gamma_2 N(O_2)] N_e \qquad\qquad (4\text{-}20)$$

Since the distribution with altitude of molecular nitrogen and molecular

oxygen are similar and since $\gamma_1 N(N_2)$ and $\gamma_2 N(O_2)$ are approximately

equal in regions where loss is important, the loss rate coefficient in

equation 4-20 will be replaced by

$$\gamma_3 N(O_2) \qquad\qquad (4\text{-}21)$$

where

$$\gamma_3 = \gamma_2 + \gamma_1 \frac{N(N_2)}{N(O_2)} \simeq 2 \gamma_2 \simeq 10^{-12} \text{ cm}^3/\text{sec} .$$

This has the added convenience of making the atomic oxygen scale

height twice the scale height of the loss rate coefficient. Thus the

effective loss rate in the F2 region can be written as

$$L = \beta N_e \qquad\qquad (4\text{-}22)$$

where β is equation 4-21.

The diffusion velocity, v_d, is limited by collisions between ions and neutral particles with ion-neutral momentum transfer collision frequencies v_{in}. From Banks (1965) the product of the collision frequencies and reduced masses in Equation 4-5 can be evaluated. At 250 km, typical values for $\mu_{in} \, v_{in}$ with O^+ ions are 3×10^{-23} for atomic oxygen, 8×10^{-25} for molecular oxygen and 9×10^{-24} for molecular nitrogen with respective neutral densities of 1×10^9, 4×10^7, and 5×10^8 cm^{-3} and a neutral temperature of 800° K. Over the F region where diffusion is important, therefore, atomic oxygen collisions predominate; the collision frequency will be taken as dependent on atomic oxygen alone.

Let v be an effective collision frequency defined as

$$v = \left(\frac{m_o}{m_o + m_i} \right) \frac{v_{io}}{\sin^2 I}$$

where the subscript "o" refers to atomic oxygen. Let H_p be the electron density scale height

$$Hp = \frac{k(T_e + T_i)}{m_i \, g} \, ,$$

and let H_o be the atomic oxygen scale height

$$H_o = \frac{k \, T_n}{m_o \, g}$$

so that the atomic oxygen density, as a function of altitude z, is

$$N(O) = N_o \exp \left((z_o - z)/H_o \right)$$

above a reference height z_o.

Then the continuity equation has the form

$$\frac{\partial N_e}{\partial t} = P_o \exp\left((z_o - z)/H_o\right) - \beta_o \exp\left(2(z_o - z)/H_o\right) N_e$$

$$+ \frac{\partial}{\partial z}\left[\frac{H_p g}{\nu}\left(\frac{1}{N_e}\frac{\partial N_e}{\partial z} + \frac{1}{He}\right)\right] - \frac{\partial(N_e W)}{\partial z} \qquad (4-23)$$

with

$$\nu = \nu_o \exp\left((z - z_o)/H_o\right).$$

For convenience, the temperatures are assumed to be isothermal; ion and neutral temperatures are assumed to be equal, i.e.

$T_i = T_n$.

Boundary conditions on the electron densities are applied from physical considerations. Below the F2 peak, diffusion rates become small due to the large neutral densities while the production and loss rates become large. Consequently, at a lower boundary altitude of 100 km production and loss rates are equated to give

$N_e = P/\beta$ at 100 km.

Above the F2 peak, the diffusion velocities of electrons and ions remains bounded while the electron densities decrease with increasing altitude. The diffusive flux, $N_e v_d$, therefore becomes small at high altitudes and approaches zero. Using the boundary condition that at great heights the diffusive flux vanishes and using Equation 4-5 for the diffusion velocity, we see that the upper boundary condition on the electron densities will be

$$\frac{1}{N_e}\frac{\partial N_e}{\partial z} \rightarrow -\frac{1}{H_p} \quad \text{as } z \rightarrow \infty \quad .$$

The exponential decrease of electron density with altitude above the F2 peak is not a desirable characteristic for numerical computations. Therefore a change of variables is made to remove the exponential variation and to put the continuity equation, 4-23, into the non-dimensional and numerically better form

$$\frac{\partial^2 \Pi}{\partial \xi^2} + \frac{\partial \Pi}{\partial \xi} \left[(1 - a + ar)\xi^{-1} + \delta \xi^{a-1} \right] + \Pi \left[-\xi^{3a-2} + ar\delta \xi^{a-2} \right] +$$

$$\xi^{-2+2a-ar} = \xi^{a-2} \frac{\partial \Pi}{\partial \gamma} \tag{4-24}$$

by the following transformations:

a = an arbitrary constant for ease of computations

$$c = \beta_o a^2 r \nu_o H_o / g$$

$$N_e = (P_o/\beta_o) c^{1/3} \Pi \xi^{ar}$$

$$\exp\left((z_o - z)/H_p) \right) = c^{-r/3} \xi^{ar}$$

$$\exp\left((z_o - z)/H_o \right) = c^{-1/3} \xi^a$$

$$t = (c^{2/3}/\beta_o) \gamma$$

$$W = (a H_o \beta_o / c^{2/3}) \delta$$

$$r = T_N/(T_i + T_e) = T_N/(T_N + T_e)$$

The independent variables ξ and γ and the dependent variable Π with parameters a, r, and δ are all non-dimensional.

Because a non-dimensional equation is used it is seen that all electron densities are directly proportional to the production rate while the density at the F2 peak is proportional to $P_o \beta_o^{-2/3} \nu_o^{1/3} H_o^{1/3}$ for a given temperature ratio r. The altitude of the peak depends on

$(H_o/3) \ln (\beta_o a^2 r v_o H_o/g)$. Similarly, the time scale for density changes depends on $\beta_o^{-1/3} v_o^{2/3} H_o^{2/3}$.

Boundary conditions on electron density are now reflected as the following conditions on Π,

at low altitudes, $\Pi \rightarrow \xi^{-a-ar}$ as $\xi \rightarrow \infty$

at high altitudes, $\Pi \rightarrow a$ constant as $\xi \rightarrow 0$.

The former condition is equivalent to production equals loss while the latter is exponential vanishing of the electron density.

Before solving Equation 4-24 we can compare the dependence of the ratio of production to loss at the F2 peak on loss rate and diffusion coefficients with the results of Rishbeth and Barron (1966). They found that the ratio was a constant (about 0.7) for a wide range of the parameter $H^2 \beta/D$ at a given altitude. In our notation the production at the peak altitude z_p ξ_p is

$$P = P_o c^{-1/3} \xi_p^a$$

and the loss is

$$L = \beta_o c^{-2/3} \xi_p^{2a} (\frac{P_o}{\beta_o}) c^{1/3} \Pi_p \xi_p^{ar}$$

Then the ratio L/P at the peak is

$$L/P = \Pi_p \xi_p^{ar}$$

This is independent of the values of diffusion and loss rate and the

neutral scale height. Thus, we can generalize their results to state that the ratio of loss to production rates at the peak of the equilibrium electron density profile is completely independent of diffusion and loss coefficients and the neutral scale height for a constant temperature ratio, r, for these particular types of production and loss processes, when the drift velocity is zero.

The time dependent differential equation for $\Pi(\xi, \gamma)$ was solved numerically by the implicit method, Diaz (1958). Central differences were used to construct a mesh of 400 altitude points (ξ_i) and two time points (γ^j). The right hand side of Equation 4-23 is

$$\xi_i^{a-2} \frac{\Pi_i^{j+1} - \Pi_i^j}{\Delta \gamma}$$

where subscripts refer to altitude mesh points and superscripts to time mesh points. It is presumed that Π_i^j is known at all altitudes and we wish to find Π_i^{j+1}. According to central difference techniques, the time derivative above represents the value at a time midway between steps j and j+1. The implicit method utilizes this condition and assumes that the left hand, or space, side of equation 4-23 is a weighted average of functions at both time steps j and j+1. The problem then is reduced to an algebraic one of grouping all the unknown dependent variables Π_i^{j+1} on one side of the equation and all the known variables including all Π_i^j on the other side to solve the resulting matrix equation.

In this work equal weighting was used so that all time dependent variables on the left hand, or space, side were replaced by one half of their values at both time steps j and j+1. This weighting is near optimum for variables changing exponentially if the time step

is not greater than a time constant. Time steps were determined as being equal to the shortest time constant encountered, i.e. $1/\beta$ sec.

Values of the parameters used in the calculations were

$z_o = 300$ km $\nu_o = 1.0$ sec^{-1}

$P_o = 78$ cm^{-3} sec^{-1} $T_N = T_i = 800^o$ K

$\beta_o = 4.32 \times 10^{-5}$ sec^{-1} $a = 3.49$

Equilibrium electron density profiles, shown in Figure 40, were computed for representative electron to ion temperature ratios, T_e/T_i, of 1.0, 2.0, and 3.0 with no drift velocity. At the F2 peak, the density decreased for higher electron temperatures by about 11% at $T_e/T_i=3.0$ compared with $T_e/T_i=1.0$. Above the peak, the densities were distributed exponentially with scale heights proportional to the temperatures. The isopycnic point above the F2 peak is apparent rather than real since it vanishes in time dependent profiles. The electron content in a one square centimeter column above 150 km increased by 45% at $T_e/T_i = 3.0$ compared with $T_e/T_i = 1.0$. No significant changes of the peak altitude were obs.

Uniform drift velocities produced larger effects as seen in Figure 41. These equilibrium profiles were computed for uniform vertical drift velocities of +10, 0, and -10 m/s with $T_e/T_i = 2.0$. Profiles at other temperature ratios were similar. The largest changes were near and above the peak where diffusion is altered by the drift velocity aiding or opposing the downward ambipolar diffusion. The relatively modest drift velocities of 10 m/s were able to change the peak electron density by +73% and -28% and the peak altitude by +30 km and -22 km for upward and downward drifts,
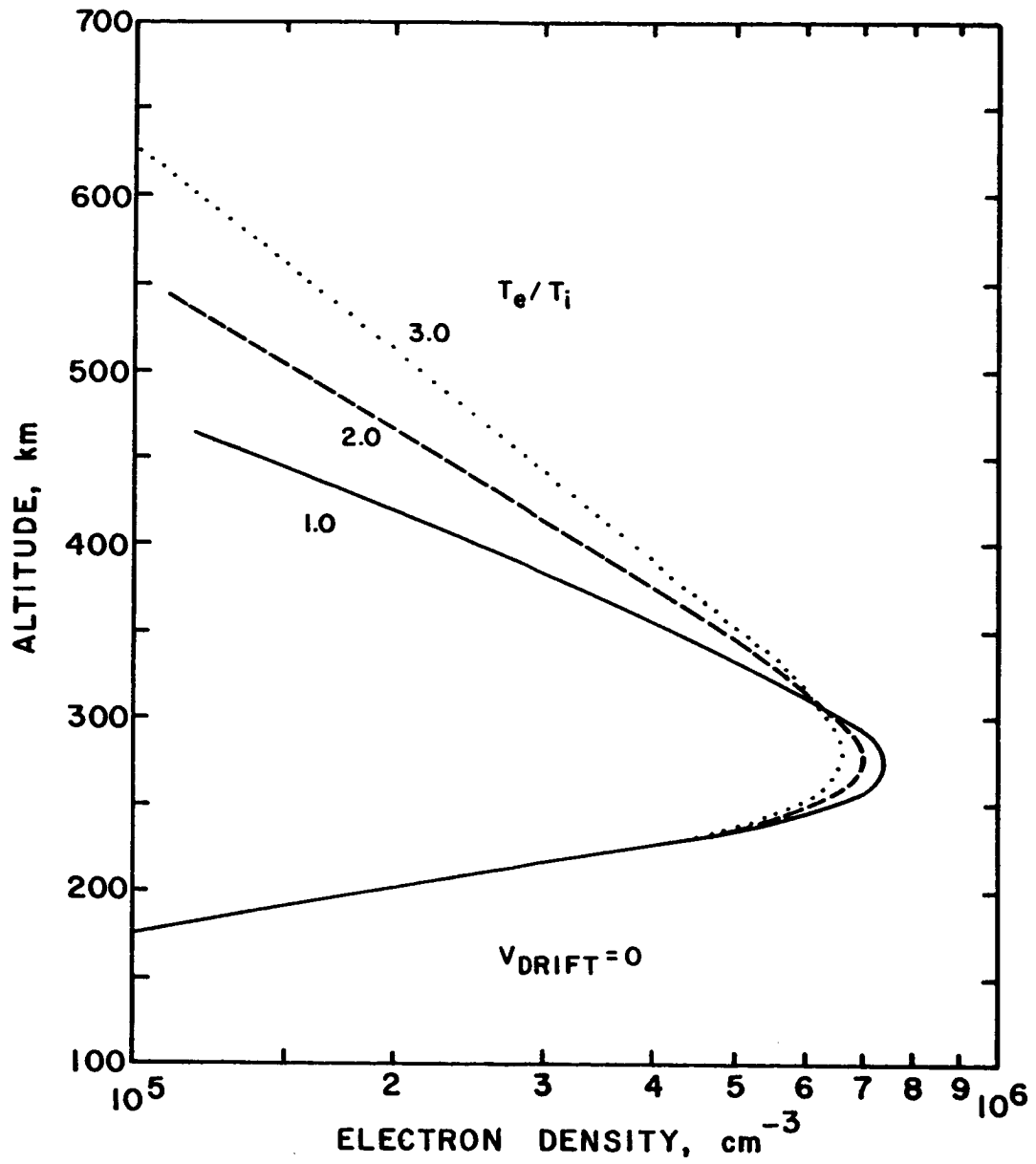
FIGURE 40. EQUILIBRIUM DENSITY PROFILES
FOR SEVERAL TEMPERATURE RATIOS.
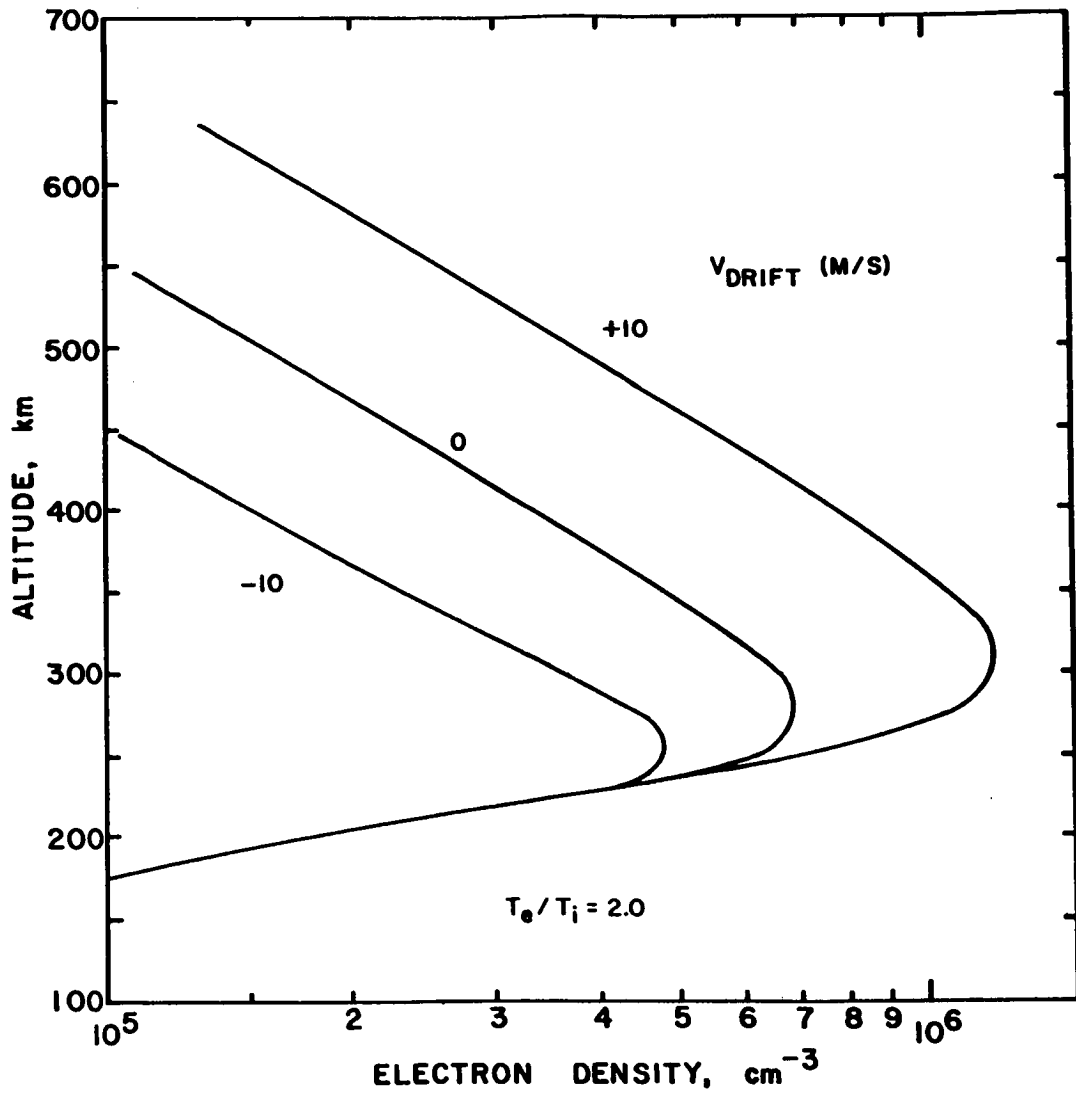
FIGURE 41.   EQUILIBRIUM   DENSITY   PROFILES
WITH   UNIFORM   DRIFT   VELOCITIES.

respectively. Unequal variation is a consequence of the exponential altitude dependence of production, loss, and diffusion. The electron content above 150 km changed by +88% and -41% compared to the no drift model. At a dip angle of 45 degrees, the 10 m/s drift velocities correspond to a north-south neutral velocity of 20 m/s or an east-west electric field of 7×10^{-4} volts/m.

The response of the model F layer to a sudden change of electron temperature is illustrated in Figure 42. The densities were initially in equilibrium at an electron temperature of 1600° K and the temperature was increased to 1800° K at time equals zero. A slow non-uniform oscillation developed about the final equilibrium density values at all altitudes with apparently lengthening periods. About one hour was required for the minimum peak density to occur; this time decreased at higher altitudes and increased below the peak. For the 200° K or 12% electron temperature change, the peak density varied by about 2%.

When an equilibrium density profile was allowed to relax from an initially upward drift velocity of 10 m/s, as seen in Figure 43, the peak density and content decreased exponentially with a time constant about 13400 seconds. Several hours were required for the layer to return near its unperturbed values.

4.3.2 Electron Temperature Profiles

We are interested in knowing the dependence of electron temperatures on electron densities and the time constants of relaxation toward equilibrium of the electron temperatures.
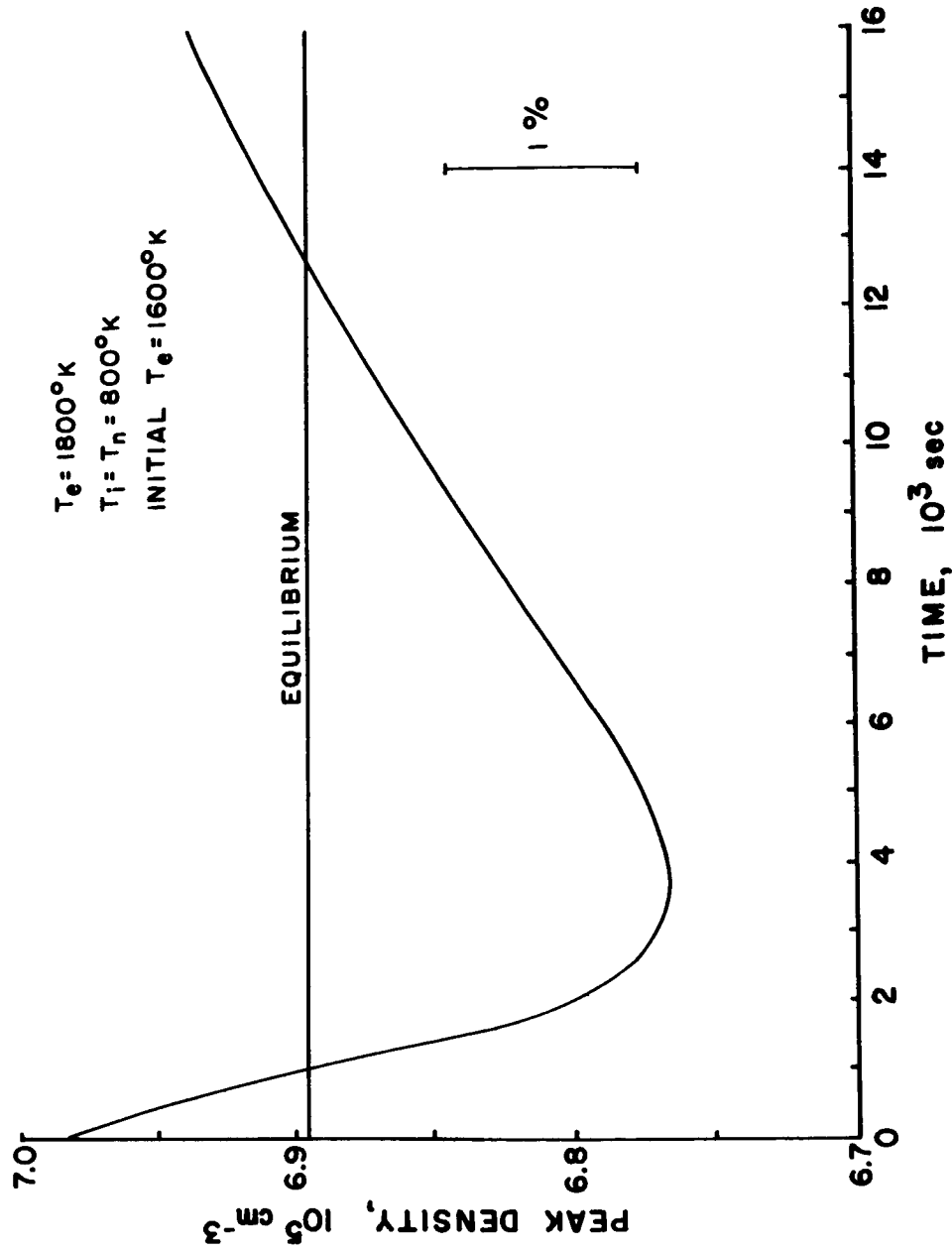
FIGURE 42. RESPONSE OF PEAK DENSITY TO ELECTRON TEMPERATURE CHANGES
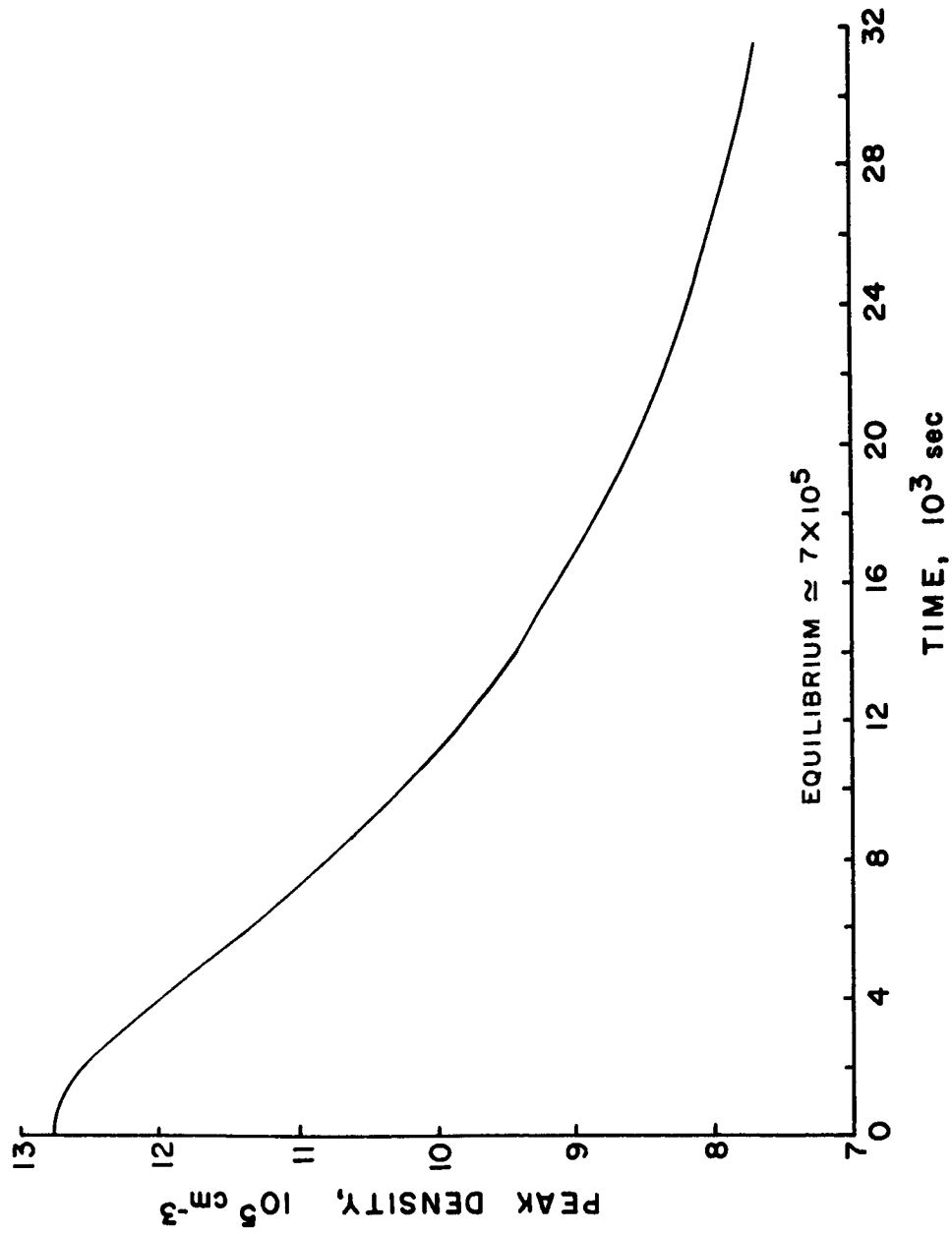
FIGURE 43. RESPONSE OF PEAK DENSITY AFTER
REMOVAL OF INITIAL + 10 m/s DRIFT

The energy equations for electron and ion gases were developed in Section 4.2 as

$$\frac{3}{2} k N_e \frac{\partial T_e}{\partial t} = Pu_e - Lu_e + \sin^2 I \frac{\partial}{\partial z} (K_{Te} \frac{\partial T_e}{\partial z}) \qquad (4-13)$$

$$Pu_i = Lu_i \qquad (4-14)$$

The ion temperature Equation 4-14 is most easily discussed first. Energy is transfered to the ion gas by electron-ion collisions from the hotter electron gas, and energy is lost to the neutral gas by ion-neutral collisions. The ions are not known to gain appreciable thermal energy in the photoionization process. The ion temperature is computed at each time and altitude by equating the electron-ion and ion-neutral energy transfer rates listed in Table 3. Only atomic oxygen ions are used.

Energy loss rates of the electron gas to the ion and neutral gases are also listed in Table 3. In the computations, losses to the neutral particles were neglected above 350 km. Energy is transfered to the ambient electron gas by collisions with energetic photoelectrons. The problem of how the photoelectrons share their energy between electrons and neutrals and how they migrate through the ionosphere has not been fully solved yet. Consequently, we shall adopt the energy production rates of Banks (1966 d) for Pu_e; and, to be consistent, the same neutral atmospheric model by Nicolet (1967) will be used. This atmospheric model has an exospheric temperature of 800° K and corresponds to solar minimum day-time conditions. The energy production rates are a maximum near 140 km due to absorption of the ionizing solar radiation, and they include high altitude non-local heating by migrating photoelectrons.

Table 3 Energy Transfer Rates, from Banks (1966 a, b)

Electron-ion

$$\frac{7.7 \times 10^{-6}}{16} \frac{(T_e - T_i)}{T_e^{3/2}} N_e^2 \; ev \; cm^{-3} \; sec^{-1}$$

Electron-neutral

rotational with O_2 and N_2

$[10^{-13} N(O_2) + 3.1 \times 10^{-14} N(N_2)] T_e^{-1/2} (T_e - T_N) N_e$

$ev \; cm^{-3} \; sec^{-1}$

vibrational with N_2 above $T_e = 800^o K$

$(1.49 + 1.5 \times 10^{-7} T_e^2) \times 10^{-15} (T_e - T_N) N(N_2) N_e ev \; cm^{-3} \; sec^{-1}$

elastic with

O: $3.74 \times 10^{-18} T_e^{1/2} (T_e - T_N) N(O) N_e \; ev \; cm^{-3} \; sec^{-1}$

O_2: $1.21 \times 10^{-18} (1 + 3.6 \times 10^{-2} T_e^{1/2}) T_e^{1/2} (T_e - T_N) N(O_2) N_e$

$ev \; cm^{-3} \; sec^{-1}$

N_2: $1.77 \times 10^{-19} (1 - 1.21 \times 10^{-4} T_e) T_e (T_e - T_N) N(N_2) N_e$

$ev \; cm^{-3} \; sec^{-1}$

Ion-neutral

$O^+ - O$ resonance

$2.04 \times 10^{-15} (T_i + T_N)^{1/2} (T_i - T_N) N(O) N_e \; ev \; cm^{-3} \; sec^{-1}$

The coefficient of electron thermal conduction, K_{Te}, is from Banks (1966c) and includes the reduction of the coefficient at low altitudes by frequent electron-neutral collisions. His coefficient is

$$K_{Te} = \frac{7.7 \times 10^5 \ T_e^{5/2}}{1 + 3.22 \times 10^4 \ \frac{T_e^2}{N_e} \ \Sigma \ N(neutrals) \ Q_D} \quad ev \ cm^{-1} sec^{-1} \ {}^oK^{-1}$$

where N(neutrals) are the densities of the major neutral species atomic and molecular oxygen and molecular nitrogen. Q_D is the electron-neutral momentum transfer cross section for each neutral species:

$$Q_D = 2.82 \times 10^{-17}(1 - 1.21 \times 10^{-4} T_e) \ T_e^{1/2} \ cm^2 \ for \ N_2$$

$$Q_D = 2.2 \times 10^{-16}(1 + 3.6 \times 10^{-2} \ T_e^{1/2}) \ cm^2 \ for \ O_2$$

$$Q_D = 3.4 \times 10^{-16} \ cm^2 \ for \ O$$

with $200 \leq T_e \leq 4500 \ {}^oK$. Summation extends over these neutral gases. By way of comparison, the electron thermal conductivity of a fully ionized gas is

$$7.7 \times 10^5 T_e^{5/2} \quad ev \ cm^{-1} \ sec^{-1} \ {}^oK^{-1}$$

At low altitudes (120 km) the coefficient of conduction becomes small because the neutral densities are large there. Hence, the thermal energy flux, $-K_{Te} \nabla Te$, also tends to become small at the

lower altitudes. The electron energy loss rate coefficients become larger with decreasing altitude because the neutral densities increase. Consequently, the electron gas is in good thermal contact with the neutral gas; and the electron temperature is largely set by local energy production and loss. As a boundary condition at the lowest altitude of 120 km we will assume that the electron temperature is controlled completely by local production and loss.

At high altitudes well above the F2 peak thermal conduction can be more important than local energy production and loss. Judging from the incoherent backscatter data, the electron temperature in the upper F region is relatively uniform with altitude so that an upper boundary condition could be imposed on the temperature gradient, or heat flux, rather than on the temperature itself. We will assume that the electron temperature gradient at the upper boundary of 800 km satisfy the equation

$$-(\sin I) \, K_{Te} \, \frac{\partial Te}{\partial Z} = \phi \text{ at 800 km}$$

where ϕ is an arbitrary thermal flux.

Equation 4-13 is non-linear in the dependent variable T_e so that some approximations must be made for time dependent solution. da Rosa (1966) linearized all electron temperature terms and solved the resulting equation by an implicit integration method. Banks (private communication) suggested that some simplification could be achieved by using a new variable θ defined as

$$\theta = T_e^{7/2}$$

and by linearizing the remaining non-linear terms implicitly as part of the integration method itself rather than make formal expansions. We will use Banks' suggestion coupled with the even weighted, central difference, implicit method of Diaz (1958) used for the electron density model calculations.

Making the transformation $\theta = T_e^{7/2}$ the thermal conduction in the vertical direction becomes

$$\sin^2 I \frac{\partial}{\partial z} \left(K_{T_e} \frac{\partial T_e}{\partial z} \right) = \frac{2}{7} \frac{\partial}{\partial z} \left(K_z \frac{\partial \theta}{\partial z} \right)$$

where $K_z = \sin^2 I \, K_{T_e} / T_e^{5/2}$, and K_z is just a constant divided by the altitude dependent electron-neutral collision reduction factor. Equation 4-13 becomes

$$\frac{\partial \theta}{\partial t} = \frac{7 \theta}{3 N_e k T_e} \left[Pu_e - Lu_e + \frac{2}{7} \frac{\partial K_z}{\partial z} \frac{\partial \theta}{\partial z} + \frac{2}{7} K_z \frac{\partial^2 \theta}{\partial z^2} \right] \qquad (4-25)$$

Implicit linearization is achieved by treating $7\theta/(3N_e kT_e)$, K_z, P_{ue}, and L_{ue} as known at the last time step while replacing the other θ terms on the left hand side of Equation 4-25 with the average of their values at that time with their unknown values at the following time step. Boundary conditions are applied by solving the equation

$$P_{ue} = L_{ue}$$

at 120 km for Te by Newton's iteration method and by setting

$$\frac{\partial \theta}{\partial z} = -\frac{7}{2} \frac{\phi}{K_z \sin I}$$

at 800 km, where ϕ is a specified energy flux. The ion temperature is evaluated with each new electron temperature profile.

Equilibrium electron temperatures were computed for several of the electron density models discussed in the preceding section. The temperatures were initially found by equating production and loss until a maximum temperature was found and then the temperatures at altitudes above this region (about 150 km) were set equal to this maximum value. For the F region, the initial temperatures were about 2900° k.

The equilibrium electron temperatures from the computations are shown in Figures 44 and 45. The results in Figure 44 are for two electron density models calculated in the preceding section,
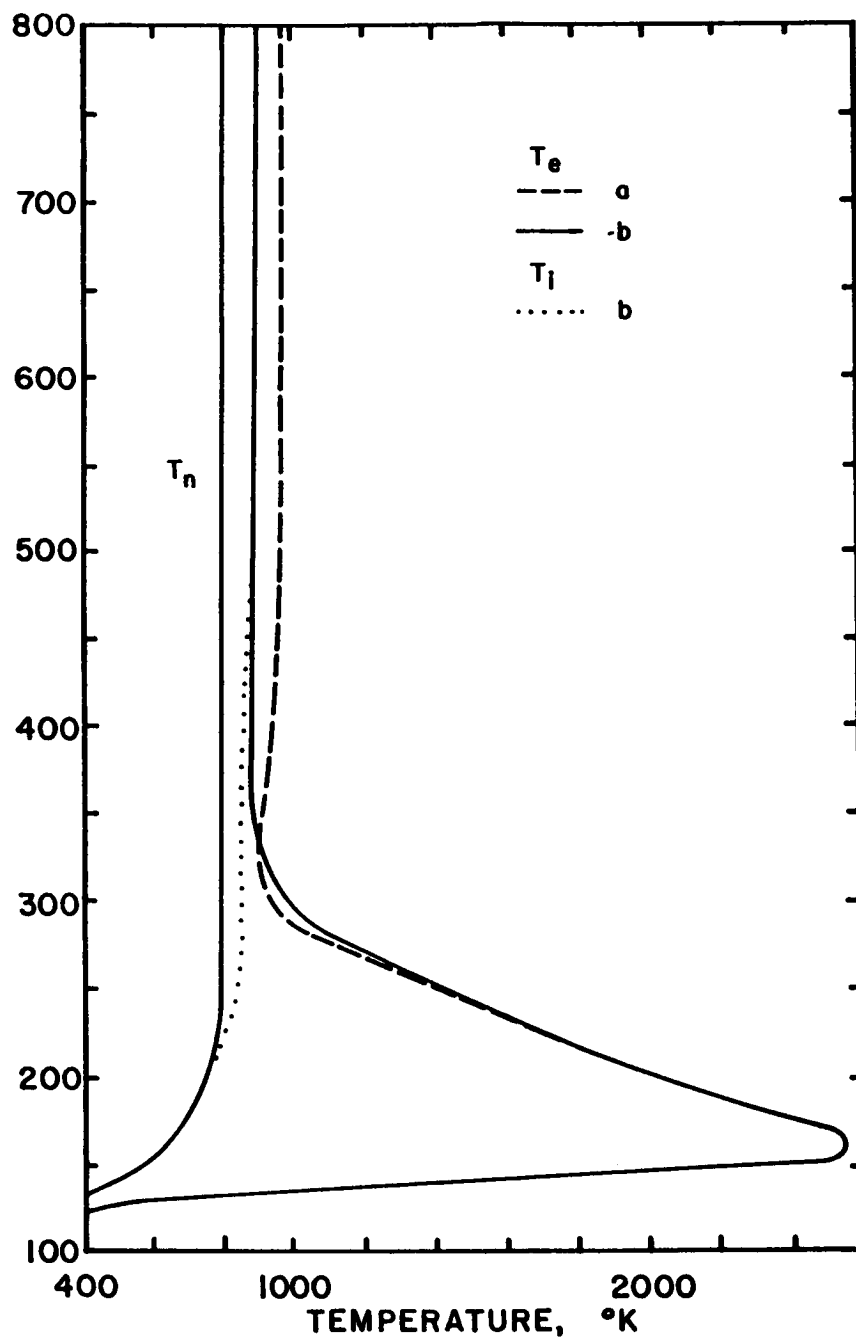
FIGURE 44. ELECTRON TEMPERATURES FOR CASE
a: ELECTRON DENSITY MODEL FOR $T_e/T_i = 1$
AND CASE b: DENSITY MODEL FOR $T_e/T_i = 3$.
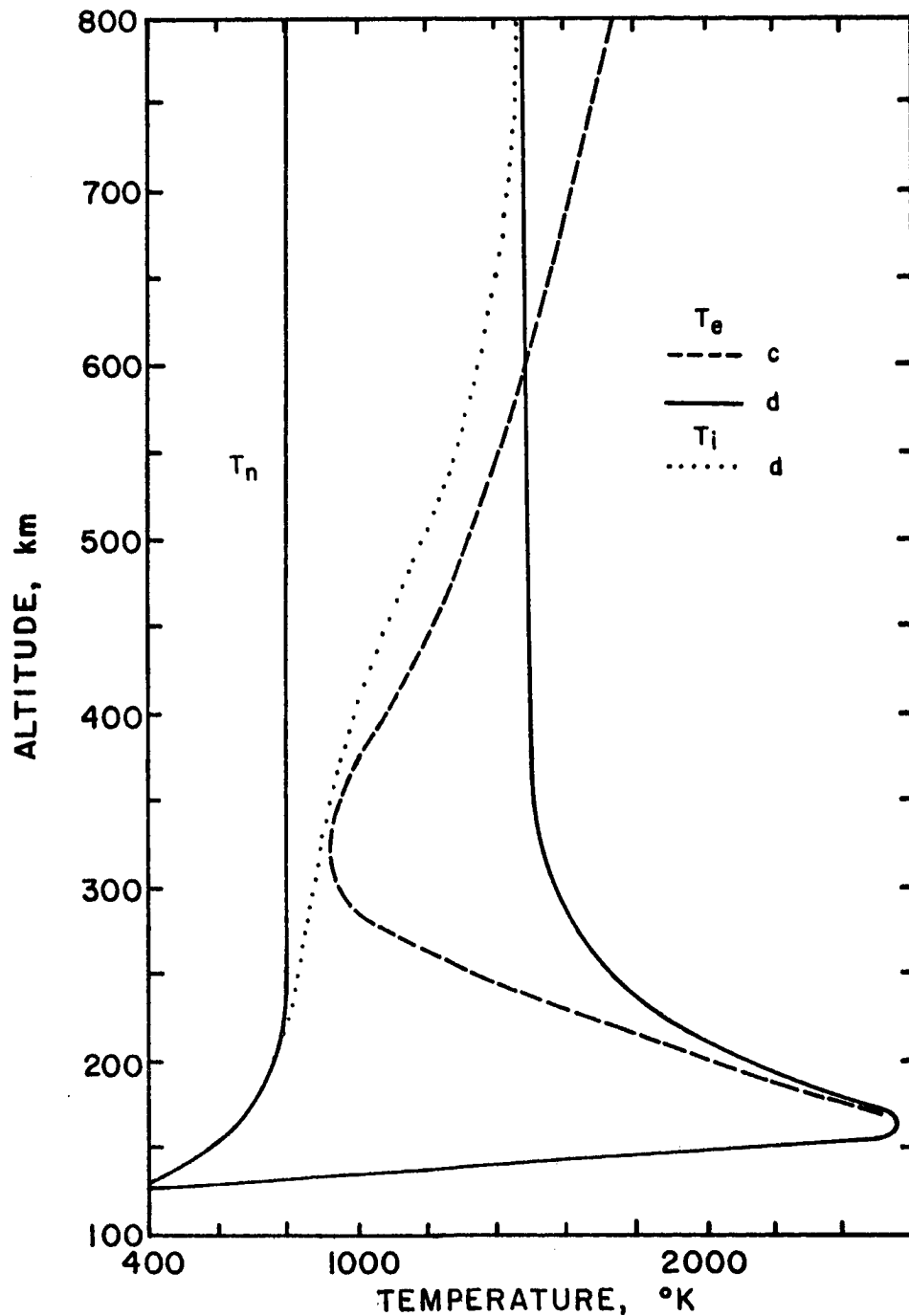
FIGURE 45. ELECTRON TEMPERATURES FOR CASE
c: -10^9 ev cm^{-3} sec^{-1} FLUX AND DENSITY MODEL
FOR $T_e/T_i = 2$ AND CASE d: DENSITY MODEL
FOR $T_e/T_i = 2$ AND -10 M/S DRIFT VELOCITY.

one for $Te/T_i = 1$ and the other for $Te/T_i = 3$ (Figure 44).
Large electron temperatures near 160 km are due to the small
electron densities of the models at that altitude; increasing
those densities would reduce the local electron temperatures.
Above 160 km, the energy production rate is insufficient to keep
the temperature above $2000^\circ k$; and minimum electron tempera-
tures are reached about 50 km above the F2 peak. Above the
peak, conduction causes nearly uniform temperatures. The
external energy flux was zero for these two calculations. Although
there are large relative density differences above the F2 peak
for these density models, the electron temperatures there show
little difference.

Two different cases are shown in Figure 45. Case (c) indicates
the electron temperatures resulting from a downward heat flux
at 800 km of 10^9 ev $cm^{-3} sec^{-1}$ with the equilibrium density
model in Figure 40 for $Te/T_i = 2$. The large temperature rise
above 320 km for case (c) is due entirely to the injected heat flux.
Case (d) in Figure 45 corresponds to zero heat flux at the upper
boundary but an electron density profile in Figure 41 for which
$Te/T_i = 2$ and a downward 10 M/S drift velocity. Reducing the
density and altitude of the F2 peak allowed higher electron
temperatures.

The time for the electron temperatures to reach equilibrium
from an initial value near $2900^\circ K$ was about ten minutes.
Relaxation was exponential in time with time constants of about
30 seconds at 200 km to 85 seconds at 400 km. The final values

of the F region temperatures were much lower than those measured at Arecibo for comparable F region electron densities.

Little temperature difference was seen between results with the two electron density models representing low and high temperatures. Addition of a large downward thermal flux did not affect the electron temperatures near the F2 peak.

CHAPTER 5 ANALYSIS OF EXPERIMENTAL DATA

5.1 Vertical Transport Velocity

The vertical transport velocity of F region electrons and ions is useful in determining if the observed density fluctuations could be caused by a transport mechanism, such as neutral atmosphere motion or electric fields. The method of computing the transport velocity from electron density profiles is taken from Chandra, Gibbons, and Schmerling (1960).

The electron density continuity equation, Equation 4-1, is integrated over an altitude range to evaluate the particle fluxes entering and leaving the volume

$$\frac{\partial}{\partial t} \int_{z_1}^{z_2} N_e \, dt = \int_{z_1}^{z_2} (P - \beta N_e) dz - (N_e v)_{z_2} + (N_e v)_{z_1}$$

(5-1)

where v is the vertical transport velocity. If the electron denisty, production rate, and loss rate coefficient are assumed known then the differences of fluxes, $N_e v$, can be computed. Further, if the velocity does not change by an order of magnitude or more between height z_1 and z_2 then, by choosing z_2 to be a region of much smaller electron density than at z_1, the velocity at the level z_1 can be estimated. In the present work the upper altitude was 700 km, and the lower altitudes were 250, 300, 350, and 400 km. We will assume that the flux at 700 km is much smaller than the values at the lower four altitudes. Consequently, the vertical transport velocity will be computed from

$$v\Big|_{z_1} = \frac{\left[\dfrac{\partial}{\partial t} \displaystyle\int_{z_1}^{700 \text{ km}} Ne \, dz - \displaystyle\int_{z_1}^{700 \text{km}} (P - \beta Ne) \, dz\right]}{Ne\Big|_{z_1}}$$

(5-2)

The loss rate coefficient, β, was assumed to be

$$\beta = N(N_2) \times 2 \times 10^{-12} \times \exp\left[(335 - T_n)/260\right]$$

(5-3)

$$+ N(O_2) \times 7 \times 10^{-12} \times \exp\left[(620 - T_n)/460\right]$$

where the rate coefficients are one half of the values constructed from Donahue's (1966) graphical data and where the neutral densities and temperature were taken from Harris and Priester's model atmospheres in CIRA 1965. The CIRA model 2 ($S_{10.7} = 75$) was used for the December data and model 3 ($S_{10.7} = 100$) for the summer data.

Production of electron-ion pairs was assumed to be directly proportional to the atomic oxygen density since effective absorbtion of the solar radiation begins at lower altitudes. No dependence on solar zenith angle was employed. The constant relating production to atomic oxygen density was determined by assuming that the ratio of loss to production at the F2 peak was about 0.7 during periods of slow density fluctuations based on the results of the electron density model computations. Theoretically, this constant is the product of the solar flux and atomic oxygen ionization cross sections integrated over all

wavelengths. During computation of the transport velocities
it was found that Donahue's (1966) loss rates, and the subsequent
production rates, were too large. Consequently, the loss
rates were halved as indicated in Equation 5-3; and the pro-
duction rates then were in agreement with the production data
of Hinteregger et al (1965). The same production constant was
used for both summer and winter data computations.

Rates of change of electron content in Equation 5-2 were
determined by eye from smooth experimental data. Generally,
the derivations were not very accurate. Considering that
production and loss rates and content changes were each unknown
by perhaps a factor of two, not much emphasis can be placed
on the magnitudes of the computed transport velocities. The
way the velocities change with time, however, is believed to
be indicative of the changes of the true velocities.

Vertical transport velocities estimated for each of the
six incoherent backscatter experiments are shown in Figures
46 through 51. The diffusion velocity component, estimated
from the electron density model studies, is about -5 to -10 m/s
near the F2 peak and perhaps twice as large at 50 km below
the peak.

During the winter, the altitude of the F2 peak tends to follow
the variations of the transport velocities with the lowest
altitudes occuring when the velocities are most negative (down-
ward). Upward velocity fluctuations usually precede electron
density increases by one half or one hour; peak density
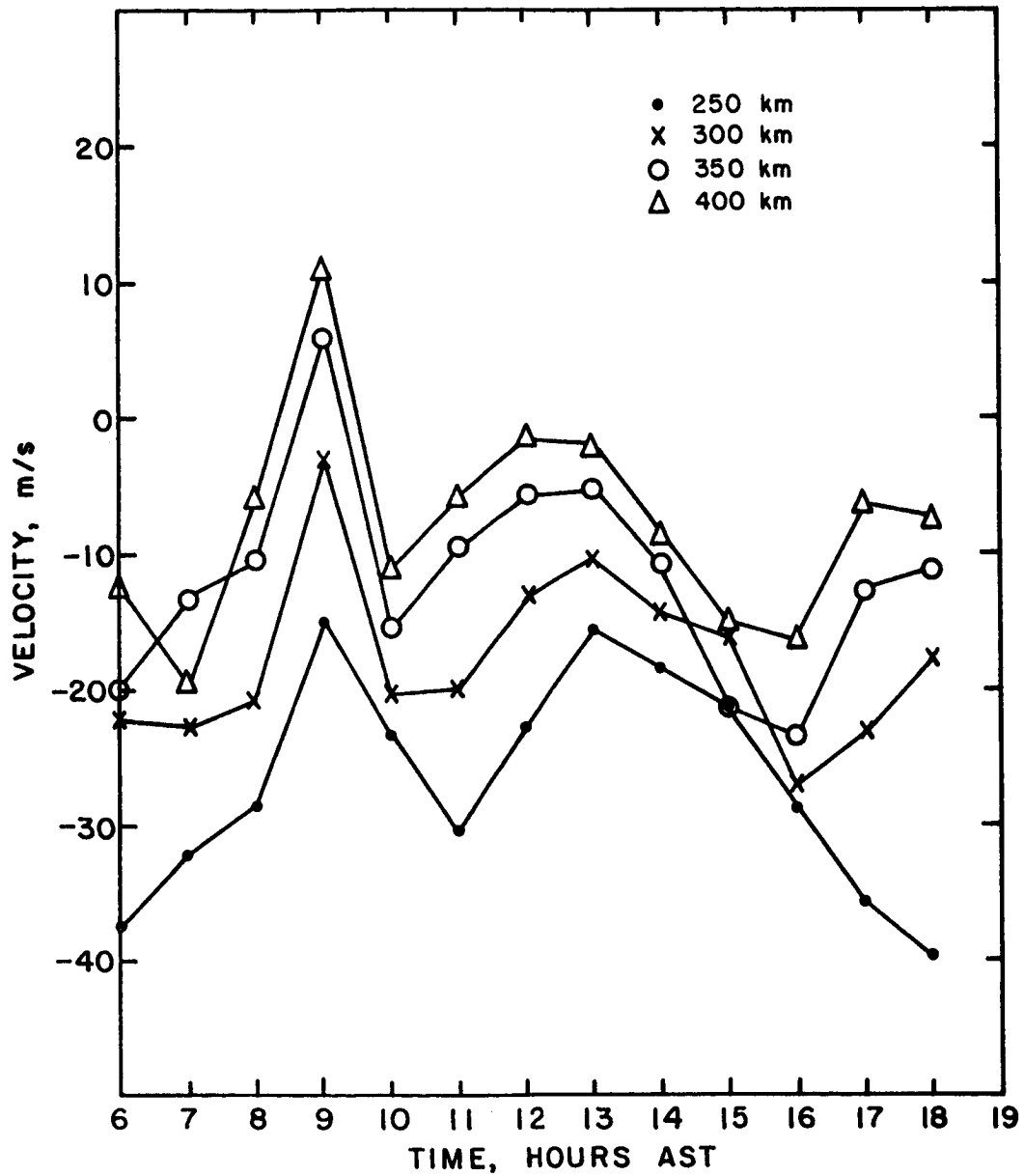
FIGURE 46 COMPUTED VERTICAL TRANSPORT VELOCITIES AT ARECIBO ON DECEMBER 15, 1965.
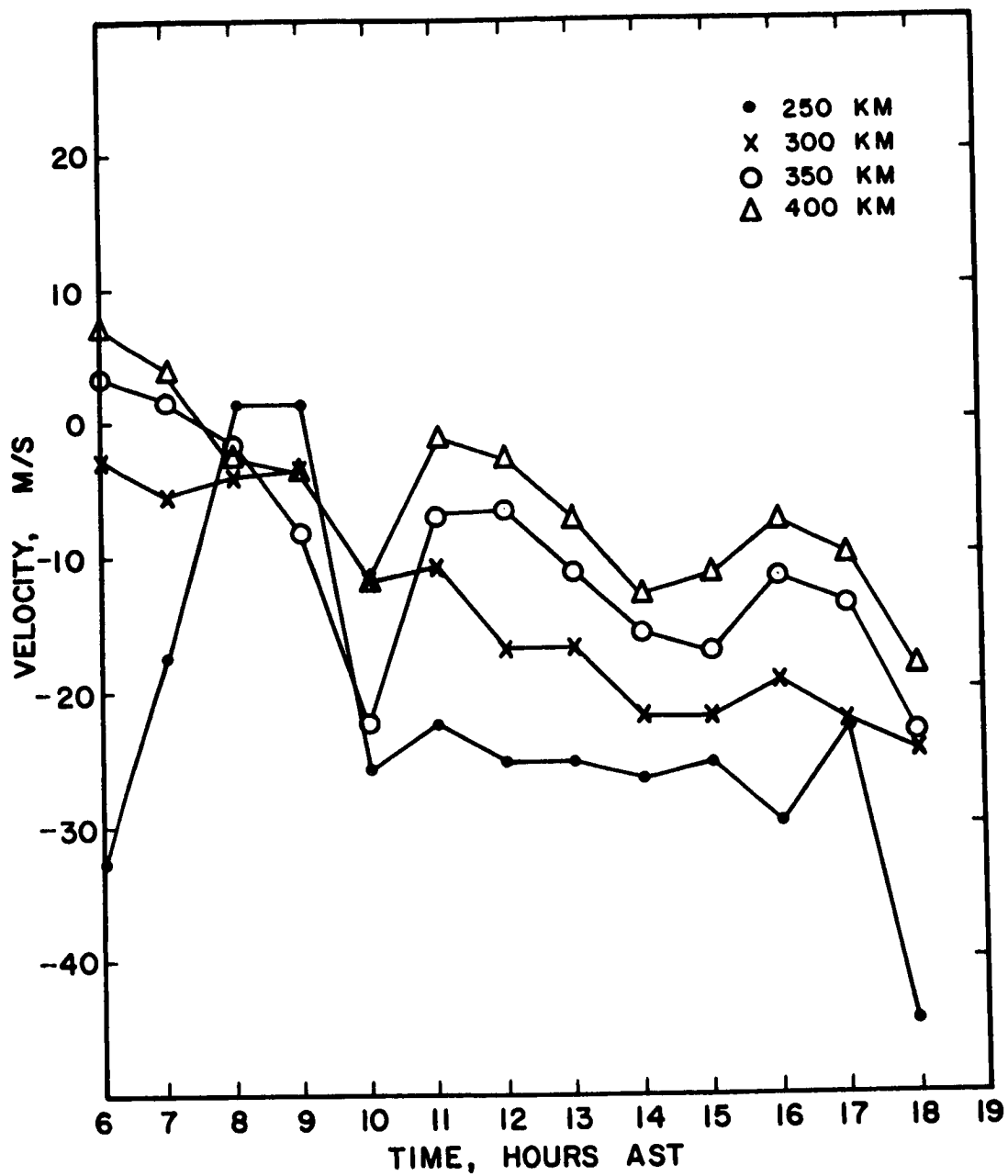
FIGURE 47. COMPUTED VERTICAL TRANSPORT
VELOCITIES AT ARECIBO ON DECEMBER 22, 1965
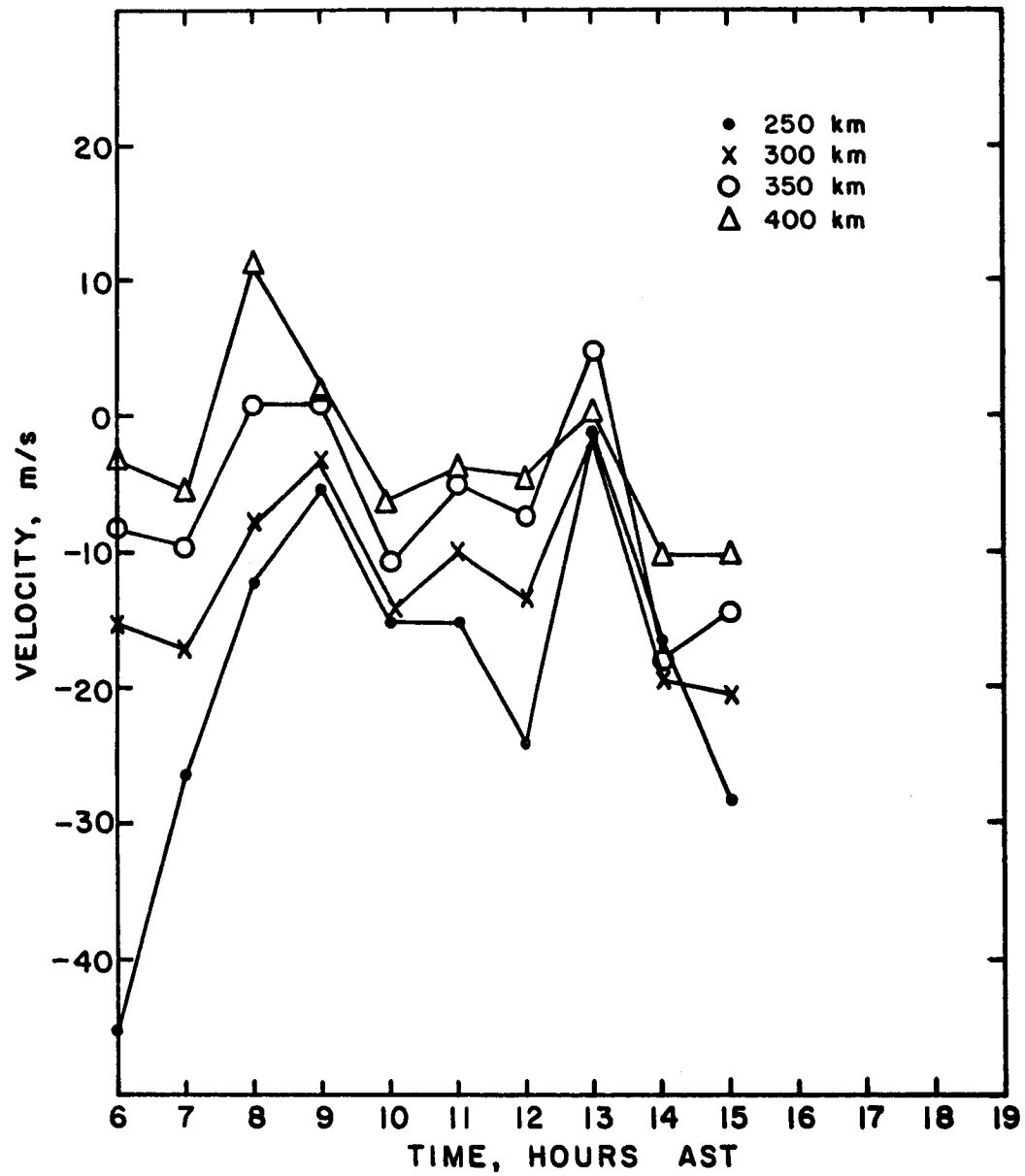
FIGURE 48   COMPUTED VERTICAL   TRANSPORT
VELOCITIES   AT ARECIBO   ON   DECEMBER
29, 1965.
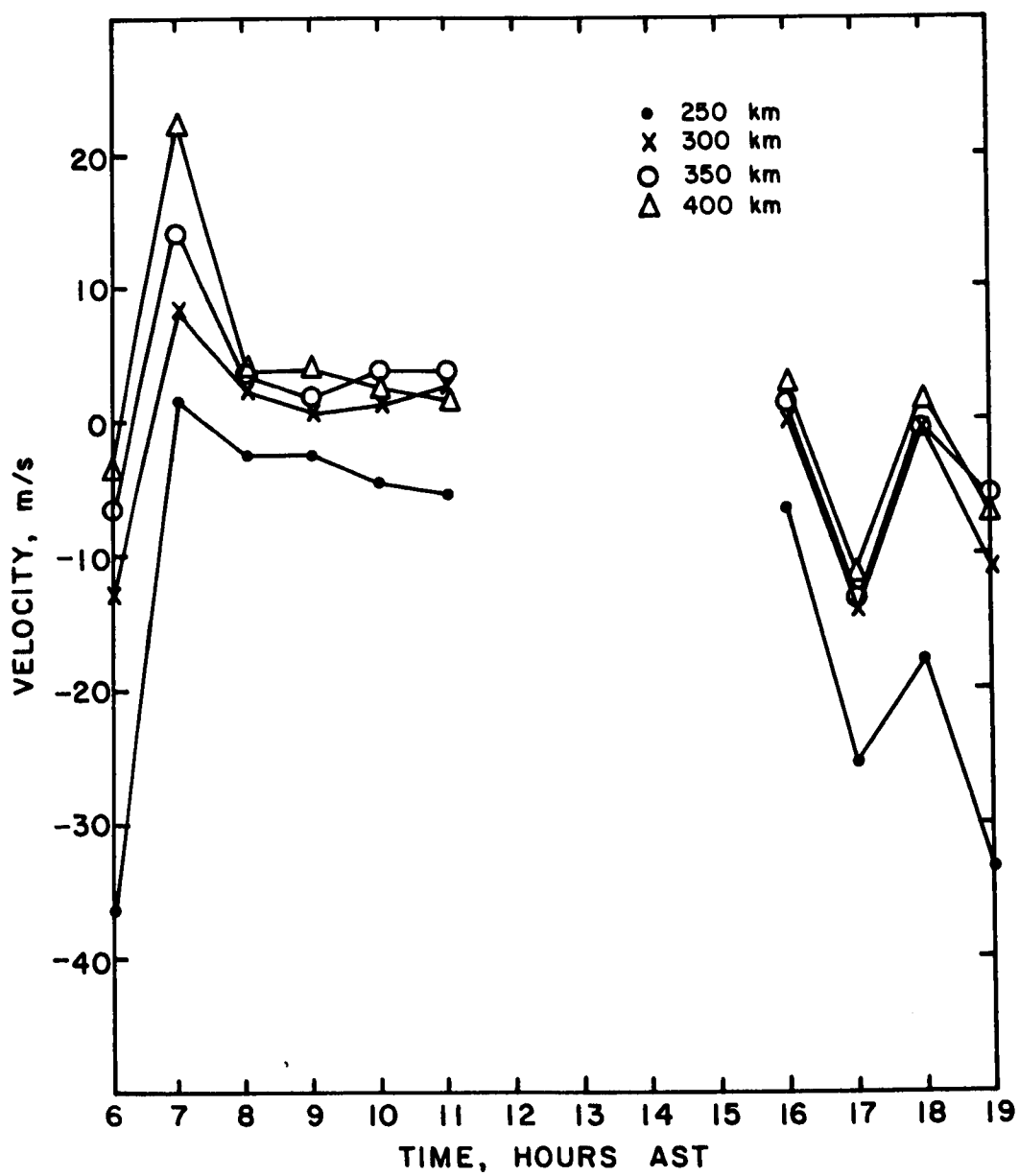
FIGURE 49   COMPUTED VERTICAL TRANSPORT
VELOCITIES AT ARECIBO ON JULY 22, 1966.
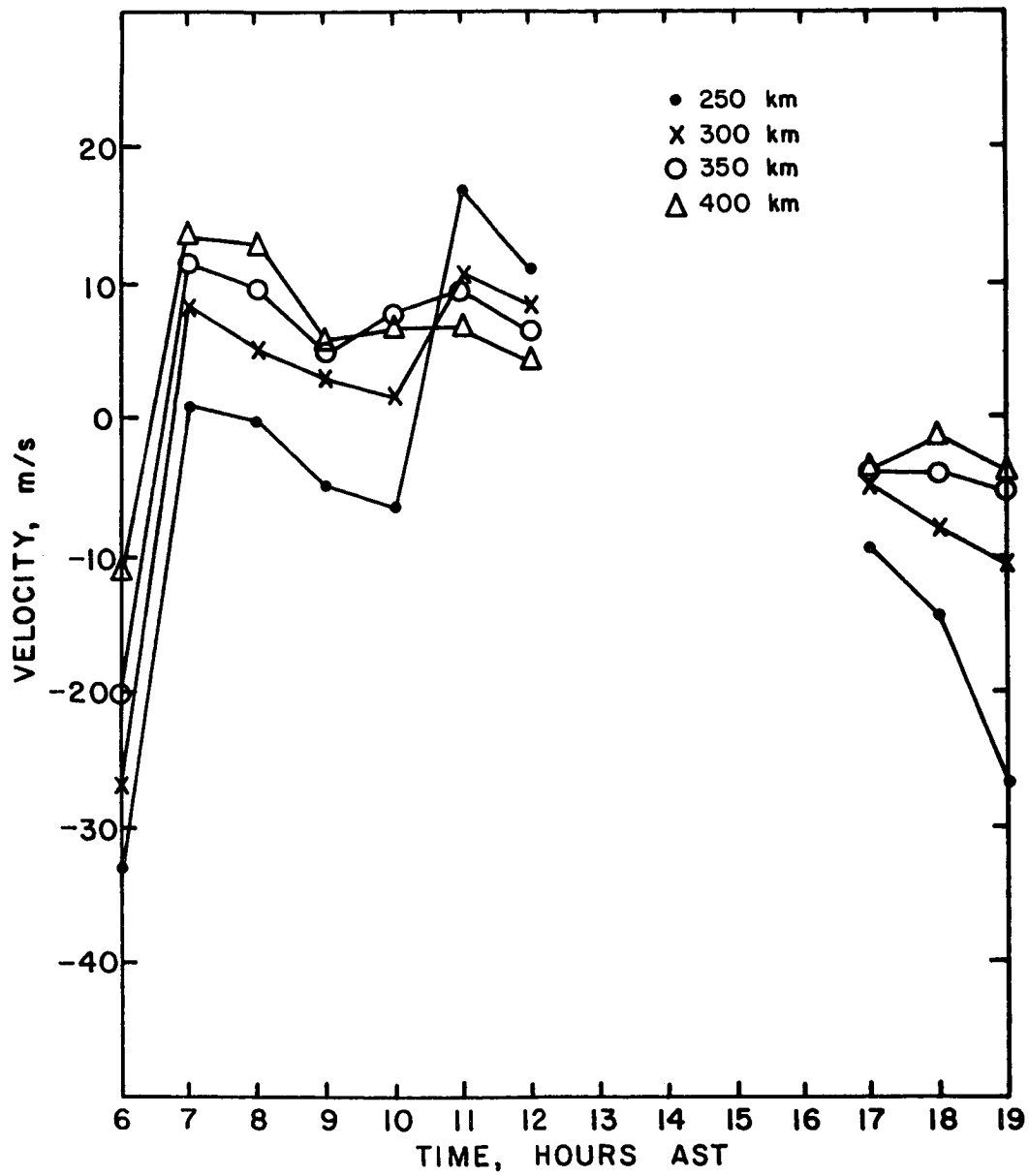
FIGURE 50   COMPUTED   VERTICAL   TRANSPORT
VELOCITIES   AT   ARECIBO   ON   JULY 30, 1966.
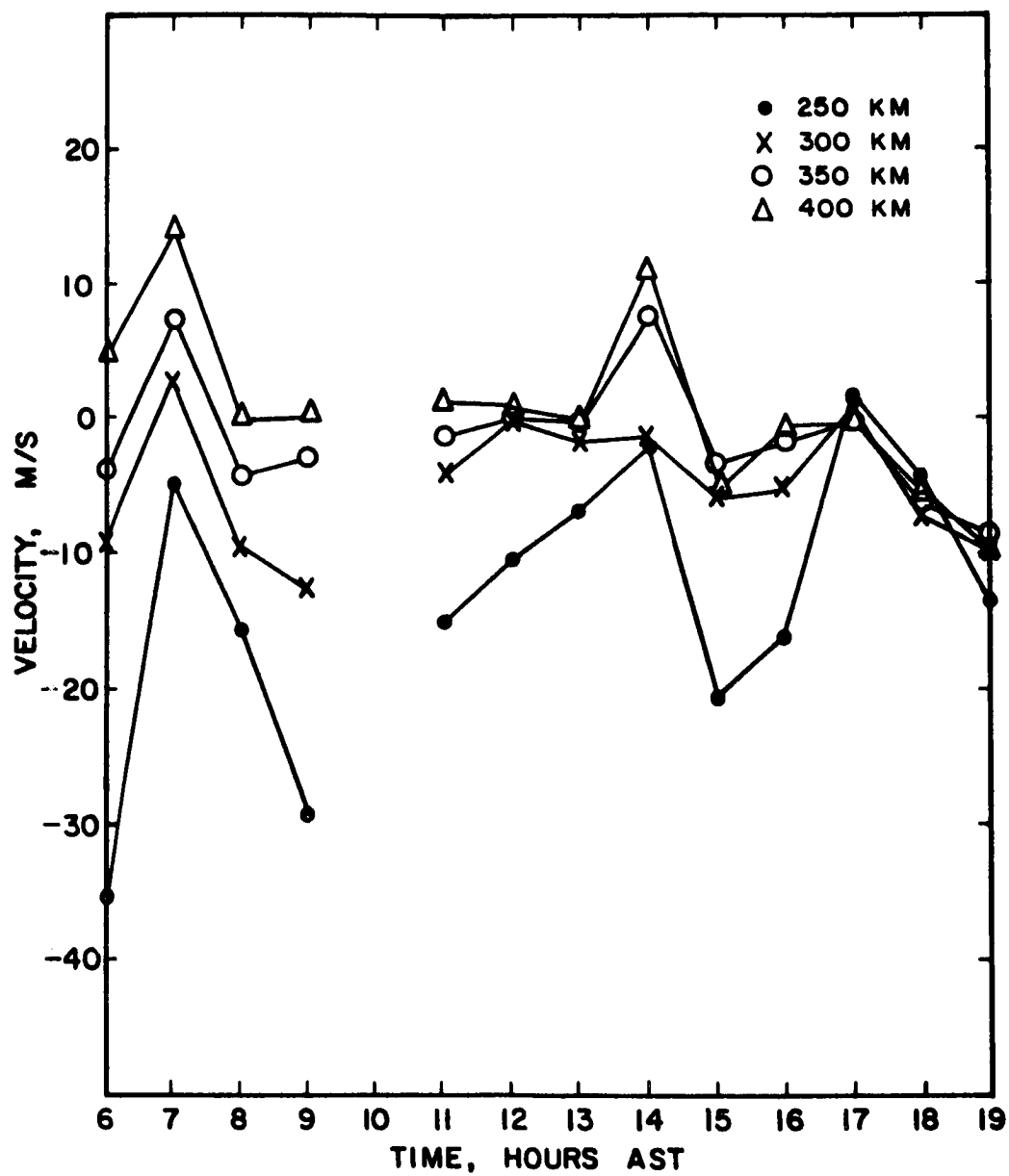
FIGURE 51. COMPUTED VERTICAL TRANSPORT
VELOCITIES AT ARECIBO ON AUGUST 17, 1966

fluctuations tend to lag behind higher altitude fluctuations by one half hour. The velocities at 250 km near sunrise (0615 AST at 100 km) and sunset (1830 AST at 100 km) are more negative than their true values since variations of solar zenith angle were not used in the calculations.

On December 15, the velocity fluctuation about 09 hours AST is associated with electron densities which rise until ten hours and with a rapid content increase until the same time. The 12 hour decrease of the F2 peak density occurs during a period of rapidly increasing electron content, decreasing velocities, and of increasing peak altitude. The afternoon density peak near 16 hours AST occurs during rapid decreases of content, altitude of the F2 peak, and velocities. The fluctuations of foF2, then, reflect expansions and compressions of the F2 region at rates faster than the normal relaxation rates.

Velocities during the morning of December 22 show an interesting pattern of upward movement only near the peak about one hour before the large peak density increase at 0930 and downward movement at all altitudes during the decreasing phase of the density fluctuation. This dual behavior of the velocities before 09 hours is not consistent with an electric field driven drift since all the velocities should have the same pattern. Neutral particle motion could explain the density fluctuation if the motion were to change direction

and strength with altitude. Transport of ionization to the
F2 peak from above and below would cause the large densities
there. Unfortunately, the data are too widely separated in
time for a detailed examination. Strong downward velocities
at 250 km during the remaining part of the day are in agree-
ment with the low altitudes of the F2 peak.

Peak electron densities on December 29 again demonstrate
that the largest values occur during the downward movement
phase of a preceding upward velocity fluctuation. The upward
velocity fluctuation between 08 and 09 hours AST followed by the
downward movement until ten hours results in rapid electron
content increases between 08 and 09 hours along with increasing
peak altitudes but the peak density is largest when the layer
movement reverses. Between ten and twelve hours the peak
densities and the peak altitude slowly decrease while the
velocities remain moderately downward. A strong, simultaneous,
upward movement beginning at 12 hours and maximizing at
13 hours results in maximum peak densities at 14 hours while
the electron content and peak altitude maximize at 1330 hours.
The morning velocity fluctuation is suggestive of a pertubation
moving downward at about 50 m/s (180 km/hour) such as a
slow speed gravity wave. The afternoon fluctuations are
simultaneous and are suggestive of an electrodynamic drift.

During the summer, the peak densities, altitude of the peak,
and the electron contents were much greater than the winter
values. The relatively constant increase of peak density and

peak altitude on July 22 were accompanied by small uniform transport velocities. A simultaneous velocity fluctuation centered on 07 hours AST signaled the beginning of the rising of the peak altitude, but there were no particular density fluctuations. In the late afternoon, the downward velocity fluctuation about 17 hours resulted in a small increase of peak density and a decrease of the electron content at all altitudes.

On July 30, the velocities indicate an upward density transport after 07 hours AST, but the altitude of the peak did not begin to increase until 08 hours. The peak density from 08 to ten hours remained relatively constant during the lifting, but it increased rapidly after ten hours as the velocities became more upward in the region of the peak.

A strong downward movement during the early morning on August 17 caused transport of ionization down to the F2 peak at rates faster than it could recombine, thus forming the 08 hour peak density fluctuation. The altitude of the peak was very low during this period, and the velocity at 250 km was strongly downward. The velocities apparently decreased after 09 hours to allow the F2 peak to move up to regions of smaller velocities. Fluctuations of the velocities between 14 and 16 hours AST are probably exaggerated because of difficulties in obtaining the rates of change of electron content.

To summarize these results, we find that the largest or least negative velocities are found during rapid electron content increases, that decreases of the F2 peak density occur during the

early part of these increases, and that the peak densities are largest during the following rapid decreases of the same event. The altitude of the peak changes at about the same time and in the same direction as the velocity fluctuations. The peak density fluctuations lag the velocity changes by about an hour as ionization is either added or removed from the peak region faster than loss or production processes can restore equilibrium. Some of the velocity fluctuations appear to be simultaneous between 250 km and 400 km such as on December 15 and 29 and on August 17 mornings while other fluctuations appear first at 400 km and require about an hour to reach to 250 km. Two fluctuations, on December 22 and July 30, are present at 250 km but are absent at 350 km and 400 km. It has not been possible to determine the absolute velocities but the summer values, except for the morning of August 17, appear to be constant and possibly slightly upward. The changes of velocity are larger than they are expected from diffusion alone.

5.2 Heat Balance

The equation representing the variation of electron temperature with time was found to be

$$\frac{3}{2} k N_e \frac{\partial T_e}{\partial t} = P_{ue} - L_{ue} + \sin^2 I \frac{\partial}{\partial z} \left(K_{T_e} \frac{\partial T}{\partial z} \right)$$

(4-13)

Time rates of change of electron temperature during the day were much smaller at Arecibo than the production and loss terms

and the time constant of relaxation was found to be short so that we will assume that the temperatures are in quasi-equilibrium.

The thermal conduction term of Equation 4-13 could not be estimated with confidence from the temperature measurements since it depends on the curvature of the temperature versus altitude profile. Thermal fluxes, $-\sin I \, K_{T_e} \, \partial T_e / \partial z$, were estimated from polynomial fits to the temperature profiles; and they were generally of the order 5×10^9 ev cm^{-2} sec^{-1} downward during the summer mornings and the winter days.

The major electron gas energy loss rate in the F2 region is to the ion gas,

$$L_{ei} = 4.8 \times 10^{-7} \frac{(T_e - T_i)}{T_e^{3/2}} N_e^2 \text{ ev cm}^{-3} \text{sec}^{-1} \qquad (5-4)$$

for atomic oxygen ions. The loss rate was computed at the central altitudes of the temperature measurements and the results for each experiment are shown in Figures 52 through 57. Electron temperatures between two and three times the ion temperature change the temperature part of the electron to ion energy loss rate by only 8%. Consequently, the variations of L_{ei} during the summer mornings and the winter days are caused almost entirely by electron density fluctuations.

Conduction is important during the density fluctuations since the production rate does not depend on the square of the electron densities. The effects of conduction are easily seen in the winter data between 10 and 14 hours AST because the electron
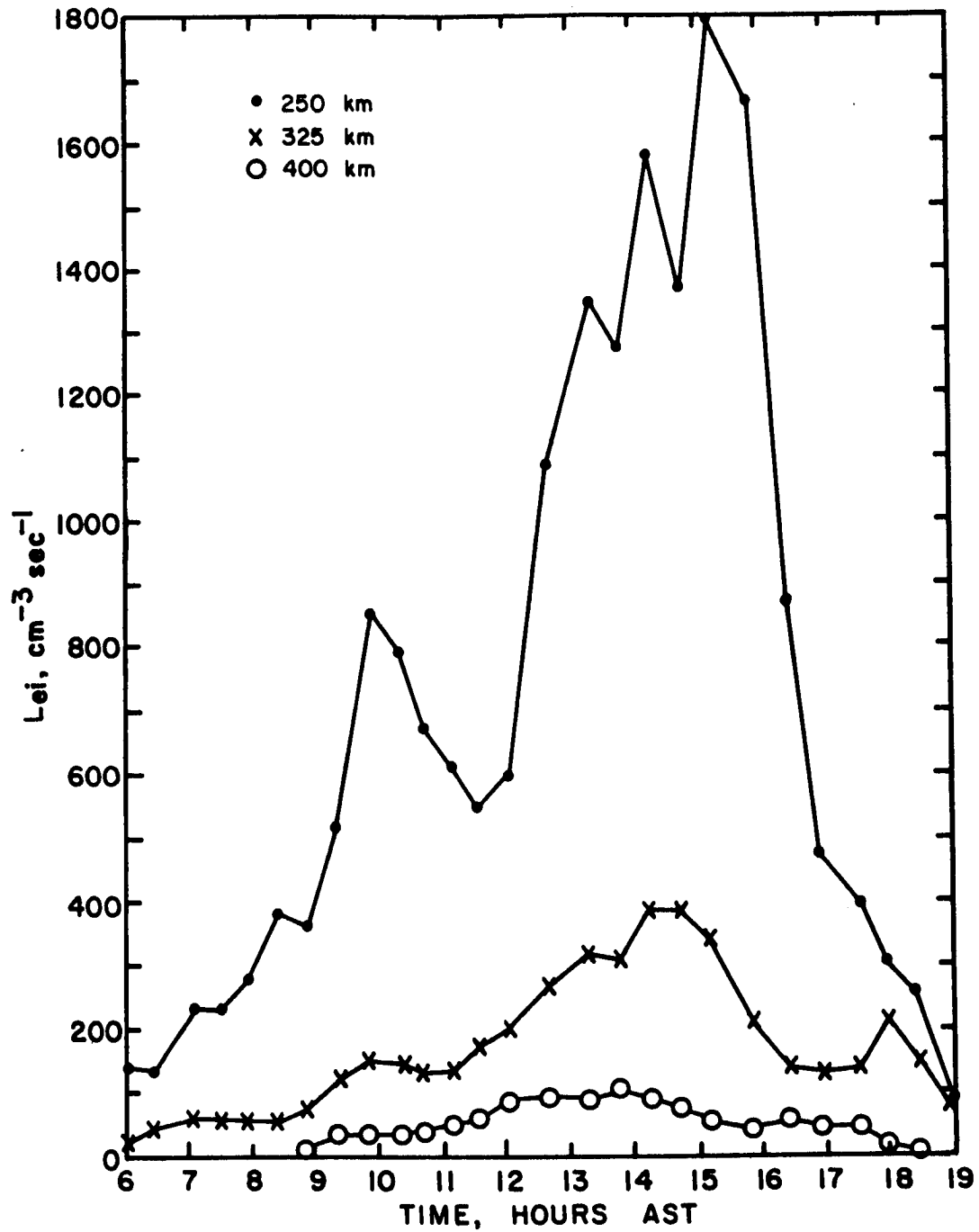
FIGURE 52   ELECTRON TO ION ENERGY LOSS RATES
ON DECEMBER 15, 1965.
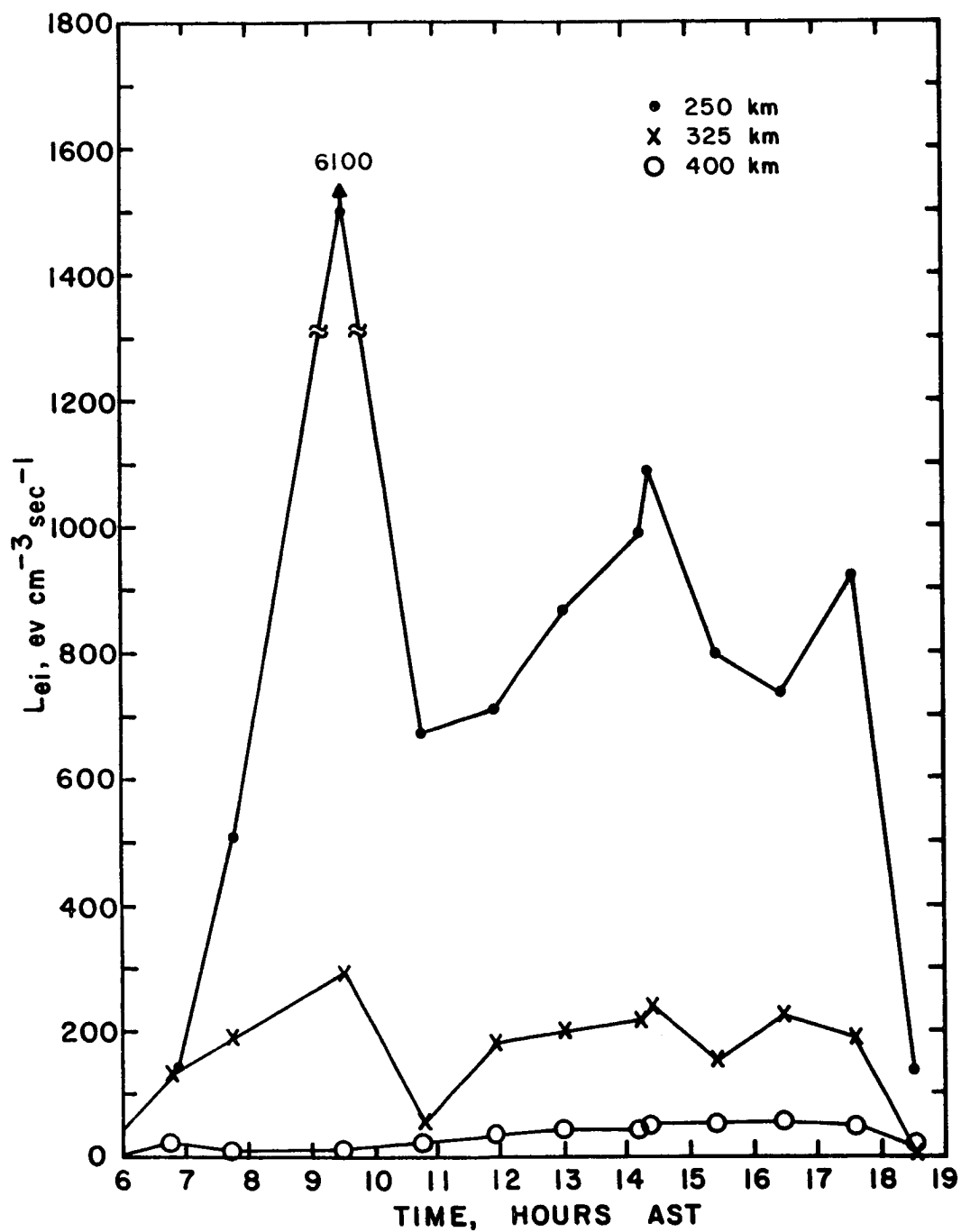
FIGURE 53 ELECTRON TO ION ENERGY LOSS
RATES ON DECEMBER 22, 1965.
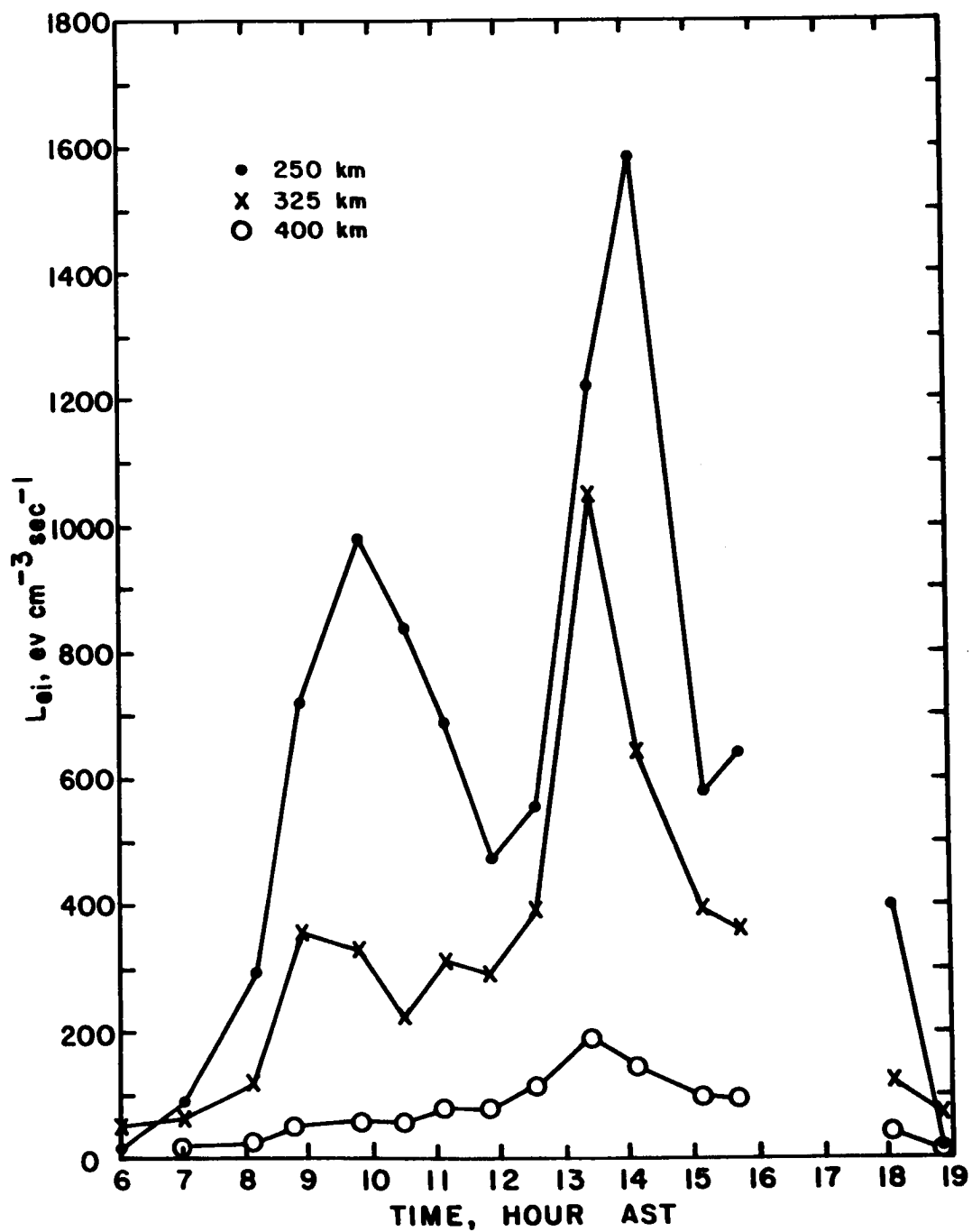
FIGURE 54 ELECTRON TO ION ENERGY LOSS RATES ON DECEMBER 29, 1965.
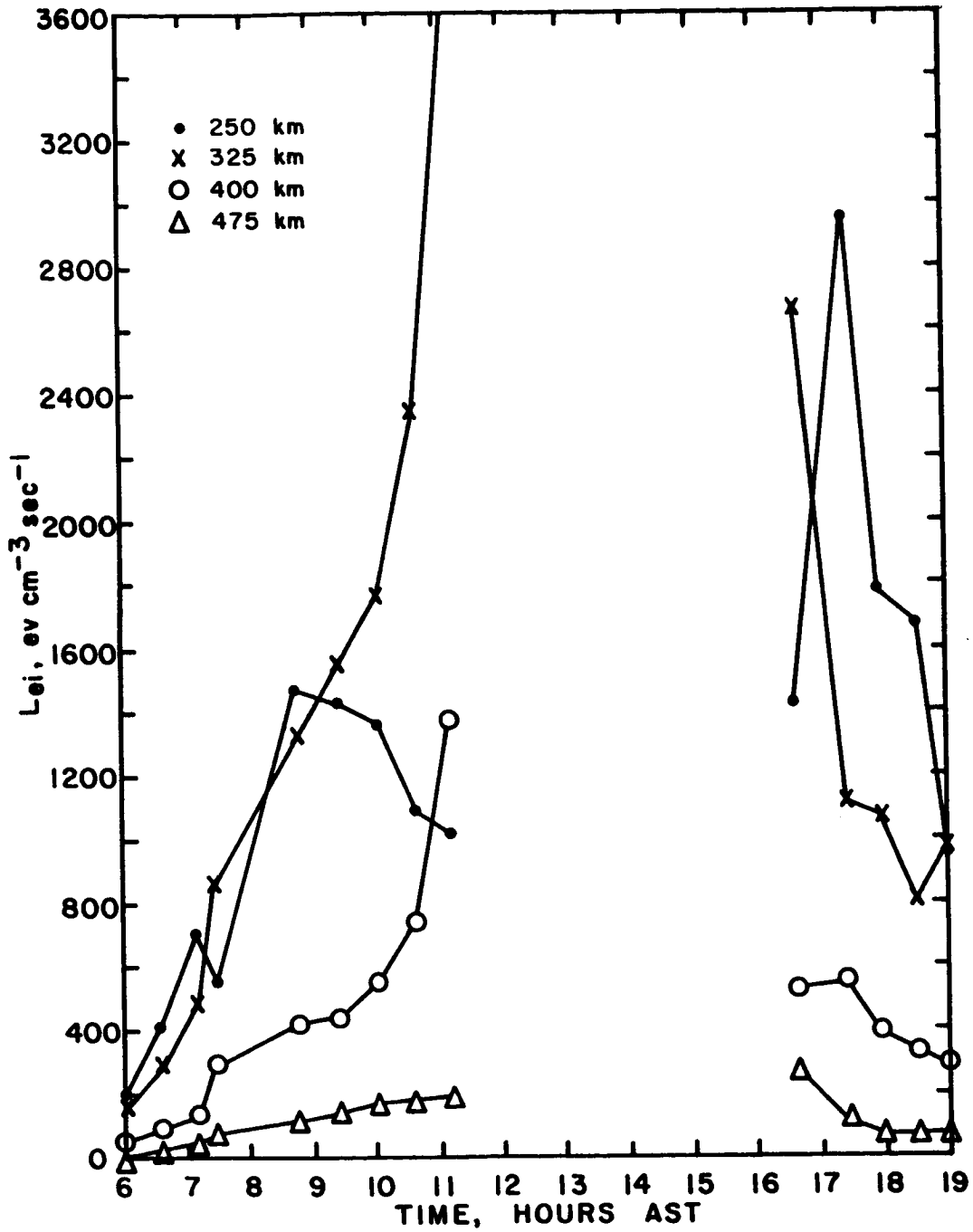
FIGURE 55 ELECTRON TO ION ENERGY LOSS
RATES ON JULY 22, 1966.
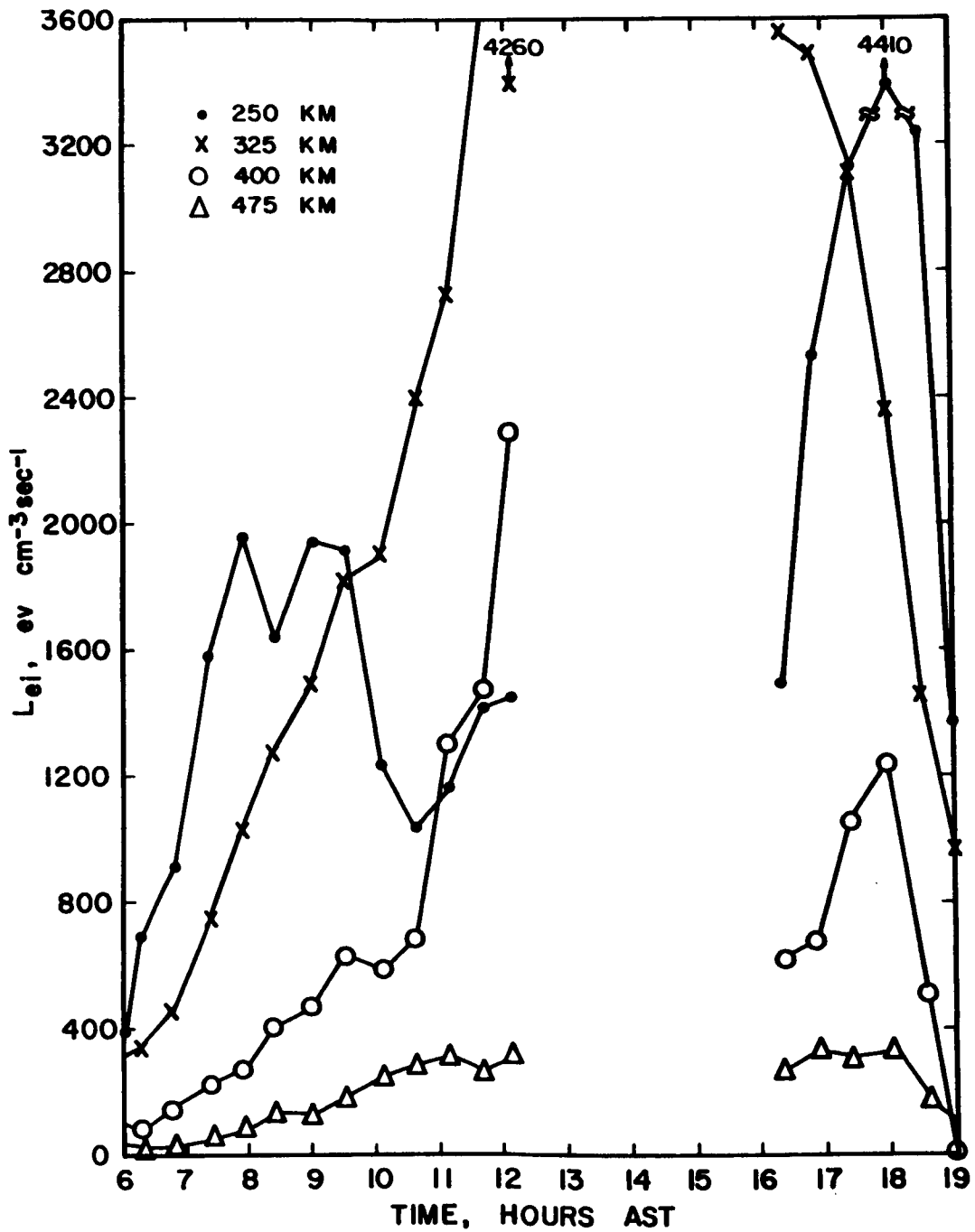
FIGURE 56.   ELECTRON   TO   ION   ENERGY   LOSS
RATES   ON   JULY   30,   1966
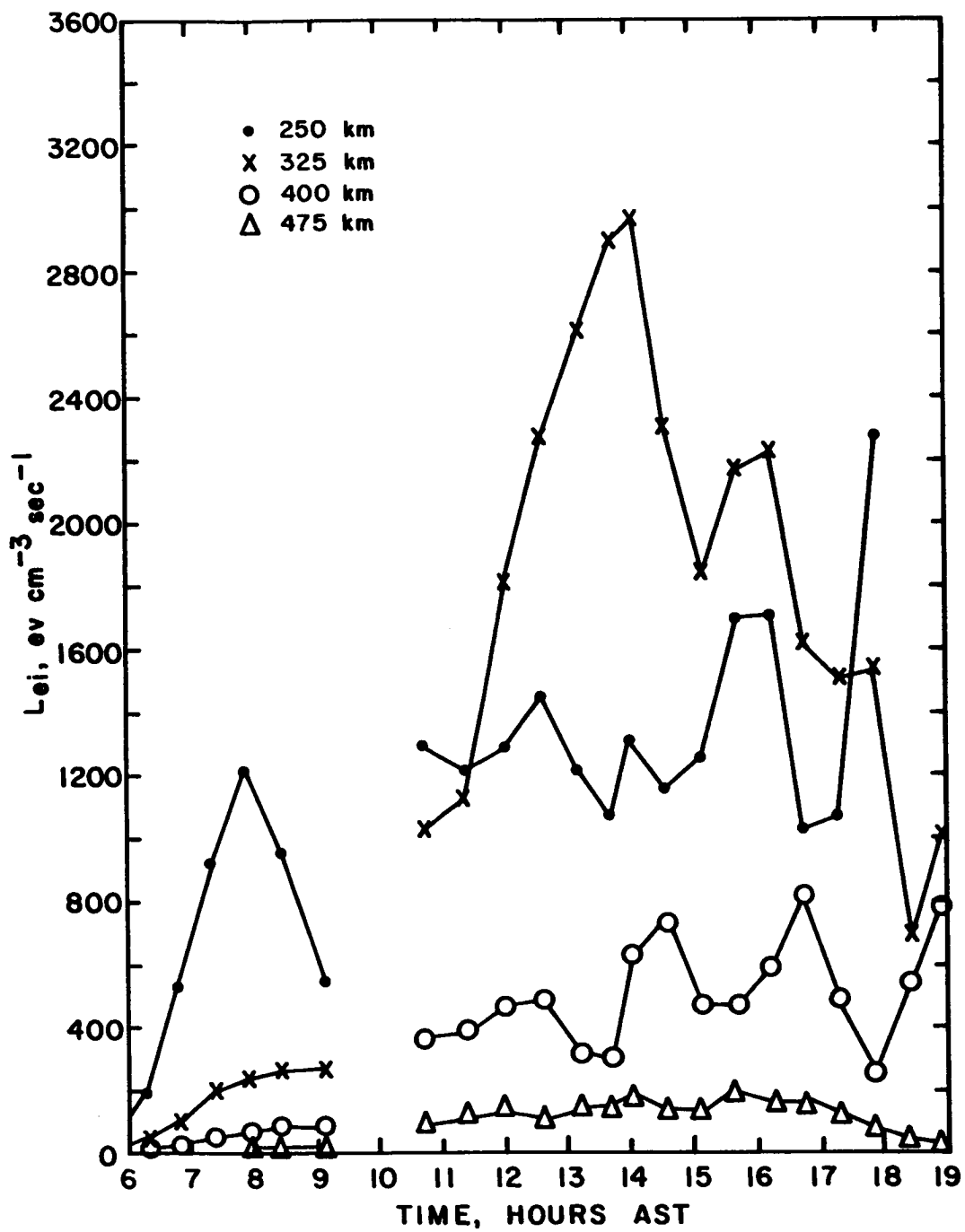
FIGURE 57   ELECTRON TO ION ENERGY LOSS
RATES ON AUGUST 17, 1966.

temperature fluctuations are much better correlated with the F2 peak electron densities than with the local electron densities. During the summer, the peak is higher and the peak densities are larger than in the winter; and the electron temperatures near the peak depend more on the local densities than on those away from the peak.

Model studies of electron temperatures in Chapter 4 with the energy production rates of Banks (1966 d) and reasonable F2 region electron density models showed much lower electron temperatures than the experimental data. Furthermore, the experimental temperatures typically increased above the peak while those of the models did not unless an upper heat flux were added. At lower F2 peak densities Banks' temperatures were comparable in size to experimental ones. Increasing the estimated energy production rates in the F2 region would help the agreement between theory and experiment but may not resolve it. Consider the 4000 ev $cm^{-3}sec^{-1}$ loss rate at 325 km on July 30, 1966 near noon. Computing the energy flux from the temperatures at each altitude given in Figure 15 we find about $4x10^9$ ev $cm^{-2}sec^{-1}$ flowing down from 475 km and $2.7x10^9$ev cm^{-2} sec^{-1} flowing up from 250 km. If this energy were distributed evenly over a 50 km altitude range about the F2 peak it would sustain a loss rate of only 1500 ev $cm^{-3}sec^{-1}$ which is much smaller than the computed losses there. The downward heat flux also suggests a heating rate of about 800 ev $cm^{-3}sec^{-1}$ somewhere between 400 and 475 km on the basis of a 50 km

scale height for the production mechanism; Banks' rate at 400 km is only 60 ev $cm^{-3} sec^{-1}$.

What appears to be required are energy production rates for the electron gas which depend on the ambient electron density. This is entirely reasonable since the photoelectrons, which supply the energy, share it between both neutral and electron gases. As the ratio of electron to neutral density increases the electron gas should receive a larger fraction of the photoelectron's energy.

5.3 Spaced Ionosondes

Values of the F2 peak critical frequency, foF2, at a number of ionosonde stations were shown in Figure 24 through 39. From these data we would like to determine how the fluctuations depend on local solar time and universal time, on latitude and longitude, and if any of them could be due to gravity waves.

The winter data at the low latitude stations, Arecibo, Jamaica, Mexico City, and Huancayo, typically consisted of morning and afternoon peaks and a midday dip of foF2. The approximate local solar and universal times at the midpoint of these fluctuations are given in Table 4 together with values for the middle latitude group of stations White Sands, Cape Kennedy, and Grand Bahama Island. Local solar time is a 24 hour clock with noon set at the time of solar zenith.

TABLE 4 TIMES OF f_oF2 FLUCTUATIONS FROM SPACED IONOSONDES

Station	Morning Peak			Midday Dip			Afternoon Peak		
	Civil Time	Universal Time	Solar Time	Civil Time	Universal Time	Solar Time	Civil Time	Universal Time	Solar Time
December 14, 1965									
WS	none			none			1130-1400	1830-2100	1130-1400
CK	0930-1030	1430-1530	0910-1010	>1100	>1600	>1040	<1330	<1830	<1310
GBI	0930	1330	0915	1130	1630	1115	<1330	<1830	<1315
AIO	--			--			1400-1500	1800-1900	1330-1430
JA	>1030	>1530	>1020	--			<1500	<2000	<1450
MC	1100	1700	1022	1230	1830	1200	1330	1430	1300
HU	1200	1700	1200	1400-1500	1900-2000	1400-1500	1730	2230	1730
December 15, 1965									
WS	0845	1545	0840	0945	1645	0940	1030-1230	1730-1930	1030-1230
CK	none			1100	1600	1040	1330	1930	1310
GBI	none			1100	1600	1045	1330	1930	1315
AIO	1015	1415	0945	1200	1600	1130	1530	1930	1500
JA	1045	1545	1040	1145-1245	1645-1745	1140-1240	1430	1930	1425
MC	--			--			1430	2030	1400
HU	0930	1430	0930	1200-1400	1700-1900	1200-1400	1800	2300	1800
December 21, 1965									
WS	none			none			1200	1900	1155
CK	1000	1500	0940	none			none		
GBI	1000	1500	0940	none			none		
AIO	1000	1400	0930	1300	1730	1230	1400-1500	1800-1900	1330-1430
JA	0930	1430	0925	1200	1700	1155	1400	1900	1355
MC	0930	1530	0900	1130	1730	1100	1400	2000	1330
HU	0900	1400	0900	1100	1600	1100	none		

TABLE 4 CONTINUED

Station	Morning Peak			Midday Dip			Afternoon Peak		
	Civil Time	Universal Time	Solar Time	Civil Time	Universal Time	Solar Time	Civil Time	Universal Time	Solar Time
				December 22, 1965					
WS	0845	1545	0840	0930	1630	0925	1115	1815	1110
CK	0815	1315	0755	1000	1500	0940	1515	2015	1500
GBI	0830	1330	0815	1000	1500	0945	1515	2015	1500
AIO	0930	1330	0900	1130	1530	1100	1500	1900	1430
JA	0930	1430	0925	1115	1615	1110	1430	1930	1425
MC	1000	1600	0930	1130	1730	1100	1430	2030	1400
HU	1200	1700	1200	1330	1830	1330	1500	2000	1500
				December 28, 1965					
WS	0845	1545	0840	1000	1700	0955	1200	1900	1155
CK	none			none			none		
GBI	none			none			none		
AIO	--			--					
JA	0945	1445	0940	1130	1630	1125	1530	1930	1500
MC	0830-1030	1430-1630	0800-1000	1200	1800	1130	1445	1945	1440
HU	none			none			1430	2030	1400
				December 29, 1965			none		
WS	0915	1615	0910	1030	1730	1025	1500	2200	1455
CK	none			1130	1630	1110	1330	1830	1310
GBI	none			1130	1630	1115	1315	1815	1300
AIO	1015	1415	0945	1200	1600	1130	1400	1800	1330
JA	none			1200	1700	1150	1400-1500	1900-2000	1400-1500
MC	1100	1700	1030	1300	1900	1230	1400	2000	1330
HU	0915	1415	0915	1200	1700	1200	1645	2145	1645

The most prominent fluctuations among these groups occured during the mornings of December 21 and 22. These fluctuations were more closely associated with local solar times than universal time. On December 21 the solar time of the morning peak increased with latitude and it was earlier at Mexico City than at Arecibo. The reverse time relation was found for the following day. The strength of the fluctuation was strongest at Arecibo, Jamaica, and Mexico City and very weak at the other stations. Disturbed ionogram traces were observed at Grand Bahama Island during the decreasing phase of both events.

The morning and afternoon peaks seem to occur at more nearly similar solar times rather that the same universal time, and from the limited number of data, they seem to occur a few minutes earlier at Cape Kennedy than at Arecibo. White Sands data were not well correlated with Cape Kennedy even though they are at the same magnetic latitudes. Changes of the fluctuations with longitude are easily seen on almost all the winter days for Arecibo, Jamaica, and Mexico City.

The summer data at Arecibo, Jamaica, and Mexico City are characterized by large afternoon values of foF2 where as the higher latitude data show almost constant values. The fluctuations at Jamaica and Arecibo were similar, at the same solar times, on July 21 and 22 and August 16 and 17. Mexico City and Arecibo data compared less well, and the phase of the August fluctuations were reversed at Mexico City. The morning foF2 dip at

Arecibo and Jamaica on August 16 and 17 was almost smoothed out at Mexico City.

To summarize, fluctuations at the three stations, Arecibo, Jamaica, and Mexico City, at the same geographic and geomagnetic coordinates were similar and occured at roughly the same local solar times. There were changes of the fluctuations between these stations, however, indicating a longitude or time dependence of the driving mechanisms. The fluctuations were greatly diminished at Cape Kennedy and Grand Bahama Island, and they were not observed at Wallops Island and Ottawa. Comparision of White Sands and Cape Kennedy data indicate that the fluctuations probably depend more on geographic than on geomagnetic latitude. No definite evidence could be found for internal gravity waves of the type discussed by Thome (1966) although there were some small scale irregularities revealed by ionograms which appeared to move downward through the F region. The similarity of the fluctuations at Arecibo, Jamaica, and Mexico City during both summer and winter suggest a common causative mechanism.

5.4 Magnetograms

The San Juan, Puerto Rico, magnetograms are applicable to this F region study only insofar as they indicate either the existence of electric fields or motions of the neutral atmosphere which may be similar to those in the F2 region.

Dougherty (1961) showed that electrodynamic drifts of the F2 region ionization would set the neutral atmosphere in motion within an hour and that the neutral motion would largely suppress vertical electrodynamic transport while increasing the effective ambipolar diffusion coefficient. Increasing the diffusion coefficient lowers the altitude, and consequently the density, of the equilibrium F2 peak. Therefore, we should expect the vertical electrodynamic drift velocities to be suppressed about an hour after beginning and the F2 peak to then move to lower altitudes and densities.

The conventional dynamo theory says that neutral atmospheric winds in the E and lower F1 regions drive the dynamo current system and electric fields result from the worldwide circulation patterns. Thus, magnetograms from a single station would be insufficient to compute the fields. We can compare the San Juan magnetograms with what is known about the Sq current system as a whole and with the electric fields for the system. Referring to Figures 4 and 9 of Maeda and Kato (1966) for the Sq current system and the estimated F region vertical electrodynamic drift velocities we find that southward currents produce the upward drifts and that these currents decrease the declination component of the geomagnetic field at San Juan.

The magnetic data in Figures 19 to 23 then indicate an upward drift in the morning after 08 hours AST in the winter and after 04 or 06 hours AST in the summer. Neutral motion

in the F2 region layer should reduce the drifts by 09 or 10 hours in the winter and by 06 or 07 hours in the summer. An afternoon downward drift would occur generally between 12 and 14 hours in both summer and winter. The backscatter data, however, indicate a general upward motion in the winter between 08 and 10 hours AST and, more importantly, a second upward movement centered near 14 hours. In the summer there is a downward movement, especially on August 17, in the morning and the absence of a downward movement in the afternoon. The conventional dynamo theory, therefore, does not predict the observed F region fluctuations.

Coupling of neutral winds in the dynamo region to those in the F2 region is probably weak since the chemical trails released from rockets indicate the existence of variable wind directions as a function of altitude through the dynamo region. These variable winds also complicate the computation of dynamo currents and electric fields since ground based magnetograms measure the vector sum of the various currents.

An alternative to the wind driven dynamo theory is that electric fields generated in the magnetosphere and transmitted along geomagnetic field lines produce the dynamo currents Fejer, (1963). Rishbeth, Megill, and Cahn (1965) estimated the time necessary for ions to accelerate the neutral atmosphere to the ion drift velocity would be of the order 3.4 hours at 140 km. during sunspot minimum daytime conditions and that this time delay would increase at lower altitudes. Therefore, we will

neglect neutral atmospheric motion in the dynamo region and suppose the currents are due entirely to an external electric field. Using Equation 17 of Maeda and Kato (1966) together with their conductivity graphs we can estimate the eastward component of the F region electric field to be roughly

$$E \simeq 1.6 \times 10^{-4} \ (\Delta D - \Delta H) \ \text{volts/meter}$$

at a dip angle of 45 degrees when ΔD and ΔH are measured in gammas to the west and north, respectively, from their unperturbed values. Over Arecibo, the vertical component W of the drift velocity, $\mathbf{E} \times \mathbf{\bar{B}} / B^2$, would be about

$$W \simeq 2.5 \ (\Delta D - \Delta H) \ \text{m/s}$$

Whether D and H have equal weighting as we have assumed depends on the values chosen for conductivities in the dynamo region. W would be reduced in the F2 region by subsequent neutral particle motion about an hour after commencement.

According to the external electric field theory, the morning decrease of D would produce an initial downward drift, and early in the afternoon there would be an upward drift. An increasing H field during the morning would add to the downward drift. The winter magnetograms indicate the downward ionization drift should begin around 07 hours for H and 08 hours AST for D and an upward drift between 12 and 14 hours. On Decmeber 22, the unusual decrease of H and the smaller decrease of D from 08 to 11 hours could lead to an

upward drift if ΔH were more important than ΔD. The similar foF2 fluctuation on the preceding day is not indicated on the magnetograms, however. Similarly, the sharp decrease of H and the increase of D on December 29 would lead to an upward drift starting after 12 hours AST. The summer magnetic data indicate stronger downward morning drifts occuring near sunrise and larger afternoon upward drifts after 12 hours. On August 16 and 17 the afternoon changes of D predict upward movements two hours earlier on August 17 than on the 16th while the reverse was found. Comparing data on July 29 and 30, we should expect larger drifts on the 30th than on the 29th.

The external electric field theory predicts some of the observed F2 region fluctuations such as downward morning and upward afternoon drifts and the large morning fluctuation on December 22; but it does not account for the general winter morning foF2 peak, nor the large peak on December 21, nor the absence of an afternoon peak on both the 21st and 22nd, nor does it give the correct phase of fluctuations after 15 hours on August 16 and 17. The wind driven dynamo theory indicates the opposite drift directions which are contrary to density fluctuation measurements. Of the two theories, the external electric field one is more successful; however, a theory is needed for the generation of the fields.

CHAPTER 6 SUMMARY AND CONCLUSIONS

6.1 Statement of the Problem

Observations of electron density and temperature at the Arecibo Ionospheric Observatory in Puerto Rico by incoherent backscatter revealed the existence of large amplitude fluctuations of both density and temperature during quiet daytime solar minimum conditions. F2 region densities and temperatures changed inversely with periods from one to four hours and with F2 peak density fluctuations as large as 100%. They occured between 180 km and an observational limit of 700 km and extended from Arecibo to Mexico City. Consequently, these are not fine structure variations with scales of only a few kilometers and derivations of a few minutes.

Investigation of the causes of the fluctuations proceeded by considering the following questions. Their order will be revised for the ease of logical development.

(a) Large electron density and temperature fluctuations are observed in the F region during the day. Can the changes in either density or temperature be explained as due to a variation of the other? Is the system of coupled electron density and temperature equations stable with respect to pertubations?

(b) Is it necessary to invoke motion of the neutral atmosphere to explain the fluctuations? If so then what types of neutral motion can be expected and what would be consistent with the experimental results?

(c) The solar energy flux is variable. To what extent can this be ruled out as a source for the fluctuations?

(d) To what extent can plasma drifts caused by electric fields be used to explain the fluctuations?

(e) How are the fluctuations correlated at different ionospheric sounding stations, and how are they related to traveling ionospheric disturbances?

(f) Are the fluctuations due to local changes of density and temperature or are they due to regions of enhanced density drifting over the station?

6.2 Discussion and Conclusions

The solar energy flux is variable. To what extent can this be ruled out as a source for the fluctuations?

Variations of the extreme ultraviolet solar flux which is responsible for creation of ionospheric electron-ion pairs would produce increases of density throughout the whole F region and over the entire sunlit hemisphere of the globe. The density fluctuation were observed to occur mainly above 180 km and at only several particular stations of the spaced ionosonde network. Therefore, solar flux variations did not cause these fluctuations.

Can the changes in either density or temperature be explained as due to a variation of the other? Is the system of coupled electron density and temperature equations stable with respect to pertubations?

The effects of electron temperature on electron densities and vice versa were studied by solving the time dependent fluid equations of the plasma. Because of computer limitations the temperature and density equations were solved independently. Several electron density models of the F2 region were computed for different isothermal electron and ion temperatures. Equilibrium solutions exhibited the known small reduction of peak electron density and enhanced density above the peak for increasing ratios of electron to ion temperatures. A sudden increase of electron temperature by $200^{\circ}K$ (12%) caused the peak electron density to oscillate slowly about its equilibrium value with less than a 2% variation and a period greater than an hour. Several of the equilibrium density models corresponding to different temperature ratios were used in conjunction with Banks' (1966d) energy production rates to compute model electron temperature profiles. Starting from high isothermal initial conditions the temperatures relaxed exponentially to equilibrium within ten minutes; time constants were less than two minutes. Low temperatures were found at and above the F2 peak and there was little variation for each of the density models.

The amplitude of changes of experimental electron densities and the F2 peak altitude were much larger than those of the models for similar $200^{\circ}K$ electron temperature variations such as on December 15. Time constants for model density changes were of the same order as the experimental fluctuations,

but those of the model electron temperatures were much shorter than the observed data. Thus, it would appear, at least from these approximate calculations, that the observed fluctuations cannot be explained by an unstable coupling of electron densities and temperatures.

Model electron temperatures were found to be much lower than experimental temperatures for similar F2 region electron densities so that ambient electron gas energy production rates needed to be increased over Banks' (1966d) values used in the calculations. It was suggested that the energy production rate for the electron gas may depend on the ambient electron density by proportional sharing of the photoelectron energies by neutral and electron gases. The density dependent energy production rate would not seriously alter the relaxation time for the electron temperatures since the photoelectrons lose their energy within a few seconds.

Are the fluctuations due to local changes of density and temperature or are they due to regions of enhanced density drifting over the station?

Plasma frequencies at the F2 peak measured by a network of nine spaced ionosondes, including Arecibo, showed fluctuations similar to Arecibo only at Jamaica and Mexico City, much smaller fluctuations at Grand Bahama Island and Cape Kennedy, and no similar fluctuations at Ottawa, Wallops Island, White Sands, and Huancayo. In addition, some fluctuations were

almost the same on pairs of adjoining days. Therefore, the fluctuations are not just local changes of density and temperature. Incoherent backscatter electron density profiles at Arecibo showed that the density fluctuations not only involved the F region from 180 km to at least 700 km but also were closely associated with variations of vertical transport velocity. Consequently, the fluctuations are not regions of enhanced density drifting over the station.

How are the fluctuations correlated at different ionospheric sounding stations, and how are they related to traveling ionospheric disturbances?

Thome (1966) found that internal gravity waves passing over Arecibo were revealed by his similar spaced ionosonde network as fluctuations of peak plasma frequency occuring at systematically later universal times as the waves traveled south toward Arecibo. The strength of these fluctuations grew at lower latitudes as the ducted waves leaked into the F2 region and amounted to a one megacycle amplitude dip at Cape Kennedy and a two megacycle dip at Jamaica. A wave velocity of about 700m/s directed to the equator was found.

Among the present data the most likely example of an internal gravity wave fluctuations occured during the afternoon of July 22, 1966. The initial fluctuation was strongest at Jamaica and succeeding ones were much weaker while similar but smaller fluctuations happened at Arecibo and Mexico City at nearly the same universal time. If the data at Wallops Island,

missing because of disturbed ionograms, before 12 hours EST
and if the small fluctuation at Ottawa near 1030 hours EST were
all manifestations of the same wave, a speed of 300-400 m/s and
a period of about three hours would be appropriate.

During the winter and during the morning of August 17 the
universal times of these fluctuations, however, did not support the
hypothesis of traveling waves. The two large fluctuations on the
mornings of December 21 and 22 which were seen at Cape
Kennedy, Grand Bahama Island, Arecibo, Jamaica, and Mexico
City were not seen at the other stations and the universal times
of these events in Table 4 are inconsistent with a traveling wave.
Therefore, traveling waves do cause large density fluctuations
at Arecibo, but the larger fluctuations presented here are not
caused by internal gravity waves.

To what extent can plasma drifts caused by electric fields
be used to explain the fluctuations?

Uniform drift velocities, whether from electrodynamic
forces or neutral particle motion, are known to cause large
changes of peak density and peak altitude of equilibrium model
F2 layers. Horizontal neutral motion at 20 m/s or an electric
field of 10^{-3} v/m near the latitude of Arecibo giving a 10 m/s
upward drift nearly doubled the peak density and increased the
F2 peak altitude by 30 km of representative density models.
Relaxation of the densities toward equilibrium after removal of
a drift was shown to procede exponentially with time constants
longer than an hour.

Vertical transport velocities in the F2 region were computed from the experimental data to determine if the density fluctuations were associated with transport velocity variations. Velocities were found by using an assumed ion-electron production model and using scaled loss rate coefficients together with the experimental electron densities in solutions of the height integrated electron density continuity equation. The electron fluxes at the upper boundary of 700 km were assumed to be much smaller than those between 250 km and 400 km so that the latter fluxes could be obtained. Because production and loss rates were not well known, the magnitude of the velocities may not be reliable, but the variations are believed to be indicative of true velocity variations.

Changes of the computed vertical transport velocities between 250 km and 400 km were found to be closely connected to the electron density fluctuations, and they were large enough to cause the fluctuations. Upward, or less downward, transport was found to begin at the same time as the densities increased, and the largest densities occured during the following downward movement. Peak density fluctuations lagged about one hour or less behind those of the velocities, but the altitude of the peak and the velocities near the peak changed almost together. Electron content in a vertical column near the peak lagged velocity variations by less than 30 minutes. Therefore, the largest densities near the peak during fluctuations resulted in part from a greater influx of ionization than could be lost immediately.

Electron density increases in the winter were preceded by less downward transport, but the midday minimum of F2 peak density was accompanied by neither excessive downward transport nor density minima above the peak. Consequently, the winter fluctuations result from upward transport and the midday dip is just a return toward equilibrium between fluctuations.

In the summer, large afternoon densities were associated with high peak altitudes and with constant small or upward transport velocities. A lower than normal F2 layer on the morning of August 17 coincided with strong downward transport near the peak. The similarity of electron densities, altitude of the peak, and strength of the velocities on this morning compared with those during the winter suggests that the transport velocity during the summer is generally much less downward than during the winter.

In the F2 region neutral atmospheric motion transports ionization along field lines while electrodynamic drifts transport it across field lines. The method used to compute the vertical transport velocities is unable to distinguish the horizontal component of motion for selection of these two mechanisms. Electric fields cause simultaneous vertical drifts at all altitudes, until inhibited by ion drag induced neutral motion, and neutral motion can cause either simultaneous or variable dirfts. Consequently, additional data are needed to distinguish between electrodynamic and neutral drifts.

Electric fields in the F2 region were inferred from San Juan, Puerto Rico, magnetograms according to two theories. The conventional theory of global charge distribution resulting from neutral winds driving the dynamo region electrical currents was found to predict F region drifts generally in the opposite direction to those of the calculated transport velocities if the work of Maeda and Kato (1966) is correct. A second, unsupported, theory suggested by Fejer (1965) is that electric fields generated in the magnetosphere drive the dynamo currents. The latter theory was applied in a crude manner to the magnetic data and the predicted drifts were in the same general direction as the density transport velocities. Coincident times and directions were found between the transport velocities and external electric field type drifts were found on some days, but there were several disagreements too. Explanation of the large fluctuations at Arecibo, Jamaica, and Mexico City, the very small ones at Cape Kennedy, and practically none to the north of Cape Kennedy would require a special low latitude dynamo region. The average San Juan magnetograms, however, blend well with those of many other stations in support of a large uniform dynamo current system (Vestine et al, 1947). It is clear that if there are electric fields of some kind associated with the dynamo current system and that these fields did not produce expected F region drifts then the theories of these fields needs to be reviewed. We conclude, therefore, although electric fields may play some role in the fluctuations, those fields inferred from the

magnetograms are not primarily responsible for the large F2 region fluctuations at Arecibo.

Neutral atmospheric winds in the F region were predicted by Geisler (1966) for middle and high latitudes. These winds, computed from static, temperature dependent neutral models were of the order 100 m/s to the poles during the day. The speeds are much higher than those indicated from velocity transport calculations of the Arecibo data. To explain the observed electron density fluctuations by winds we would require in the winter:

a) southward gusts of 20-30 m/s for one or two hours during the morning and again the evening

b) very small speeds to the north of Arecibo

c) vertical speed variations at some times

d) some changes with longitude

e) possible generally northward speeds of about 20 m/s during the day,

and in the summer:

a) generally small speeds throughout the day

b) roughly 50 m/s northward gusts on the mornings of August 16 and 17 with speeds decreasing with altitudes above 250 km

and generally:

a) moderate north-south speeds at 20 degrees north geographic latitude

b) much reduced north-south speeds north of Arecibo

c) generally consistent circulation patterns as a function
   of longitude with small variations

d) fair correlation from day to day but less from week
   to week.

Despite this list of special requirements, the theory of F region
atmospheric circulation has not been developed sufficiently
to confirm or deny any of them. When non-sinusoidally changing
neutral temperatures and ion drag effects with an unsymmetrical
magnetic equator are considered it might be possible to have
regional wind systems of the types discussed here. Differences
between summer and winter at Arecibo would be expected since
the center of the heated atmosphere passes directly over Arecibo
during the summer and 30 to 40 degrees to the south during
the winter.

However, as Chapter 5 shows, the magnitudes, time scales,
and relative directions of the density fluctuations correlate
reasonably well with vertical drifts. Thus, we speculate that
one single mechanism could be responsible for these fluctuations
if this mechanism were a wind of the kind just described.

One further question arose during this investigation with
particular reference to the large summer afternoon electron
densities at Arecibo, Jamaica, and Mexico City. Could these be
due to spreading of the Appleton equatorial anomaly; and,
if so, could the winter fluctuations come from the same source?

The centers of the anomaly's enhanced density ridges move
out as far as 20 degrees from the magnetic equator in the

afternoon; Arecibo, Jamaica, and Mexico City are 30 degrees
north of the magnetic equator. World maps of mean F2 peak
plasma frequencies prepared by Zacharisen (1959, 1960) showed
that the northern anomaly ridge was strongest and farthest north
during summer afternoons and that Arecibo was on its shoulder.
In the winter, the ridge is weaker and was shifted down to the
geographic equator; Arecibo was not on the shoulder.

Plasma flow along field lines from the anomaly can be
discarded because the transport velocity calculations show that
the electron density fluxes decrease rather than increase above
the F2 peak, and the fluctuations were preceded by upward
rather than downward transport. Horizontal transport of
ionization would require electric fields to cross the geomagnetic
field lines, and the magnetogram data indicated that electric
fields were not well correlated with many of the fluctuations.
Summer afternoon velocities were generally constant despite
magnetic field diurnal variations. Consequently, if the
anomaly were to appear to spread to Arecibo, then neutral winds
would be the most likely agent.

6.3 Suggestions for Further Work

Electron and ion temperatures are important in
determining the electron density distribution above the F2
peak. More detailed electron temperature profiles throughout
the F region during the day would provide better estimates

of the energy fluxes and conduction of the ambient electron gas.
Additional theoretical work and measurements are needed at the
same time about the problems of photoelectron production,
transport, and energy loss rates over the whole ionosphere.

Two difficulties were encountered in studying the
mechanisms for electron density fluctuations. They were
insufficient knowledge of what the electric fields and neutral winds
should be in the ionosphere. These two forces are not necessarily
separate in the ionosphere. Analysis with spherical harmonic
fitting of global data and diurnally periodic solutions are not
likely to account for the irregular features which caused the
density fluctuation at Arecibo. Studies of neutral winds in the
F region and the dynamo region should be approached more as
initial value problems with time dependent electron densities
and with neutral temperature variations similar to those of
low altitude ion temperatures from backscatter experiments.
Measurements are needed of electric fields, neutral motion
(winds and waves), and, equally as important, the transport
velocities of the ionization itself throughout the day over a
wide range of latitudes.

BIBLIOGRAPHY

Banks, P. M., "Energy Transfer and Charged Particle Temperatures in the Upper Atmosphere," Ph.D. thesis, Penn. State Univ., 1965.

_____, "Collision Frequencies and Energy Transfer: Electrons," Planet. Space Sci. 14, 1085, 1966 a.

_____, "Collision Frequencies and Energy Transfer: Ions," Planet. Space Sci. 14, 1105, 1966 b.

_____, "Electron Thermal Conductivity in the Ionosphere", Earth Planet. Space Sci. Letters 1, 151, 1966 c.

_____, "Charged Particle Temperatures and Electron Thermal Conductivity in the Upper Atmosphere", An. Geophys. 22, 577, 1966 d.

_____, "Thermal Conduction and Ion Temperatures in the Ionosphere", Earth Planet. Space Sci. Letters 1, 270, 1966 e.

_____, "The Temperature Coupling of Ions in the Ionosphere", Planet. Space Sci., 15, 77, 1967 a.

_____, "Ion Temperatures in the Upper Atmosphere", J. Geophys. Res. 72, 3365, 1967 b.

Bowles, K. L., "Incoherent Scattering by Free Electrons as a Technique for Studying the Ionosphere and the Exosphere: Some Observations and Considerations", J. Res. 65D, 1, 1961.

Buneman, O., "Fluctuations in a Multicomponent Plasma", J. Geophys. Res. 66, 1978, 1961.

Chan, K. L. and D. G. Villard, "Observation of Large-Scale Traveling Ionospheric Distrubances by Spaced-Path High Frequency Instantaneous-Frequency Measurements", J. Geophys. Res. 57, 973, 1962.

Chandra, S., J. J. Gibbons, and E. R. Schmerling, "Vertical Transport of Electrons in the F Region", J. Geophys. Res. 65, 1159, 1960.

Chapman, S. and J. Bartels, Geomagnetism, Oxford Univ. Press, London, 1940.

Cospar International Reference Atmosphere 1965, North Holland
Pub. Co., Amsterdam, 1965.

Cummack C. H., "Spectrum Analysis of the Critical Frequency
of the F_2-layer", J. Atmosph. Terr. Phys. 28, 447, 1966.

Cummings, J. D., "Theoretical Electron Distributions in the
Nocturnal F-2 Region at Mid-latitudes", Penn. State Univ.
Ionosphere Res. Lab. Sci. Rpt. 275, 1966.

Dalgarno, A., M. B. McElroy, and R. J. Moffett, "Electron
Temperatures in the Ionosphere", Planet. Space Sci. 11,
463, 1963.

Diaz, J. B., "Partial Differential Equations" in Handbook of
Automation, Computation, and Control, ed. by Grabbe, Ramo,
and Wooldridge, Wiley Pub. Co., New York, 1958.

Donahue, T. M., "Ionospheric Reaction Rates in the Light of
Recent Measurements in the Ionosphere and Laboratory",
Planet. Space Sci. 14, 33, 1966.

Dougherty, J. P., "On the Influence of Horizontal Motion of
the Neutral Air on the Diffusion Equation of the F Region",
J. Atmosph. Terr. Phys. 20, 167, 1961.

_____, and D. T. Farley, "A Theory of Incoherent Scattering
of Radio Waves by a Plasma 3. Scattering in a Partly
Ionized Gas", J. Geophys. Res. 68, 5473, 1963.

Doupnik, J. R. and J. S. Nisbet, "Electron Temperature and
Density Fluctuations in the Daytime Ionosphere", in Electron
Density Profiles in Ionosphere and Exosphere, ed. by
J. Frihagen, North Holland Pub. Co., Amsterdam, 1966.

Evans, J. V., "An F Region Eclipse", J. Geophys. Res. 70,
131, 1965.

Fejer, J. A., "Scattering of Radio Waves by an Ionized Gas in
Thermal Equilibrium in the Presence of a Uniform Magnetic
Field", Can. J. Phys. 39, 716, 1961.

_____, "Motions of Ionization", in Physics of the Earth's Upper
Atmosphere, ed. by Hines, Paghis, Hartz, and Fejer,
Prentice Hall, Englewood Cliffs, N. J., 1965.

Friedman, J. P., "Propagation of Internal Gravity Waves
in a Thermally Stratified Atmosphere", J. Geophys. Res.
71, 1033, 1966.

Geisler, J. E. and S. A. Bowhill, "Ionospheric Temperatures at Sunspot Minimum", J. Atmosph. Terr. Phys. 27, 457, 1965.

_____ and S. A. Bowhill, "Exchange of Energy Between the Ionosphere and the Protonosphere", J. Atmosph. Terr. Phys. 27, 1119, 1965.

_____, "Atmospheric Winds in the Middle Latitude F-region", J. Atmosph. Terr. Phys. 28, 703, 1966.

Gordon, W. E., "Incoherent Scattering of Radio Waves by Free Electrons with Applications to Space Exploration by Radar", Proc. IRE 46, 1824, 1958.

Haerendel, G., R. Lust, and E. Rieger, "Motion of Artificial Ion Clouds in the Upper Atmosphere", Max-Planck-Institute fur Physik und Astrophysik report 27/66, 1966.

Hagfors, T., "Density Fluctuations in a Plasma in a Magnetic Field, with Applications to the Ionosphere", J. Geophys. Res. 66, 1699, 1961.

Hanson, W. B. and F. S. Johnson, "Electron Temperatures in the Ionosphere", Memoires Soc. R. Liege 4, 390, 1961.

_____, "Electron Temperatures in the Upper Atmosphere", in Space Research III, North Holland Pub. Co., Amsterdam, 1963.

_____, and R. J. Moffett, "Ionization Transport Effects in the Equatorial F Region", J. Geophys. Res. 71, 5559, 1966.

Heisler, L. H., "Observation of Movement of Pertubations in the F-region", J. Atmosph. Terr. Phys. 25, 71, 1963.

_____, "A Universal Time Control of Temperate Zone F2-region Ionization", J. Atmosph. Terr. Phys. 28, 153, 1966.

Hines, C. O., "Internal Atmospheric Gravity Waves at Ionospheric Heights", Can. J. Phys. 38, 1441, 1960.

_____, "On the Nature of Traveling Ionospheric Disturbances Launched by Low-altitude Nuclear Explosions", J. Geophys. Res. 72, 1877, 1967.

Hinteregger, H. E., L. A. Hall, and G. Schmidtke, "Solar XUV Radiation and Neutral Particle Distribution in July 1963 Thermosphere", in Space Research V, North Holland Pub. Co., Amsterdam, 1965.

Holt, E. H. and R. E. Haskell, Foundations of Plasma Physics, Macmillian Co., New York, 1965

Kato, S., "Horizontal Wind Systems in the Ionospheric E Region Deduced from the Dynamo Theory of the Geomagnetic Sq Variation, Part II", J. of Geomag. Geoelect. 8, 24, 1956.

King, J. W., D. Eccles, A. J. Legg, et al, "An Explanation of Various Ionospheric and Atmospheric Phenomena Including the Anomalous Behavior of the F Region", Internal Memo. 191, D.S.I.R. Radio Res. Station, Slough, England, 1964.

_____ and H. Kohl, "Upper Atmospheric Winds and Ionospheric Drifts Caused by Neutral Air Pressure Gradients", Nature 206, 699, 1965.

Kohl, H. and J. W. King, "Atmospheric Winds Between 100 and 700 km and Their Effects on the Ionosphere", URSI XV General Assembly, Munich, 1966.

Maeda, K. and S. Kato, "Electrodynamics of the Ionosphere", Space Sci. Rev. 5, 57, 1966.

Mahajan, K. K., "Extent of Thermal Non-equilibrium in the Ionosphere", to appear in J. Atmosph. Terr. Phys., 1967.

Moorecroft, D. R., "On the Power Scattered from Density Fluctuations in a Plasma", J. Geophys. Res. 68, 4870, 1963.

Nicolet, M. "Composition and Constitution of the Earths Environment", in Geophysics The Earths Environment, ed. by DeWitt, Hieblot, and Lebeau, Gordon and Breach Pub. Co., New York, 1963.

_____, "Aeronomy", in Handbuch der Physik, Geophysik, Band XLIX, Springer Verlag, 1967.

Nisbet, J. S., "Factors Controlling the Shape of the Upper F Region Under Daytime Equilibrium Conditions", J. Geophys. Res. 68, 6099, 1963.

Perkins, F. and R. Wand, "Analysis of the Ionospheric Incoherent Scatter Signal by Digital Methods", Cornell Univ. Rpt. CRSR 207, 1965.

Renau, J., H. Camnitz, and W. Flood, "The Spectrum and Total Intensity of Electromagnetic Waves Scattered from an Ionized Gas in Thermal Equilibrium in the Presence of a Static Quasi-uniform Magnetic Field", J. Geophys. Res. 66, 2703, 1961.

Rishbeth, H. and D. W. Brown, "Equilibrium Electron Distributions in the Ionospheric F2-layer", J. Atmosph. Terr. Phys. 18, 234, 1960.

_____, "A Time-varying Model of the Ionospheric F2-layer", J. Atmosph. Terr. Phys. 26, 657, 1964.

_____, L. R. Megill, and J. H. Cahn, "The Effect of Ion-drag on the Neutral Air in the Ionospheric F-region", An. Geophys. 21, 235, 1965.

_____, "The Effect of Winds on the Ionospheric F2 Peak", J. Atmosph. Terr. Phys. 29, 225, 1967.

da Rosa, A. V., "The Theoretical Time-dependent Thermal Behavior of the Ionospheric Electron Gas", J. Geophys. Res. 71, 4107, 1966.

Salpeter, E. E., "Scattering of Radio Waves by Electrons above the Ionosphere", J. Geophys. Res. 65, 1851, 1960.

_____, "Effect of the Magnetic Field on Ionospheric Backscatter", J. Geophys. Res. 65, 982, 1961.

_____, "Density Fluctuations in a Nonequilibrium Plasma", J. Geophys. Res. 68, 1321, 1963.

Sharofsky, I. P., I. B. Bernstein, and B. B. Robinson, "Condensed Presentation of Transport Coefficients in a Fully Ionized Plasma", Phys. Fluids 6, 40, 1963.

Thomas, L., "Electron Density Distributions in the Daytime F_2 Layer and Their Dependence on Neutral Gas, Ion, and Electron Temperatures", J. Geophys. Res. 71, 1357, 1966.

Thome, G., "A Study of Large-Scale Traveling Disturbances in the Ionosphere Using the Arecibo UHF Radar", Ph.D. thesis, Cornell Univ., 1966.

Tornatore, G. H., "Drift Effects on Parameters of the Upper F-Region Under Daytime Equilibrium Conditions", Penn. State Univ. Ionosph. Res. Lab. Sci. Rpt. 221, 1964.

Vestine, E. H. et al, "The Geomagnetic Field, Its Description and Analysis", Carnegie Institution of Washington Pub. 580, 1947.

Volland, H., "Heat Conduction Waves in the Upper Atmosphere", J. Geophys. Res. 72, 2831, 1967.

Yerg, D. G., "Observations of Ionospheric Drifts and Related Phenomena with Spaced Radio Receivers", Univ. of Puerto Rico Sci. Rpt. 3, 1955.

_____, "Observations and Analysis of Ionospheric Drift", J. Atmosph. Terr. Phys. 8, 247, 1956.

Yonezawa, T., "On the Influence of Electron-ion Diffusion Exerted Upon the Formation of the F2 Layer", J. Radio Res. Lab. 5, 165, 1958.

Zacharisen, D. H., "World Maps of F2 Critical Frequencies and Maximum Usable Frequency Factors", NBS Tech. Note 2, 1959.

_____, "Supplementary World Maps of F2 Critical Frequencies and Maximum Usable Frequency Factors", NBS Tech Note 2-2, 1960.

ACKNOWLEDGMENTS